



NOVA
NOVA SCHOOL OF
SCIENCE & TECHNOLOGY

DEPARTAMENT OF
CHEMISTRY

Tatiana Pereira Fernandes
BSc in Biochemistry

The potential neuroprotective role of carboxyhemoglobin (COHb) against hemorrhagic stroke

Master in Molecular Genetics and Biomedicine
NOVA University Lisbon
September 2024



The potential neuroprotective role of carboxyhemoglobin (COHb) against hemorrhagic stroke

Tatiana Pereira Fernandes

BSc in Biochemistry

Adviser: Helena Luísa de Araújo Vieira
Associate Professor, NOVA University Lisbon

Examination Committee:

Chair: Margarida Casal Ribeiro Castro Caldas Braga,
Associate Professor, NOVA University Lisbon

Rapporteurs: Rita de Oliveira Teodoro,
Associate Professor, NOVA Medical School, University Lisbon,

Adviser: Helena Luísa de Araújo Vieira
Associate Professor, NOVA University Lisbon

THE POTENTIAL NEUROPROTECTIVE ROLE OF CARBOXYHEMOGLOBIN (COHB) AGAINST HEMORRHAGIC STROKE

Copyright © Tatiana Pereira Fernandes NOVA School of Science and Technology, NOVA University Lisbon.

The NOVA School of Science and Technology and the NOVA University Lisbon have the right, perpetual and without geographical boundaries, to file and publish this dissertation through printed copies reproduced on paper or on digital form, or by any other means known or that may be invented, and to disseminate through scientific repositories and admit its copying and distribution for non-commercial, educational or research purposes, as long as credit is given to the author and editor.

Acknowledgements

Gostaria de começar por expressar a minha enorme gratidão a todas as pessoas que me acompanharam e ajudaram na realização desta tese de mestrado.

À minha orientadora, Doutora Helena Vieira, pela oportunidade que me deu, por toda a confiança que depositou em mim e pelo conhecimento e motivação que sempre estiveram presentes e que me permitiram crescer tanto pessoalmente como profissionalmente.

Um agradecimento também à Investigadora Inês Mollet por toda a ajuda e pelos vários conselhos e conhecimentos que me transmitiu.

Aos meus colegas e amigos de laboratório, Catarina, Rodrigo e Cristina, por partilharmos tanto os bons como os maus momentos, pelas nossas conversas de almoço, por todos os risos que tornaram os dias mais fáceis, e principalmente por toda a alegria que me trouxeram nesta fase da minha vida. Obrigada também à Sara, ao Luís e ao Zé, que apesar de não estarem no laboratório também fizeram parte destes momentos felizes.

Às minhas amigas da faculdade, Ana e Sara, que apesar de não estarmos juntas continuaram a estar sempre presentes.

Aos meus amigos e amigas de sempre, Filipe, Bia, Diogo e Inês por todos os nossos convívios e por todos os momentos de alegria de que fizeram parte e que me deram motivação e energia para continuar. Um obrigado especial à minha melhor amiga, Beatriz Potra, por toda a companhia, por todos os risos e momentos juntos, por todos os desabafos e por todas as palavras de apoio e de amizade.

Ao meu namorado, Francisco, que foi um dos meus maiores apoios, não só este ano, mas todos os anteriores. Obrigada por ouvires todas as minhas tristezas e preocupações mas também todas as minhas conquistas e felicidades. Obrigada por toda a alegria, motivação e confiança que sempre me deste e por nunca me deixares ir abaixo nem desistir, sem ti não teria conseguido.

À minha família, especialmente aos meus pais, Carlos e Sandra, e aos meus pais emprestados, Laura e Hélder. Um grande obrigado por todo o vosso apoio e por terem sempre acreditado em mim mesmo quando eu própria não acreditei. Obrigada por todas as vossas palavras de motivação, por todos os vossos conselhos, por todo o amor e carinho que me deram e por sempre me ouvirem e me garantirem que tudo ia correr bem. Obrigada por serem a minha maior força e me motivarem a ser uma pessoa melhor.

Abstract

Stroke is the leading cause of death in Portugal and a major global cause of permanent neurological disability. Although hemorrhagic stroke accounts for just 15% of all stroke cases, it poses a higher risk of mortality by triggering harmful biological processes, including oxidative stress, increased neuroinflammation, neuronal damage and blood-brain barrier (BBB) dysfunction. Cell-free hemoglobin (Hb), released after the rupture of red blood cells, is easily oxidized into pro-oxidant forms like methemoglobin (MetHb) that further contribute to these harmful processes. Addressing the harmful effects of pro-oxidant MetHb represents a potential therapeutic strategy for hemorrhagic stroke.

Carbon monoxide (CO), a gas endogenously produced by the stress-response enzyme heme-oxygenase, has been shown to have cytoprotective, anti-inflammatory, antioxidant, and anti-apoptotic effects. This gas binds to reduced Hb with high affinity forming carboxyhemoglobin (COHb), which is traditionally considered a marker of CO toxicity. However, recent studies have suggested that COHb may have a neuroprotective role by stabilizing Hb in its reduced state and preventing the formation of toxic heme byproducts.

The goal of this study was to evaluate the potential protective effects of COHb against cell-free Hb toxicity by assessing its effects in microglia, neurons, and endothelial cells, focusing on neuroinflammation, cell viability, and BBB integrity.

The results showed that while both COHb and MetHb induced oxidative stress, COHb led to significantly lower levels of reactive oxygen species (ROS) production and neuroinflammation in microglia compared to MetHb. However, COHb did not show a cytoprotective effect on neuronal viability compared to MetHb. In terms of BBB integrity, the results were inconclusive, suggesting the need for further investigation into COHb's protective mechanisms.

Overall, these findings highlight the therapeutic potential of COHb in treating hemorrhagic stroke by mitigating the damaging effects of cell-free Hb. Nevertheless, additional research is necessary to better understand its neuroprotective and anti-neuroinflammatory mechanisms and its impact on preserving BBB integrity.

Keywords: Hemorrhagic stroke, cell-free hemoglobin, carboxyhemoglobin, neuroinflammation, neuroprotection, oxidative stress

Resumo

O Acidente Vascular Cerebral (AVC) é a principal causa de morte em Portugal e uma das principais causas de incapacidade neurológica permanente a nível mundial. Embora o AVC hemorrágico constitua apenas 15% de todos os casos de AVC, apresenta um maior risco de mortalidade ao desencadear processos biológicos nocivos, incluindo stress oxidativo, aumento da neuroinflamação, danos neuronais e disfunção da barreira hemato-encefálica (BHE). A hemoglobina (Hb) livre, libertada após a rutura dos eritrócitos, é facilmente oxidada em formas pró-oxidantes, como a metemoglobina (MetHb), que contribuem ainda mais para estes processos prejudiciais. A abordagem dos efeitos tóxicos da MetHb pró-oxidante representa uma potencial estratégia terapêutica para o AVC hemorrágico.

O monóxido de carbono (CO), um gás produzido endogenamente pela enzima de resposta ao stress heme-oxigenase, demonstrou ter efeitos citoprotetores, anti-inflamatórios, antioxidantes e anti-apoptóticos. Este gás liga-se à Hb reduzida com elevada afinidade, formando carboxihemoglobina (COHb), que é tradicionalmente considerada um marcador de toxicidade do CO. No entanto, estudos recentes sugerem que a COHb pode desempenhar um papel neuroprotetor, estabilizando a Hb no seu estado reduzido e impedindo a formação de subprodutos tóxicos do heme.

O objetivo deste trabalho foi avaliar os potenciais efeitos protetores da COHb contra a toxicidade da Hb livre, avaliando os seus efeitos na microglia, nos neurónios e nas células endoteliais, centrando-se na neuroinflamação, na viabilidade celular e na integridade da BHE.

Os resultados mostraram que, embora tanto a COHb como a MetHb tenham induzido stress oxidativo, a COHb conduziu a níveis significativamente mais baixos na produção de espécies reativas de oxigénio (ROS) e de neuroinflamação na microglia, em comparação com a MetHb. No entanto, a COHb não mostrou um efeito citoprotetor na viabilidade neuronal em comparação com a MetHb. Em termos de integridade da BHE, os resultados foram inconclusivos, sugerindo a necessidade de mais investigação sobre os mecanismos de proteção da COHb.

No geral, estes resultados realçam o potencial terapêutico da COHb no tratamento do AVC hemorrágico, atenuando os efeitos nocivos da Hb livre. No entanto, é necessária mais investigação para compreender melhor os seus mecanismos neuroprotetores e anti-neuroinflamatórios e o seu impacto na preservação da integridade da BHE.

Palavras-chave: AVC hemorrágico, hemoglobina livre, carboxihemoglobina, neuroinflamação, neuroproteção, stress oxidativo

Table of contents

1. Introduction	1
1.1. Brain and brain cells	1
1.1.1. Neurons.....	1
1.1.2. Glial cells	2
1.1.3. Brain endothelial cells	4
1.1.4. Blood-brain barrier.....	6
1.2. Stroke	6
1.2.1. Pathophysiology of hemorrhagic stroke	8
1.2.2. Microglia, neuroinflammation and blood-brain barrier in hemorrhagic stroke	10
1.2.3. Currently available therapies.....	13
1.3. Carbon monoxide (CO)	14
1.3.1. Biological role of carbon monoxide	15
1.3.2. CO-releasing molecules.....	18
1.4. Hemoglobin and red blood cells	19
1.4.1. Red blood cells.....	19
1.4.2. Hemoglobin function.....	19
1.4.3. Hemoglobin and red blood cells' antioxidant defenses.....	21
1.4.4. Cell-free hemoglobin.....	25
1.5. Carboxyhemoglobin (COHb)	27
1.5.1. COHb does not indicate CO toxicity	28
1.5.2. COHb as a cytoprotective molecule.....	30
1.5.2.1. COHb formation as a protective mechanism against cell-free Hb oxidation and toxicity.....	30
1.5.2.2. COHb as an antioxidant factor	31
1.5.2.3. Other possible protective functions of COHb.....	32
1.5.3. Advantages of COHb as a potential therapeutic agent.....	33
2. Aims	35
3. Materials and methods	37
3.1. Cell lines and maintenance	37
3.1.1. SH-SY5Y.....	37
3.1.1.1. Maintenance	37

3.1.1.2.	Neuronal differentiation and plating	37
3.1.1.3.	Thawing	38
3.1.1.4.	Freezing	38
3.1.2.	BV-2 cell line	38
3.1.2.1.	Maintenance	38
3.1.2.2.	Plating	38
3.1.2.3.	Thawing	39
3.1.2.4.	Freezing	39
3.1.3.	hCMEC/D3 cell line	39
3.1.3.1.	Maintenance	39
3.1.3.2.	Cell differentiation and plating	40
3.1.3.3.	Thawing and freezing	40
3.2.	Preparation of Hemoglobin, Methemoglobin and Carboxyhemoglobin solution	40
3.2.1.	Methemoglobin with Fe ³⁺ (MetHb)	41
3.2.2.	Reduced hemoglobin with Fe ²⁺ (Hb)	41
3.2.3.	Carboxyhemoglobin (COHb)	41
3.3.	Griess assay – nitrite quantification	43
3.3.1.	Standard calibration curve	43
3.3.2.	Griess assay sample preparation	43
3.4.	ELISA assay – TNF- α quantification	44
3.4.1.	ELISA assay sample preparation	44
3.5.	DCF assay – ROS quantification	45
3.5.1.	DCF assay sample preparation	45
3.6.	Protein extraction and quantification	46
3.7.	Flow cytometry – cell viability assessment	46
3.7.1.	Flow cytometry sample preparation	47
3.8.	Lucifer yellow assay – cell permeability assessment	48
3.8.1.	Standard calibration curve	49
3.8.2.	Sample preparation and calculations	49
3.9.	Immunofluorescence microscopy – assessment of tight junction integrity	50
3.9.1.	Sample preparation	50
3.10.	Statistical analysis	51
4.	Results	53
4.1.	Preparation of the Hemoglobin solution	53

4.2. Neuroinflammatory response of microglia – assessment of neuroinflammatory biomarkers after MetHb and COHb treatment	54
4.2.1. Nitrite quantification.....	54
4.2.2. ROS quantification	56
4.2.3. TNF- α quantification	57
4.3. Neuronal viability and oxidative stress – assessment of cell death and stress biomarkers after MetHb and COHb treatment	59
4.3.1. Neuronal viability in differentiated and non-differentiated SH-SY5Y cells	59
4.3.2. ROS quantification	61
4.4. Blood-brain barrier (BBB) integrity – assessment of BBB permeability and tight junction integrity	62
4.4.1. BBB permeability assay	62
4.4.2. Endothelial tight junction (ZO-1) integrity – immunofluorescence microscopy.....	64
5. Discussion and conclusions	67
6. References	71
7. Annexes	81

List of Figures

Figure 1 - Schematic representation of the structure of a neuron and synaptic connections.....	2
Figure 2 - Main types of glial cells in the CNS and PNS and some of their corresponding functions. .	4
Figure 3 - Schematic representation of adherens and tight junction proteins in blood-brain barrier endothelial cells.....	5
Figure 4 - Schematic representation of ischemic and hemorrhagic stroke.	7
Figure 5 - Simplified mechanism of the inflammation, blood-brain barrier disruption and brain edema development following intracerebral hemorrhage.....	10
Figure 6 - Schematic representation of microglia-induced neuroinflammation after stroke.....	12
Figure 7 - Process of oxidative heme degradation by heme-oxygenase.....	15
Figure 8 - Summary of carbon monoxide's key physiological functions.....	16
Figure 9 - The most studied CO-Releasing Molecules (CORMs).....	18
Figure 10 - Hemoglobin redox states.....	22
Figure 11 - Schematic representation of the antioxidant defense mechanisms within red blood cells..	23
Figure 12 - Schematic illustration of the pathways involved in the reduction of MetHb (Fe^{3+}) to Hb (Fe^{2+}).....	25
Figure 13 - Schematic representation of the pathways activated by extracellular hemoglobin	27
Figure 14 – Schematic representation of the preparation process for MetHb, reduced Hb, and COHb solutions.....	42
Figure 15 - Schematic representation of Griess assay protocol.....	44
Figure 16 - Schematic representation of DCF assay protocol.....	46
Figure 17 - Flow cytometry gating strategy.....	47
Figure 18 - Schematic representation of cell viability assay protocol.....	48
Figure 19 – Schematic representation of the Lucifer yellow assay protocol.	50
Figure 20 - Apparent permeability coefficient (P_{app}) formula.....	50
Figure 21 - Hemoglobin absorption spectra from 350 to 700 nm.....	53
Figure 22 - Comparison between nitrite levels in BV-2 cells pre-treated with PBS, MetHb, COHb and Hb (Fe^{2+}) solutions and control samples	55
Figure 23 - ROS quantification in BV-2 cells pre-treated with PBS, MetHb and COHb solutions.....	57
Figure 24 - TNF- α concentration percentage in BV-2 cells pre-treated with PBS, MetHb and COHb solutions.....	59
Figure 25 - Cell viability (%) assessment of non-differentiated and differentiated SH-SY5Y cells pre-treated with PBS, MetHb, COHb and Hb (Fe^{2+}) solutions and co-treated with CCCp.....	61

Figure 26 - ROS quantification in differentiated SH-SY5Y cells pre-treated with PBS, MetHb and COHb solutions.....	62
Figure 27 - Apparent permeability coefficient values of hCMEC/D3 cells pre-treated with PBS, MetHb and COHb solutions.....	64
Figure 28 - Confocal microscopy images of immunofluorescence staining of the tight junction protein zonula occludens-1 (ZO-1) in hCMEC/D3 cells pre-treated with PBS, MetHb and COHb solutions .	65
Annex Figure 1 – NO quantification in BV-2 cells pre-treated with PBS, MetHb, COHb and Hb (Fe ²⁺)	81
Annex Figure 2 – Griess assay standard curve.....	82
Annex Figure 3 – ELISA assay standard curves.....	82
Annex Figure 4 - Cell viability (%) assessment of non-differentiated and differentiated SH-SY5Y cells pre-treated with PBS, MetHb, COHb and Hb (Fe ²⁺) solutions.....	83

Abbreviations and formulas

A

AA – Ascorbic Acid

AJ – Adherens Junctions

ATP – Adenosine Triphosphate

B

BBB – Blood-Brain Barrier

BECs – Brain Endothelial Cells

bFGF – basic Fibroblast Growth Factor

BSA – Bovine Serum Albumin

C

CAT- Catalase enzyme

CCCP – Carbonyl cyanide m-chlorophenyl hydrazone

CD – Cluster of Differentiation

cGMP – cyclic Guanosine Monophosphate

CNS – Central Nervous System

CO – Carbon Monoxide

CO₂ – Carbon Dioxide

COHb – Carboxyhemoglobin

CORM – Carbon Monoxide-Releasing Molecules

D

DAMPs – Damage-Associated Molecular Patterns

DCF – 2',7'-dichlorofluorescein

DHA – Dehydroascorbic Acid

DMEM-F12 – Dulbecco's Modified Eagle Medium: Nutrient Mixture F-12

DMSO - Dimethyl sulfoxide

E

EBM-2 – Endothelial Basal Medium - 2

EDTA – Ethylenediaminetetraacetic acid

EGF – Endothelial Growth Factor

ELISA – Enzyme-Linked Immunosorbent Assay

F

FBS – Fetal Bovine Serum

G

GPx – Glutathione Peroxidase

GSH – Reduced form of Glutathione

GSSG – Oxidized form of Glutathione

H

Hb – Hemoglobin

HBSS – Hank's Balanced Salt Solution

HCl – Hydrochloric acid

HMGB1 – High Mobility Group Box 1 protein

HO – Heme-Oxygenase enzyme

HSP32 – Heat Shock Protein 32

H₂O₂ – Hydrogen Peroxide

H₂S – Hydrogen Sulfide

I

ICH – Intracerebral Hemorrhage

IGF – Insulin-like Growth Factor

IL – Interleukin

L

LY – Lucifer Yellow dye

M

MAPK – Mitogen-Activated Protein Kinase

MHC II – Major Histocompatibility Complex II

MMPs – Matrix Metalloproteinases

N

NaCl – Sodium chloride

NADH – Nicotinamide Adenine Dinucleotide

NADPH – Nicotinamide Adenine Dinucleotide Phosphate

NF- κ B – Nuclear Factor kappa B

NO – Nitric Oxide

NO₂⁻ – Nitrite

NOS – Nitric Oxide Synthase

NOD – Nitric Oxide Dioxygenase

O

·O₂⁻ - Superoxide Anion

P

PAR-1 – Proteinase-Activated Receptor 1

PBS – Phosphate Buffered Saline

Pen/Strep – Penicillin-Streptomycin

PI – Propidium Iodide

PKG – Protein Kinase G

PNS – Peripheral Nervous System

PPP - Pentose Phosphate Pathway

PRDX2 – Peroxiredoxin 2 enzyme

R

RA – Retinoic Acid

RBC – Red Blood Cell

RIPA – Radioimmunoprecipitation assay buffer
RNS – Reactive Nitrogen Species
ROS – Reactive Oxygen Species
RPMI-1640 – Roswell Park Memorial Institute Medium
RT – Room Temperature

S

SAH – Subarachnoid Hemorrhage
SDS – Sodium Dodecyl Sulfate
sGC – soluble Guanylate Cyclase
SOD- Superoxide Dismutase enzyme

T

tBHP – tert-Butyl Hydroperoxide
TJ – Tight Junctions
TLRs – Toll-Like Receptors
TNF- α – Tumor Necrosis Factor alpha
Trx – Thioredoxin enzyme

U

UV-Vis – Ultraviolet-Visible

V

VEGF – Vascular Endothelial Growth Factor

Z

ZO-1 – Zonula occludens-1

1. Introduction

1.1. Brain and brain cells

The central nervous system (CNS), consisting of the brain and spinal cord, serves as the body's coordinating system, responsible for sensing and controlling all the cognitive processes, movements and endocrine system. The peripheral nervous system (PNS), which extends throughout the body and works in collaboration with the CNS, is comprised of an intricate network of nerves that transmit nerve impulses, in the form of electrical signals, between the sensory organs and the brain, which processes, coordinates, and interprets data very rapidly.¹

The central organ of the CNS is the brain, the most complex organ in the body, featuring an intricate network of about 100 billion neurons in constant communication. The nervous system also includes glial cells, which are non-neuronal cells dedicated to supporting and protecting neurons, in order to improve the complex functions of the CNS.¹

1.1.1. Neurons

Neurons are composed of a cell body, called the soma, and several processes known as neurites, which are classified into dendrites and axons. The soma serves as the central core with multiple short dendrites extending from the soma. These dendrites increase the neuron's surface area, allowing it to receive signals from other neurons. A single, often myelinated axon extends from the soma, conducting signals to other cells, facilitating communication between neurons or transmitting signals to other types of cells. The axon can branch into many extensions, allowing the originating cell to influence many other cells (Figure 1). The extent of branching in both axons and dendrites is indicative of neuronal function, with more extensive dendritic branching correlating with a higher number of inputs received by the neuron.^{2,3}

Similar to other cells, the soma contains a nucleus surrounded by cytoplasm with various organelles. Among these organelles, ribosomes, the endoplasmic reticulum and the Golgi apparatus are essential for protein transcription, translation and processing. These proteins are then directed to specific locations within the soma, dendrites or axon. Additionally, neurons have a cytoskeleton made up of several types of neurofibrils, which are crucial for the formation and shaping of the neuronal processes and facilitating substance transport along them.^{2,3}

Neurons respond to stimuli by transmitting and receiving electrical signals known as nerve impulses. The signals are initially received by the dendrites, transmitted to the soma, and then propagated along

the axon to transmit the signal onward.¹ Nerve impulses can travel throughout the body in milliseconds, either within the CNS or between the CNS and PNS or other organs. The impulses are transmitted from one neuron to another through synapses, the points of connection between them (Figure 1).³

There are two main types of synapses, chemical synapses and the less common electrical synapses. Chemical synapses consist of the presynaptic terminal, synaptic cleft, and postsynaptic terminal.⁴ Specialized signal molecules called neurotransmitters are released to the synaptic cleft by the presynaptic neuron at these synapses. Following their recognition, these neurotransmitters bind to the postsynaptic side's specific receptors.⁴ Electrical synapses, on the other hand, are highly specialized junctions between neurons that allow electric signals to be transferred rapidly and directly between cells.⁵

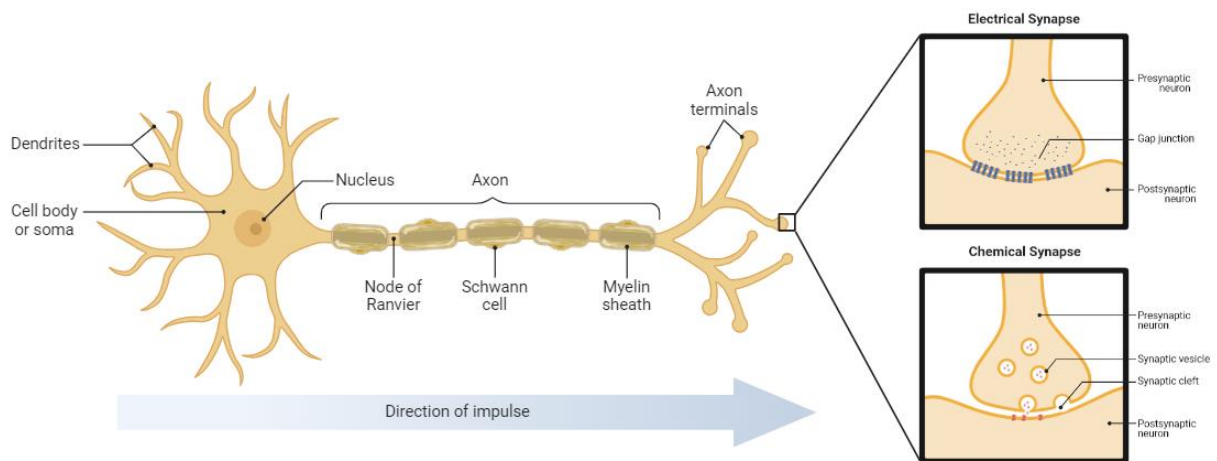


Figure 1 - Schematic representation of the structure of a neuron and synaptic connections. The figure shows the structure of a neuron, including dendrites, soma, axon, myelin sheath, and axon terminals. The direction of impulse transmission is indicated by an arrow. Two types of synapses are depicted: electrical synapse and chemical synapse.

1.1.2. Glial cells

Glial cells were first discovered in the 19th century when scientists observed a non-neuronal, interstitial element in the CNS, comprised of cells distinct from neurons. Initially, these cells were believed to function exclusively as “nerve glue” by providing structural support to neurons.⁶ However, it is now understood that glial cells have many important functions during development and in the mature nervous system, being indispensable for neuronal functioning. Although extensive research has been done to identify these additional functions, the complete capabilities of glial cells remain unclear.⁶

In mammals, depending on the species, glial cells represent between 33% and 66% of the total brain composition. The main glial cell types include astrocytes, microglia and oligodendrocytes in the CNS, and Schwann cells in the PNS.^{6,7}

Astrocytes are the most abundant glial cells in the adult CNS, making them one of the most thoroughly studied glial populations.⁶ These cells have numerous radiating processes, some of which extend to blood capillaries, where they modulate the blood brain barrier (BBB) and regulate cerebral blood flow. Astrocytes play a key role in maintaining neuronal metabolism by guaranteeing the availability of glucose and lactate, and they may also regulate water entry into the brain through aquaporins.^{2,3} Their processes often surround nerve terminals, where they modulate synaptic transmission by modulating neurotransmitter concentration in the synaptic cleft.^{2,7} In fact, astrocytes are also vital in clearing the excess neurotransmitters like glutamate from the synaptic cleft, thus preventing excitotoxicity. They do this through high-affinity uptake sites for the major brain neurotransmitters and the expression of glutamate transporters, converting glutamate into glutamine that is released from astrocytes for neurons to reuse.² It is also thought that during synaptic activity, astrocytic receptors are activated, resulting in an increase in their intracellular Ca^{2+} levels.² Astrocytic Ca^{2+} waves control vasomodulation increasing blood perfusion for supporting increased neuronal activity. Furthermore, astrocytes regulate potassium levels in the extracellular space, maintaining K^+ homeostasis, and deliver glutathione to neurons, which is required for antioxidant defense. GABA transporters on astrocytes also contribute to balance excitatory and inhibitory signals in the brain.^{2,3,7}

Microglia are the nervous system's primary immune and phagocytic cells. They are located in normal brain in a resting state and transform into a mobile, active macrophage upon brain homeostasis disruption during disease or injury by sensing pathological alterations in the brain. These cells are known to transition from a “resting” state to an “activated” state in response to disruptions in brain homeostasis, which can be triggered by injury, infection, or neurodegenerative disease.^{3,6} This microglia activation involves several key processes, including cell proliferation, migration towards a chemoattractant, simplification of cell morphology, and phagocytosis to clear damaged tissue.⁶ In their “resting” state, microglia are characterized by highly branched processes that constantly monitor their surroundings for foreign material, damaged cells, or cellular debris. Moreover, they possess receptors for various neurotransmitters, which suggests that they may also detect local neuronal activity.^{3,6} When they identify any abnormalities, microglia become activated and shift into amoeboid cells with macrophage-like properties, while more microglia cells rapidly migrate to the site. In this activated state, they release inflammatory molecules and phagocytose the harmful elements in order to protect neurons and maintain homeostasis.^{3,6}

Oligodendrocytes in the CNS and myelinating **Schwann cells** in the PNS are responsible for forming the myelin sheath around axons, which ensures the rapid transmission of electrical signals by insulating the nerve fibers. Beyond this, these cells provide essential trophic support, contributing to axonal maintenance and health. They influence the structural and electrical properties of axons by regulating their diameter and the distribution of ion channels in specific regions. Additionally, while oligodendrocytes mainly focus on sustaining axons, Schwann cells in the PNS also influence the regeneration of damaged axons.^{3,7}

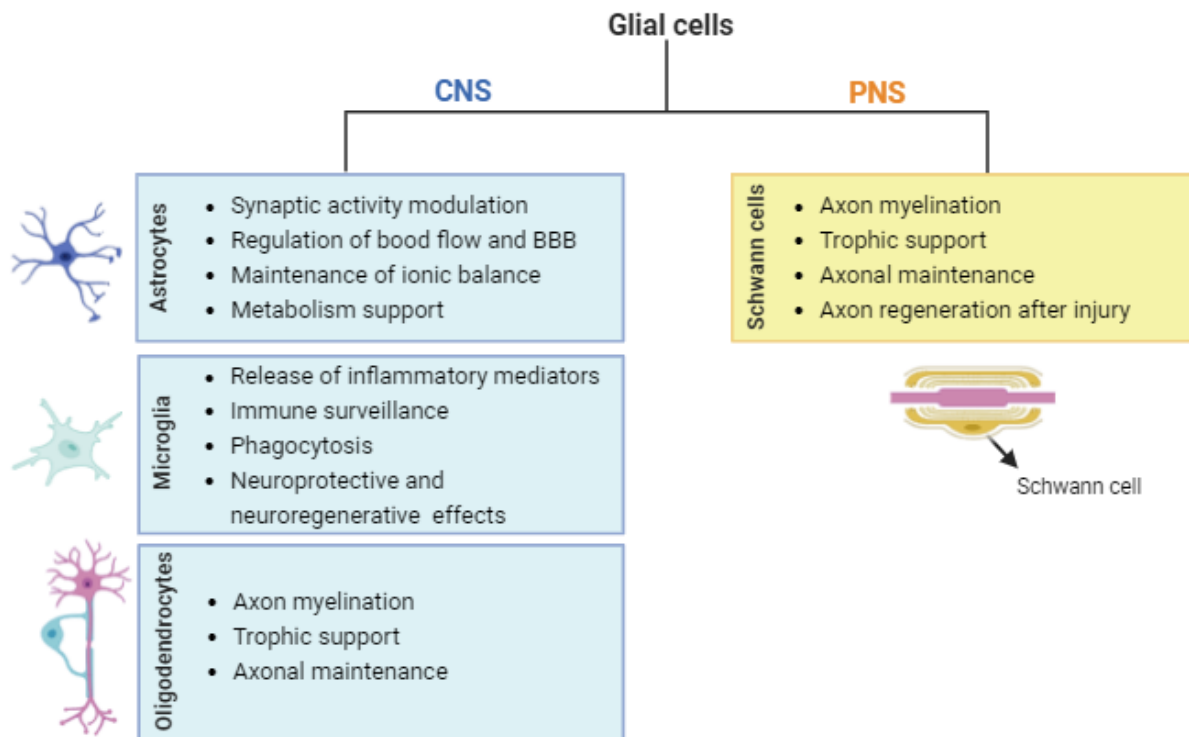


Figure 2 - Main types of glial cells in the CNS and PNS and some of their corresponding functions.

The complexity of brain processes is mainly determined by the intricate neuron-glia interactions, which are essential for regulating fundamental aspects of brain development including neurogenesis, myelination, synapse formation, neuronal metabolism, neuronal migration, proliferation, differentiation, and neuronal signaling.⁸

1.1.3. Brain endothelial cells

Brain endothelial cells (BECs) are specialized cells that line the interior surfaces of brain capillaries, playing an important role in the formation of the blood-brain barrier (BBB), which is essential for maintaining the brain's homeostasis.² These cells are tightly connected, creating a strong physical barrier by limiting the movement of molecules between cells (paracellular permeability). BECs also control the passage of ions and other molecules, serving as metabolic and transport barriers. For example, using enzymes and ATP-dependent transporters, like P-glycoprotein, they help remove harmful agents from the brain back into the bloodstream, guaranteeing that only required nutrients reach the brain while protecting it from potentially damaging substances.^{2,9}

BECs' integrity is supported by a structure composed of transmembrane proteins that form complex junctions between adjacent cells. These junctions, which include both adherens junctions (AJ) and tight junctions (TJ), are essential for maintaining cell adhesion and controlling paracellular permeability (Figure 3). While AJs are present throughout the vasculature and play essential roles in endothelial cell adhesion, paracellular permeability, and the formation of TJs, TJs are specific to BECs and are crucial for maintaining the selective permeability of the BBB.^{2,9}

TJs consist of various transmembrane proteins, such as occludin and claudin, that connect to cytoplasmic accessory proteins like zonula occludens (ZO-1, -2 and -3), catenins and cingulin.⁹ These proteins are connected to the actin cytoskeleton, offering structural stability and contributing to the dynamic modulation of BBB permeability both in normal physiological conditions and during pathological events. TJs also contribute to the polarization of BECs by ensuring adequate transporter distribution between the brain-facing (abluminal) and blood-facing (luminal) membranes.^{2,9}

BBB dysfunction, which is a key event in neurological disorders, occurs when the functions and properties of BECs and TJs are compromised during disease.^{2,9}

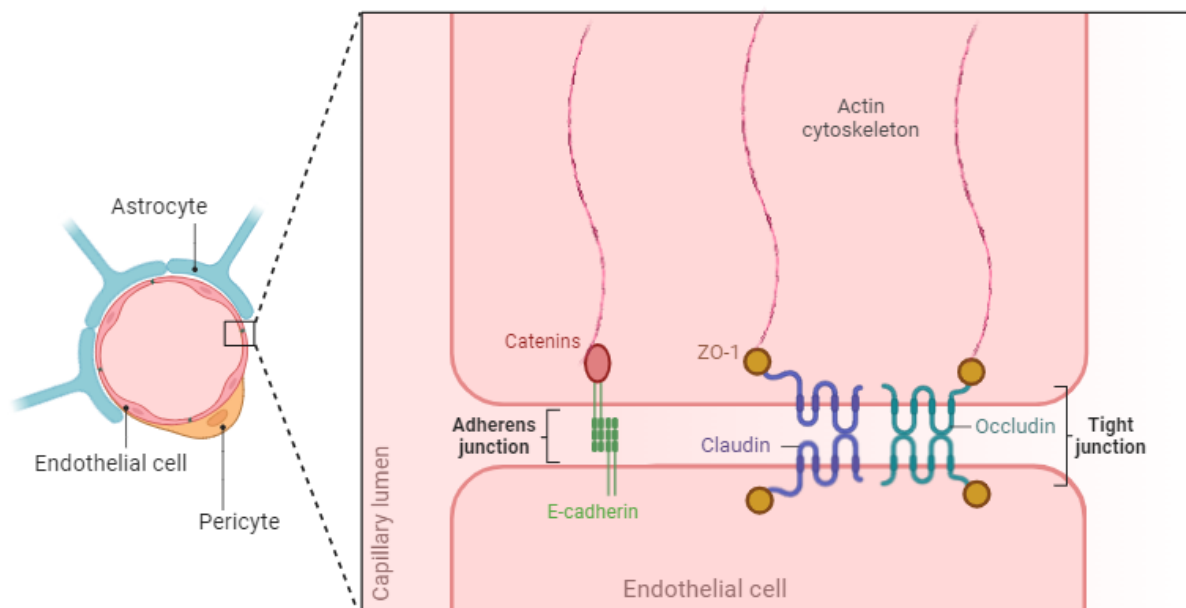


Figure 3 - Schematic representation of adherens and tight junction proteins in blood-brain barrier endothelial cells. The figure illustrates the key adherens and tight junction proteins in BBB endothelial cells. Adherens junctions (cadherins and catenins) maintain cell adhesion, while tight junctions (claudins, occludins, and ZO proteins) regulate permeability, ensuring the selective barrier function of the BBB. (Figure adapted from Sweeney, Melanie D. et al 2019)

1.1.4. Blood-brain barrier

The blood-brain barrier (BBB) plays a key role in maintaining isolated the CNS microenvironment, which is essential for neuronal function. The barrier is a complex system of cellular components made up of endothelial cells connected by tight junctions, pericytes, astrocytes, perivascular microglia and basal lamina.¹⁰ The BBB regulates molecular transport into and out of the CNS, maintaining tight control over the chemical composition of the neuronal environment. It prevents blood cells, neurotoxic plasma components and pathogens from entering into the brain, while facilitating the flow of nutrients and metabolites between the brain and circulation.¹¹

Systemic inflammation, infection, autoimmune diseases, trauma, vascular disorders such as stroke, and neurodegenerative diseases are often associated with an increased permeability of the BBB. This increased permeability allows the infiltration of inflammatory mediators like immune cells and other damaging factors into the brain, which can compromise neuronal function.¹¹ These changes can occur through alterations in the tight junctions, affecting paracellular permeability, or through enhanced transcytosis via the transcellular route across the cerebral endothelium.¹²

The regulation of brain endothelial cell permeability is complex, involving TJ translocation, decreased expression of TJ proteins, and phosphorylation of the TJ complex. Many extracellular mediators, including cytokines like TNF- α and IL-1, reactive oxygen species (ROS), nitric oxide, and various inflammatory agents like prostaglandins and histamine, can induce a leaky BBB.² These mediators influence BBB permeability through intracellular signaling pathways involving protein kinases (A, G, C), small G proteins (rho and rac), mitogen-activated protein kinase (MAPK) pathways (JNK, ERK, p38 MAPK), and Wnt and endothelial nitric oxide synthase (eNOS) pathways, leading to BBB disruption.²

1.2. Stroke

Stroke is the second leading cause of death and the third leading cause of combined death and disability globally, with more than 12.2 million new cases reported and about 6.5 million stroke-related deaths every year.¹³ Furthermore, the lifetime risk of experiencing stroke has also increased by 50% over the past two decades, now affecting one in four individuals.¹³ In Portugal, stroke remains the leading cause of both death and disability.¹⁴ While progress has been made in stroke management, the consequences of post-stroke care significantly impact families, caregivers, the healthcare system and the economy, since this disease often results in long-term disability for the survivors, limiting their ability to do daily activities.¹⁵ As a result, there is a great demand and ongoing work of clinicians and researchers to better

comprehend the underlying pathological mechanisms of stroke and to develop novel, efficient treatments against it.¹⁵

Stroke is a neurological disorder caused by an impaired blood flow to the brain, either due to clots that obstruct arteries (ischemic stroke) or ruptured blood vessels causing bleeding (hemorrhagic stroke), as represented in Figure 4. Ischemic stroke, the most common type, represents about 85% of casualties in stroke patients, while hemorrhagic stroke accounts for the remaining. In ischemic stroke, a blockage prevents blood from reaching the brain, whereas in hemorrhagic stroke, sudden bleeding or leaky blood vessels disrupt normal blood flow.¹⁵ This disruption in oxygen and nutrient supply leads to neuroinflammation and oxidative stress, which can cause cell death and brain tissue damage.¹⁵ Although hemorrhagic stroke is less frequent than ischemic stroke, it is significantly more dangerous, with a mortality rate of 40-50% and significant morbidity among survivors.^{16,17}

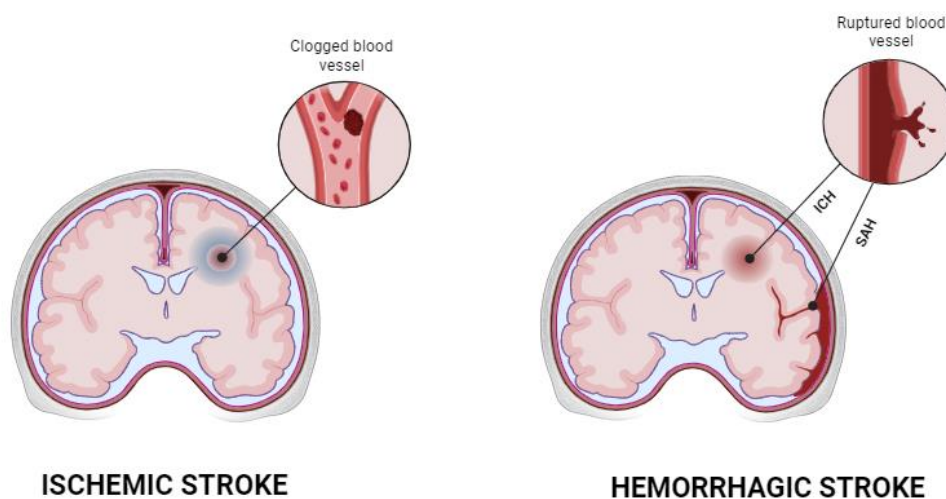


Figure 4 - Schematic representation of ischemic and hemorrhagic stroke. In ischemic stroke, blood flow to the brain is blocked, leading to oxygen deprivation and neuronal damage. In hemorrhagic stroke, the rupture of blood vessels causes bleeding in the brain, resulting in tissue damage and increased intracranial pressure.

Stroke is a multifactorial disease influenced by many factors such as age, sex, geography, race, socioeconomic status, history of cardiac diseases, diabetes mellitus, smoking, alcohol consumption, hypertension and past history of transient ischemic attacks. These factors greatly influence the prevalence, incidence, mortality, and survival rates of both types of stroke.^{15,16}

1.2.1. Pathophysiology of hemorrhagic stroke

Hemorrhagic stroke accounts for about 10-15% of all stroke cases annually. It can be classified into subarachnoid hemorrhage (SAH) or intracerebral hemorrhage (ICH), the most common type and severe.¹⁵ In SAH, a head injury or aneurysm causes blood to accumulate in the brain's subarachnoid space. In ICH, excessive blood accumulation in the brain parenchyma is caused by blood vessel rupture. The primary causes of ICH include excessive use of thrombolytic and anticoagulant medications, hypertension and impaired vasculature.¹⁵

Over the next 30 years, it is anticipated that this number will increase as the global population continues to age. Trends from German registry data suggest that due to an aging population, the total number of ICH patients will increase by approximately 35.2% between 2009 and 2050, assuming that the incidence rate of ICH remains unchanged.¹⁸ Demographic changes are expected to lead to a higher total number of ICH cases and more elderly patients in the future. More specifically, the total number of individuals aged 80 years old and over in the European Union is estimated to increase by approximately 144% from 2010 to 2050. Therefore, the number of ICH patients admitted to hospitals in the European Union is expected to rise in the coming decades.¹⁸

Stroke is a complex disease involving various signaling pathways and mechanisms that affect multiple cells and systems. In the case of hemorrhagic stroke, more specifically ICH, brain injury is caused by factors such as inflammation, BBB dysfunction, oxidative stress, apoptosis, and necrosis.¹⁹⁻²¹ During ICH, blood quickly accumulates within brain parenchyma resulting in the disruption of normal brain anatomy and an increase in local pressure. The primary brain injury occurs within minutes to hours following the beginning of the bleeding (depending on hematoma growth), mainly due to the mechanical damage caused by the mass effect of the expanding hematoma.^{20,21} There is not much that can be done to treat the primary brain injury during this initial damage. Hemorrhagic volume and hematoma growth are critical factors that influence the ICH outcome and mortality, with some studies suggesting that hypertension may exacerbate hemorrhage expansion and contribute to further brain injury.^{20,21}

Secondary brain injury in ICH is caused by a series of events that lead to neurological deterioration, mainly due to the presence of intraparenchymal blood. There is increasing evidence that many mechanisms contribute to this secondary damage, including the formation of edema, the generation of free radicals, inflammatory responses, and the direct cytotoxic effects of by-products resulting from hematoma degradation (Figure 5).^{20,21}

After ICH, the leakage of blood components, especially erythrocytes and plasma proteins, along with damage-associated molecular patterns (DAMPs) such as extracellular matrix components, nucleic acids, lipid mediators, uric acid and ATP released from necrotic and damaged tissue, creates a highly oxidative,

cytotoxic and inflammatory environment to the adjacent healthy brain cells.²¹ Initially, it was hypothesized that extravasated blood plasma components such as complement proteins, immunoglobulins and coagulation factors, contributed to tissue damage. Within 24 hours following the ICH, red blood cells begin to lyse, releasing cytotoxic hemoglobin (Hb) and its degradation products, heme and iron.²¹ These substances enhance the damage to brain tissue by generating free radicals, namely free iron (Fe^{2+}) that can react with hydrogen peroxide through a Fenton reaction, leading to the formation of hydroxyl radical that causes extensive oxidative damage to proteins, carbohydrates, lipids and nucleic acids.²¹

Thrombin, a serine protease, plays a crucial role in the hemostatic response. It is immediately produced in the brain following ICH and influences various cell types, including endothelial cells, astrocytes, microglia and neurons. Alongside hemoglobin and iron released from the hematoma, thrombin is considered a significant contributor to secondary brain injury.^{19,20} While thrombin is necessary in low concentrations to facilitate hemostasis, at higher levels it can be harmful, leading to apoptosis and early cytotoxic edema. Additionally, thrombin can activate the complement cascade and matrix metalloproteinases (MMPs), leading to increased BBB permeability.¹⁹

The disruption of the BBB is a defining characteristic of brain injury caused by ICH, leading to secondary brain damage.¹⁹ This loss of BBB integrity is further exacerbated by the deficiency of tight junction proteins, such as claudin-5, zonula occludens-1, and occludin, which are crucial for maintaining the barrier's structural integrity.²⁰

Apoptosis plays a significant role in neurological disorders like intracerebral hemorrhage (ICH). It is influenced by factors such as a lack of neurotrophic factor, excessive glutamate receptor activation, and increased oxidative stress.²⁰ ROS are central to this process, leading to the peroxidation of lipids, nucleic acids, and proteins. The combined effects of hydrogen peroxide (H_2O_2) and nitric oxide (NO) can induce neuronal apoptosis through pathways involving p38 MAPK and caspase-3 activation. Furthermore, nitric oxide synthase and peroxynitrite overproduction disrupts mitochondrial function and enhances the expression pro-apoptotic genes, contributing to neuronal cell death.²⁰

Additionally, inflammatory processes significantly affect the pathology of secondary brain damage following hemorrhagic stroke (see Section 1.2.2).^{22,23}

to activate after injury.^{21,23} Microglia can have either a pro-inflammatory M1 phenotype or an anti-inflammatory M2 phenotype.^{22,23} M1 microglia release harmful cytokines like IL-1 β , IL-6 and TNF- α , as well as pro-oxidant enzymes such as inducible nitric oxide synthase (iNOS).²² Conversely, M2 microglia are associated with neuroprotection and tissue regeneration, secreting anti-inflammatory cytokines like IL-10 and neurotrophic factors, exhibiting arginase activity and phagocytizing cell debris.²² The balance between M1 and M2 phenotypes is important in determining whether microglia promote inflammation or help with recovery after brain injury.²²

Within minutes after ICH, microglia quickly react to danger-associated molecular patterns (DAMPs) like nucleic acids, ATP and high mobility group box 1 (HMGB1), which are released from damaged neurons.²² These DAMPs interact with microglial receptors, including Toll-like receptors (TLRs) such as TLR4, initiating a neuroinflammatory cascade. This activation results in the upregulation of pro-inflammatory genes through the nuclear factor- κ B (NF- κ B) signaling pathway.^{22,24} In addition to DAMPs, components present in blood such as thrombin, fibrin, and heme also trigger inflammation through the TLR/NF- κ B pathway, with hemoglobin specifically inducing an inflammatory response by promoting the assembly of TLR2/TLR4 heterodimers. Experimental evidence shows that inhibiting TLR4 reduces brain edema and neurological deficits in ICH.²²

NF- κ B is a ubiquitous transcription factor that targets genes that encode adhesion molecules (like the ones involved in immune cell extravasation), immune receptors, cell surface receptors, cytokines, chemokines, metalloproteinases (like MMP-9), acute phase proteins and inflammatory enzymes.²¹ The secretion of inflammatory cytokines, such as TNF- α and IL-1 β , further amplifies the NF- κ B pathway and perpetuates inflammation.¹⁹ Additionally, by inducing heme-oxygenase activity and increasing iron- and ROS-induced toxicity, NF- κ B may exacerbate local inflammation.¹⁹ Moreover, oxidative stress, through the generation of free radicals that function as signaling molecules, can also enhance NF- κ B activation, thereby intensifying inflammation.²¹

Microglia are also activated by thrombin through the MAPK and proteinase-activated receptor-1 (PAR-1) pathways, leading to an increase in TNF- α production and neuronal death.²²

Besides pro-inflammatory cytokines, activated M1 microglia also release chemokines, and ROS through the action of NADPH oxidase, exacerbating the inflammatory response by recruiting neutrophils through chemokines like CXCL2.²² These cells interact with the adaptive immune system by presenting antigens through major histocompatibility complex class II (MHCII), and CD80 and CD86 expression, enhancing early neuroinflammation and recruiting blood-derived leukocytes, which can worsen neuronal damage in ICH.^{22,24} Despite their role in promoting inflammation, microglia are crucial for hematoma resolution and recovery after ICH. As mentioned before, microglia have an important function in clearing cellular debris and phagocytosing blood components, using scavenger receptors like CD36 or CD91.^{21,22} Once activated, these cells transform into rounded, ameboid, highly phagocytic cells

that help reducing secondary damage and facilitating tissue repair and recovery following ICH.²² Moreover, microglia express the enzyme heme-oxygenase, responsible for the degradation of the oxidative heme, which allows them to clear red blood cells, free hemoglobin, and heme, further decreasing oxidative stress in the brain.^{19,21}

Reactive astrocytes also contribute to neuroinflammation by secreting MMPs, cytokines and iNOS. They also regulate glutamate excitotoxicity and brain inflammation by downregulating the production of microglial inflammatory mediators.¹⁹

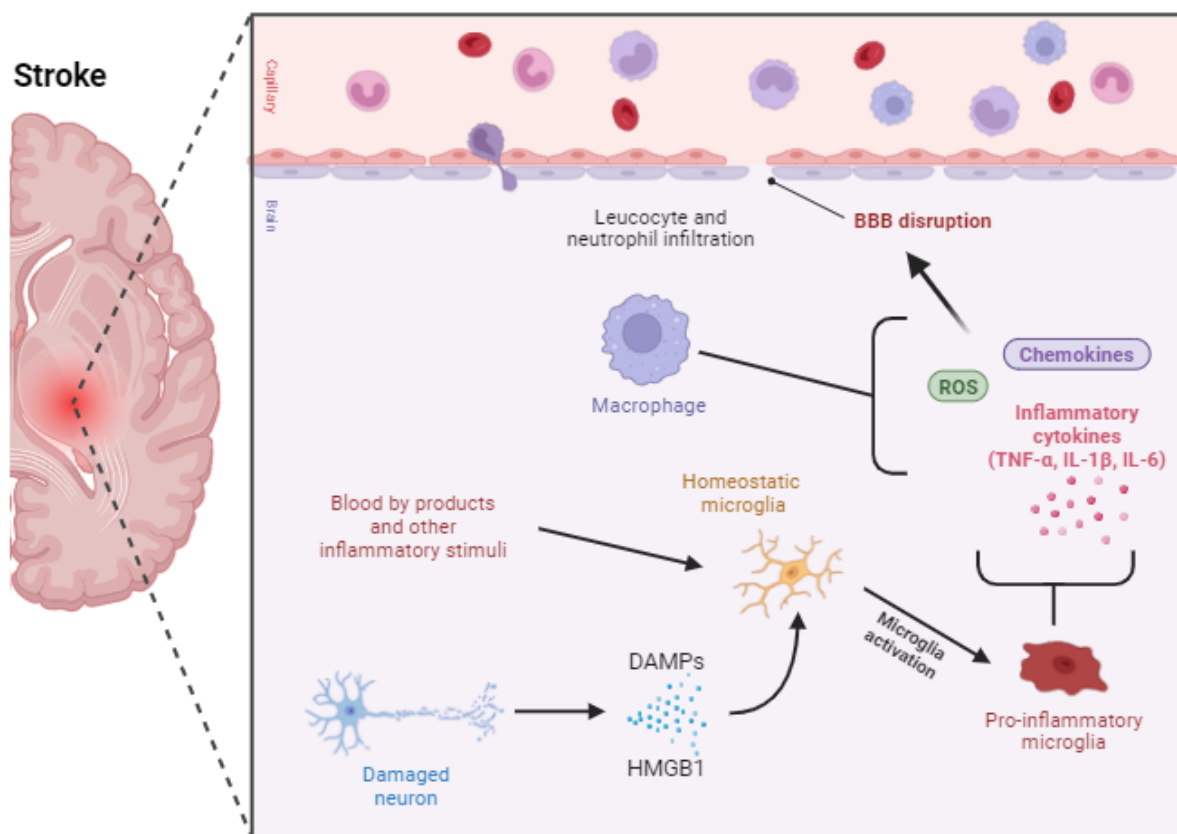


Figure 6 - Schematic representation of microglia-induced neuroinflammation after stroke. The activation of microglia following stroke promotes the release of pro-inflammatory cytokines, reactive oxygen species (ROS), and nitric oxide (NO). The inflammatory response contributes to neuronal injury, blood-brain barrier disruption, and exacerbates the brain's post-stroke damage. (Figure adapted from Alsbroo, Diana L. et al. 2023)

ICH is known to cause delayed BBB dysfunction and increased permeability. A potential explanation for this could be ICH-induced ischemia, where the mass effect of the hematoma increases intracranial pressure and reduces cerebral blood, both of which can increase BBB permeability.¹² However, the precise impact of ischemia in brain injury following ICH remains debated with evidence suggesting that

blood flow around the hematoma may not be significantly reduced. This implies that other factors, such as blood components or inflammation, might directly increase BBB disruption.¹²

Following an ICH, the rupture of red blood cells results in the release of hemoglobin, whose degradation leads to the generation of neurotoxic heme and iron. The release of iron promotes the production of free radicals which can damage endothelial cells and activate signaling pathways that regulate BBB permeability.^{12,25} The accumulation of iron accelerates the production of ROS, causing lipid peroxidation and protein oxidation. This process not only damages pericytes but also disrupts tight junction proteins in the BBB.²⁵ The inflammatory response triggered by the blood components from the hemorrhage further compromises the BBB.¹²

The dysfunction of the BBB is significantly influenced by MMPs, which are endopeptidases involved in the remodeling of the extracellular matrix. MMPs contribute to increased vascular permeability, which contributes to brain edema.¹⁹ Furthermore, increased formation of stress fibers induced by ICH leads to endothelial cell contraction and the formation of intercellular gaps, thereby enhancing even more BBB permeability.²⁰

In summary, experimental evidence suggests that targeting these proinflammatory and prooxidative pathways may help manage ICH and mitigate its harmful effects.

1.2.3. Currently available therapies

Preventing hemorrhagic stroke mostly focuses on modifying risk factors at both the population and individual levels, whereas managing stroke involves treating its underlying mechanisms. Although extensive research has been done in the past twenty years, a simple method for treating all the different causes of stroke has yet to be discovered.¹⁵

Several studies have demonstrated that craniotomy and early hematoma evacuation in individuals with spontaneous ICH may be successful at reducing cerebral pressure, making it a standard therapeutic treatment. However, the efficacy of this approach has been questioned due to different outcomes and the lack of strong evidence supporting long-term benefits.²⁶

Elevated blood pressure is frequently observed following ICH and reducing it has been shown to lower long-term morbidity and mortality. However, the best timing and amount of blood pressure reduction remains debated. Supporters for early intervention suggest that it may reduce risks of hematoma expansion and cerebral edema, while those opposed worry that this intervention could increase secondary brain injury by inducing cerebral ischemia in the tissue surrounding the hematoma.^{19,26}

Intracranial hypertension can result from the accumulation of intracranial content, such as the mass effect from the hematoma or cerebral edema. Increased intracranial pressure is dangerous as it can decrease cerebral perfusion pressure, leading to reduced blood flow and subsequent hypoperfusion. Typical strategies include elevating the head of the bed, administering osmotic agents like mannitol or hypertonic saline, and in more severe cases, considering surgical options like mentioned before.^{19,26}

In patients taking blood-thinning medication, rapid reversal of the anticoagulant's effects is essential to reduce the risk of hematoma expansion. This is done using agents like vitamin K, fresh frozen plasma, or a prothrombin complex concentrate, which contains essential clotting factors II, VII, IX, and X, which restores normal blood coagulation. Additionally, recombinant activated factor VII (rFVIIa) may also be used to stabilize clotting and prevent further bleeding.^{19,26}

In addition to the mechanical brain damage from the expanding hematoma, a promising approach in ICH therapy involves neutralizing the toxic effects of blood in the brain tissue. Cytotoxic hemoglobin and iron released from the lysis of red blood cells trigger oxidative stress and inflammation, contributing to brain injury after ICH (as mentioned in Sections 1.2.1. and 1.2.2.).²⁷ Since these damaging processes occur several days after the initial hemorrhage, therapies targeting blood-derived injury may have a longer window of effectiveness compared to treatments for ischemic stroke.²⁷

1.3. Carbon monoxide (CO)

Carbon monoxide (CO) is commonly known as a poisonous gas when inhaled at higher concentrations.²⁸ Since ancient times, the presence of a noxious fume has been acknowledged during the combustion of carbon-containing materials like coal or wood. In the 18th century, the chemical composition of CO was identified following the recognition that combustion processes produced gas. Only in 1846 Claude Bernard demonstrated CO's harmful effects on the body, showing how it could induce hypoxia by binding to hemoglobin (Hb) and forming carboxyhemoglobin (COHb), displacing oxygen.²⁸ In the 19th century, CO was detected in exhaled human air, which was initially associated to environmental pollution and smoking, but later was recognized as a product of gut microbiome metabolism.²⁸ Later, in the early 20th century, evidence emerged supporting the endogenous presence of CO in human blood, resulting in the demonstration of endogenous CO formation from hemoglobin catabolism in 1949, taking around two more decades for the identification of the heme-oxygenase (HO) enzyme.^{28,29}

The initial and rate-limiting stage in the oxidative degradation of heme is catalyzed by HO (encoded by HMOX genes). Heme cleavage leads to the release of heme iron (Fe^{2+}) and the production of CO and

biliverdin which is then converted to bilirubin by an NADPH-dependent reductase (represented in Figure 7).^{29,30}

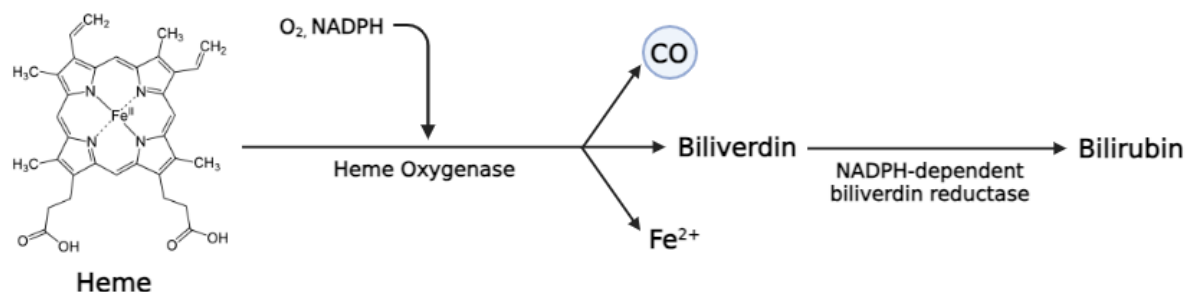


Figure 7 – Process of oxidative heme degradation by heme-oxygenase. The enzyme catalyzes the conversion of heme into biliverdin, carbon monoxide (CO), and free iron.

HO has two main isoforms, HO-1 and HO-2, which are inducible and constitutive respectively. HO-1 is an inducible heat shock protein (HSP32) that responds to various stress-related factors such as inflammation, ROS, injury, ischemia, hypoxia and hypothermia.²⁸ The common characteristic among many of these stressors in their ability to generate ROS, indicating that HO-1 has strong cytoprotective effects on the cells. On the other hand, HO-2 is constitutively expressed in certain tissues like the brain, testes, and gastrointestinal tract. As a result, cells that express HO-2 produce CO consistently, while HO-1 driven CO production is variable depending on environmental stimuli.^{28,31}

Endogenously produced CO primarily binds to Hb and is mostly expelled through exhalation, while a small portion of around 10-15% binds to other hemoproteins in extravascular tissues. Less than 1% of CO remains dissolved in bodily fluids and an additional small percentage is oxidized to CO₂ by cytochrome c oxidase before being eliminated from the body.³²

1.3.1. Biological role of carbon monoxide

CO was initially considered to be only a by-product of heme metabolism, but the recognition of NO as a gaseous messenger in the body instead of a toxic gas, changed the view about CO. Extensive research over the last two decades has highlighted CO's homeostatic and protective properties. Although CO is traditionally viewed as a silent killer, experimental data have revealed that small and controlled doses of CO gas have shown unexpected physiological benefits (Figure 8), including modulation of vascular tone³³, blood pressure regulation³⁴, control of cell proliferation^{35,36}, anti-inflammatory^{37,38}, anti-apoptotic^{39,40} and antioxidant properties⁴¹, and cytoprotection against tissue injury.⁴² So far, an

increasing number of studies also suggests that HO-derived CO may function as a signaling molecule in the brain and CNS, acting as a neurotransmitter in a variety of neurological processes.³⁰

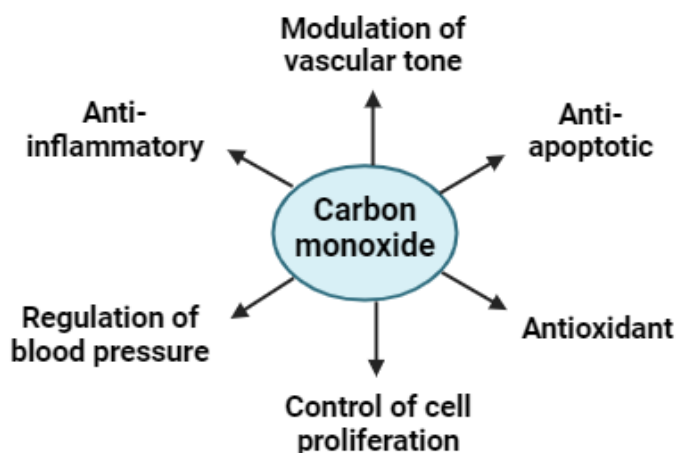


Figure 8 - Summary of carbon monoxide's key physiological functions involved in the modulation of oxidative stress, neuronal survival, and blood-brain barrier integrity.

CO's functional activity is mainly related to its high affinity for transition metals, particularly iron, which is the most abundant transition metal in cells; as a result, CO mainly targets iron-containing heme proteins like Hb. In biological systems CO is described to only bind to reduced iron Fe^{2+} , limiting the number of heme proteins to which CO can target.⁴³ These heme-containing proteins are essential for various cellular processes, including oxygen transport, mitochondrial respiration and cellular signaling pathways. In vitro studies indicate that CO can interfere with the activity of these enzymes, suggesting that its biological effects in vivo may be mediated through binding to these enzymes.³⁰

Currently known physiological signaling effects of CO involve a small number of well-defined pathways. CO modulates cellular functions primarily by activating soluble guanylate cyclase (sGC) through direct binding to its heme iron. This activation leads to an increase in cyclic guanosine monophosphate (cGMP) levels, which in turn activates protein kinase G (PKG). PKG mediates various downstream effects, such as vasodilation and regulation of anti-inflammatory and antiproliferative responses, impacting overall cellular homeostasis.^{30,44}

CO signaling involves additional mechanisms besides the activation of the sGC/cGMP pathway. Another mechanism involves the modulation of MAPK activation, which may be connected to the cGMP pathway, depending on the model. While MAPKs do not directly bind to CO, they act as downstream targets in CO signaling, with CO downregulating proinflammatory cytokine production via p38 MAPK-dependent pathways, resulting in anti-inflammatory and tissue-protective effects.^{30,43,44}

Additionally, CO can influence Ca^{2+} -dependent K^+ channel activity, which affects cellular excitability, neurotransmitter release, and many other cellular functions.^{30,43,44}

Many hypothesized functions of CO as a neural messenger are associated to its role in activating the brain's sGC/cGMP pathway.³⁰ It has also been demonstrated that CO can dilate cerebral arteries and arterioles by activating large-conductance Ca^{2+} -activated K^+ channels in smooth muscle cells through a mechanism independent of sGC activation, promoting a healthy brain vascular system.⁴⁵

In the context of vasodilation, research indicates that both exogenous and endogenous (HO-derived) CO can enhance cGMP levels in vascular smooth muscle cells.^{46,47} In studies involving rat-tail artery smooth muscle cells, CO induced hyperpolarization by increasing outward K^+ currents, which inhibited voltage-gated Ca^{2+} channels, resulting in relaxation of the smooth muscle.⁴⁸ Under certain conditions, CO can also bind to and activate NOS, promoting NO production. This suggests that CO has a regulatory role in vascular tone through the modulation of NO generation.⁴⁹

Addressing its other properties, many other mechanisms have been described. As for its anti-apoptotic effects, low dose CO pre-treatment in various models of disease and/or tissue injury, such as ischemia/reperfusion injury, demonstrates a net anti-apoptotic effect in vivo. In endothelial cells, CO appears to inhibit TNF- α induced apoptosis, likely through the p38 MAPK pathway.⁵⁰ Furthermore, both HO-1 and CO have been shown to interact with NF- κ B-dependent anti-apoptotic genes, providing protection against TNF- α -mediated apoptosis in endothelial cell.³⁰ CO's anti-apoptotic effects also extend to other cell types, including neurons^{51,52} and astrocytes^{53,54}, where it can act through various mechanisms.

Regarding CO's anti-inflammatory properties, it has been demonstrated that CO can modulate and limit neuroinflammation in microglia. This is achieved by inhibiting the release of inflammatory mediators, including nitrites and pro-inflammatory cytokines such as TNF- α and IL-1 β , while simultaneously promoting the production of anti-inflammatory cytokines like IL-10. CO seems to influence multiple pathways involved in the cellular inflammatory response, ranging from direct enzymatic inhibition to interactions with MAPK pathways. However, additional research is needed to understand the exact mechanisms through which CO transduces these signals.^{55,56}

CO can also bind to the ferrous heme group of cytochrome c oxidase (complex IV), the final electron acceptor of the mitochondrial respiratory chain, instead of oxygen, thus inhibiting its activity. In fact, high concentrations of CO lead to cytotoxicity by inhibiting mitochondrial respiration.⁵⁷ Nevertheless, when this inhibition occurs with low levels of CO, it can become an important regulator of mitochondrial respiration. It can cause a partial uncoupling of the electron transport chain, leading to altered electron flow and increased production of ROS. These CO-induced low levels of mitochondrial ROS serve as signaling molecules that influence various cellular processes, including the regulation of the balance

between glycolysis and oxidative phosphorylation, mitochondrial biogenesis stimulation and the modulation of the pentose phosphate pathway.⁵⁷

Since so many beneficial properties of CO have been discovered so far, there is a lot of active clinical study and scientific research being done on the therapeutic potential of administering low doses of CO.

1.3.2. CO-releasing molecules

As already mentioned, many biological functions of CO have been identified, which has led to significant efforts to make use of its benefits for human health.⁵⁸ Administering low concentrations of CO can be achieved through inhalation. However, this method presents many complications due to the gas's lack of tissue specificity and toxicity. To address these issues, researchers have focused on developing pro-drugs able to deliver CO, commonly known as CO-releasing molecules (CORMs).⁵⁸ These CORMs, which are often based on transition metal carbonyl complexes or organic compounds, are capable of delivering CO in a more controlled and targeted manner, significantly reducing systemic toxicity associated with COHb formation. CORMs have demonstrated the capacity to mimic the effects of CO gas, such as inducing vasodilation, preventing organ rejection after transplantation, and also exhibiting anti-inflammatory, anticoagulant, anti-apoptotic and anti-bacterial properties. This targeted and controlled CO delivery promotes therapeutic efficacy and extends our understanding of CO's biological mechanisms.⁵⁸



Figure 9 - The most studied CO-Releasing Molecules (CORMs). Schematic diagram with the chemical structures of three of the most studied CORMs: CO-RM2, CO-RM3, and CO-RMA1. These CORMs are designed to deliver controlled doses of CO for therapeutic purposes. (Figure adapted from Rochette, Luc et al. 2013).

1.4. Hemoglobin and red blood cells

1.4.1. Red blood cells

Mature red blood cells (RBCs) or erythrocytes are produced in the bone marrow and circulate through the bloodstream with a life span of around 120 days.⁵⁹ These cells consist of a plasma membrane that encloses a viscous concentrated solution of proteins. Because of the lack of cytoplasmic organelles and the absence of a nucleus, these cells can undergo significant shape changes to pass through narrow capillaries, with the purpose of transporting oxygen from the lungs to various cells, tissues and organs throughout the body while also facilitating the return of carbon dioxide to the lungs.⁵⁹ This important biological function is mainly performed by hemoglobin (Hb), which constitutes more than 98% of the total protein content within RBCs.⁵⁹ To guarantee proper tissue oxygenation, it is essential to maintain an adequate levels of Hb in the bloodstream. With a concentration of 150 g/L in the blood, an adult human normally contains around 1 kg of Hb.^{43,60}

1.4.2. Hemoglobin function

Hemoglobin (Hb) is a highly conserved protein present in the RBCs of almost all vertebrates, with approximately 64.5 kDa, and is composed of four globular protein subunits: two alpha (α) and two beta (β) polypeptide chains.^{59,60} Each subunit incorporates one prosthetic heme group which consists of a protoporphyrin IX molecule bound to a reduced ferrous ion (Fe^{2+}) that is capable of binding one molecule of oxygen (O_2). As a result, the Hb tetramer can bind up to four O_2 molecules. This ability is facilitated by the combination of the two α - β dimers, which promotes the essential "heme-heme" interaction, crucial for effective oxygen uptake and distribution.^{43,59,60}

As mentioned above, the main function of Hb is to bind and transport O_2 to tissues in the organism, sustaining the cellular energy need and maintaining homeostasis.⁴³ However, Hb can also bind to other gaseous molecules, including carbon dioxide (CO_2), nitric oxide (NO), hydrogen sulfide (H_2S) and carbon monoxide (CO).^{43,61}

CO_2 is a metabolic by-product of oxidative metabolism (also known as respiration) produced during the citric acid cycle.⁶² While most CO_2 exits cells mainly through passive diffusion across the membrane, certain CO_2 channels can facilitate its transport. Once outside the cell, this gas not only participates in the maintaining of blood's buffering system, but also acts as a physiologic regulator in several cellular signaling pathways, influencing tissue homeostasis and modulating immune responses by reducing inflammation and innate immune activation.^{43,62}

Carbonic anhydrase is an essential component of the blood's buffering mechanisms, catalyzing the hydration of CO₂ to produce carbonic acid (H₂CO₃). This carbonic acid is then transported to the lungs, where carbonic anhydrase facilitates its dissociation into bicarbonate (HCO₃⁻) and H⁺, allowing CO₂ to be released and exhaled.⁶³ Any residual CO₂ in tissues is bound by Hb and transported to the lungs for exhalation. When CO₂ levels increase or pH decreases (indicating higher CO₂ tension), Hb's affinity for oxygen decreases while its affinity for CO₂ increases, facilitating the delivery of O₂ to tissues. Therefore, CO₂ acts as an allosteric modulator that regulates Hb-O₂ affinity, a process for O₂ delivery in the tissues and CO₂ uptake and elimination. Besides that, since CO₂ also as a signaling function, its binding to Hb indirectly regulates these physiological processes.^{43,63}

NO is a well-recognized gasotransmitter and plays an important role as a signaling molecule, mostly known for its function as endothelial-derived relaxing factor.⁴³ NO can be synthesized by many types of mammalian cells primarily through enzymatic and non-enzymatic processes. The production of NO through enzymatic mechanisms involves nitric oxide synthase (NOS), while its non-enzymatic generation mainly occurs through the reduction of nitrites.⁴³ NO signaling is essential for maintaining vascular homeostasis by modulating vascular tone, preventing blood clot formation, and regulating endothelial adhesion molecule expression. Additionally, it plays a key role in protein modification processes, skeletal muscle contraction, CNS signaling, inflammation regulation and enhancing immune defense against infections.⁴³

Red blood cells (RBCs) influence the bioactivity of NO released from cells by quickly capturing this gas through binding to Hb. In this way, Hb serves as a regulator of NO's activity. Within RBCs, NO exhibits distinct reactions with oxyHb-Fe²⁺ and deoxyHb-Fe²⁺.^{43,63,64} NO can have different roles, acting as either a signaling molecule or a toxin, depending on whether it generates ROS through interactions with heme (ferrous iron) or hemin (ferric iron). This dual nature is advantageous for eliminating microbes but may also harm proteins, DNA, and lipids.⁴³ On the other hand, Hb can act as a nitric oxide dioxygenase (NOD), converting NO and O₂ into nitrates and thus decreasing NO's potential as a source of ROS. This capacity of Hb is very important for maintaining continuous energy supply essential for cellular bioenergetics and homeostasis, and for minimizing cell damage. However, it also suggests that NO's function as a signaling molecule may be impaired, which could lead to decreased blood flow.⁴³

Similar to NO and CO, H₂S is an essential gasotransmitter and signaling molecule, continuously synthesized by a variety of enzymes including 3-mercaptopyruvate sulfurtransferase, cystathionine γ -lyase, and cystathionine β -synthase.⁶¹ At low concentrations (from nanomolar to micromolar) H₂S is involved in multiple physiological roles, such as cytoprotection, metabolic suppression, and the modulation of vasodilation and vasoconstriction. However, at higher concentrations, H₂S can become highly toxic.⁶¹

H₂S rapidly associates with MetHb, resulting in the formation of a MetHb-sulfide complex, where the H₂S molecule binds to the ferric heme. However, this complex is short-lived, maintaining stability for

only a few minutes. Eventually, MetHb is reduced back to its functional form, Hb (Hb-Fe²⁺), through a process known as reductive sulfhydrylation, which also results in the production of polysulfides and thiosulfates. Although the exact mechanism is not yet fully understood, evidence suggests that MetHb may have a physiological role in the transport and metabolism of H₂S.⁶¹

As mentioned in Section 1.3.1., CO acts as both a signaling molecule and a gasotransmitter, showing properties such as antioxidant, anti-inflammatory, and anti-apoptotic effects, while also contributing to the regulation of vascular tone. While NO may bind to both ferrous and ferric hemes, CO selectively binds to reduced (ferrous) iron centers. Upon binding to the reduced iron-heme in hemoglobin, CO forms carboxyhemoglobin (COHb) with an affinity 210 to 250 times greater than that of O₂.⁴³ However, the precise physiological role of COHb and its potential protective effects, particularly under pathological conditions, remain unclear.

1.4.3. Hemoglobin and red blood cells' antioxidant defenses

As noted in Section 1.4.1., RBCs are characterized by the absence of nuclei and most cellular organelles, which optimizes their capacity for O₂ transport by containing a high concentration of Hb (~98% of total protein).⁵⁹

RBCs must present a robust antioxidant machinery since their high O₂ tension along with reduced iron of Hb are factors involved in the generation of a strong pro-oxidant environment within RBCs.⁶⁵ During O₂ transport by RBCs, Hb's heme iron must remain in its reduced Fe²⁺ state to bind O₂ effectively. However, this reduced iron is susceptible to oxidation and, through a slow autooxidation reaction, this Fe²⁺ iron is gradually oxidized to Fe³⁺ MetHb, producing superoxide (O₂⁻) as a byproduct.⁶⁵ Even though this reaction occurs slowly under normal oxygen conditions, it is significantly accelerated in hypoxic conditions, such as those in microcirculation, leading to increased amounts of produced superoxide. Both superoxide and H₂O₂ are highly reactive that can interact with Hb and other cellular components, exacerbating oxidative stress.^{43,65}

Although MetHb is incapable of binding O₂, RBCs use MetHb reductase to convert it back to functional Fe²⁺ Hb. Any remaining MetHb can release free heme, which interacts with the RBC membrane disrupting skeletal proteins and inducing lipid peroxidation.^{43,65}

Besides the autooxidation reaction, RBCs are also exposed to extracellular oxidants and reactive nitrogen species (RNS), such as NO, produced by nitric oxide synthase (NOS), and nitrite (NO₂⁻). These reactive species can also interact with Hb and contribute to nitrosative stress. In the RBCs, NO can rapidly react with oxygenated Hb-Fe²⁺, undergoing oxidation by using O₂ to transform into nitrate (NO₃⁻

) and forming MetHb (Fe^{3+}), which is subsequently recycled by reductase enzymes.⁶⁵ Conversely, when NO reacts with deoxygenated Hb (Fe^{2+}), a reductive reaction occurs where NO can either bind to the heme, forming deoxyHb- Fe^{2+} NO (iron nitrosyl Hb), or act as a nitrite reductase converting nitrite into NO.^{43,63,64} Although these reactions occur rapidly, any superoxide generated from the autoxidation of oxyHb reacts even more quickly with NO than with Hb, resulting in the formation of peroxynitrite. This highly reactive species is also formed in the interstitial spaces of the endothelium and can diffuse into RBCs, causing cellular damage.^{43,65}

H_2O_2 plays a major role in initiating a cascade of oxidative reactions within RBCs. It reacts with Hb- Fe^{2+} to produce MetHb (Fe^{3+}) and with oxidized Hb- Fe^{3+} to form ferrylHb (Fe^{4+}).^{43,65} The ferryl form of Hb can lead to further ROS generation, protein radical formation, and heme degradation, releasing iron and producing heme degradation products. The accumulation of these heme degradation products and iron on the RBC membrane is associated with RBC cellular aging and the binding of autologous IgG, which may indicate the expression of senescent antigens on the cell surface.^{43,65}

Figure 10 illustrates the various redox states of Hb and its interactions with NO, CO and H_2O_2 .

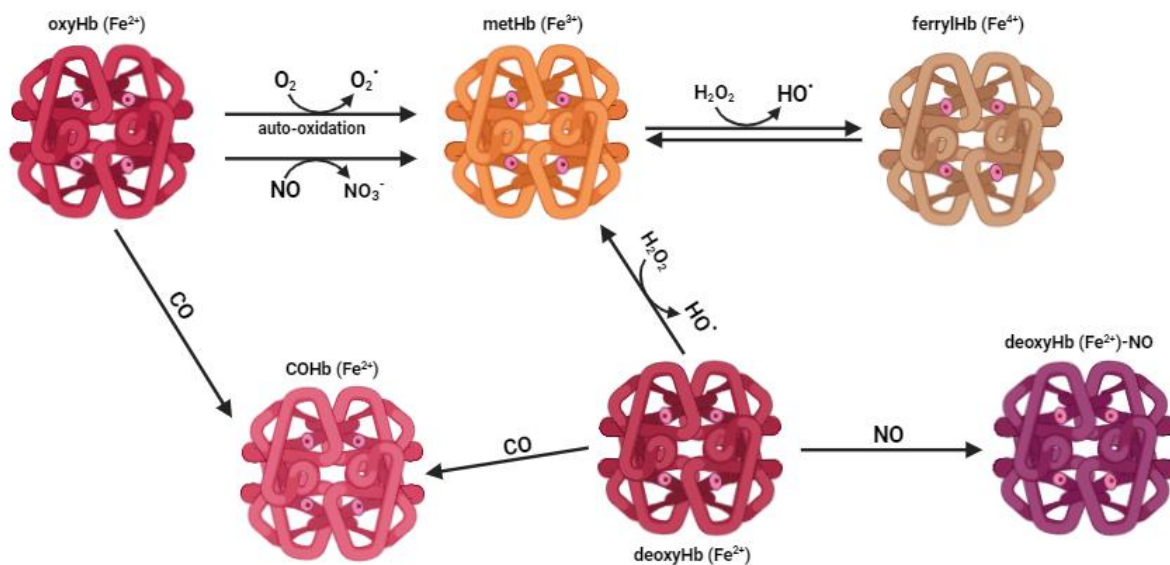


Figure 10 - Hemoglobin redox states: oxyhemoglobin (oxyHb), methemoglobin (MetHb), carboxyhemoglobin (COHb), ferrylhemoglobin (ferrylHb), deoxyhemoglobin (deoxyHb) and nitrosyl-hemoglobin (deoxyHb-NO). (Figure adapted from Carrola, André et al. 2023)

In order to minimize the toxic effects associated with these redox reactions, RBCs have a robust antioxidant defense system that preserves Hb in its functional reduced Fe^{2+} state. This antioxidant machinery includes enzymes such as superoxide dismutase (SOD1), catalase (CAT), glutathione peroxidase (GPx), and peroxiredoxin-2 (PRDX2), which effectively neutralize and detoxify reactive

oxygen and nitrogen species.⁶⁵ In addition to these enzymes, the presence of high concentrations of non-enzymatic antioxidants, including ascorbic acid (AA) and reduced glutathione (GSH), also contribute to minimize oxidative stress (Figure 11).⁶⁵

SOD1 converts the superoxide anion into O_2 and H_2O_2 . Catalase is then responsible for detoxifying H_2O_2 by breaking it down into water and O_2 . GPx also plays an important role in protecting RBCs from oxidative stress by reducing H_2O_2 and organic hydroperoxides to water and alcohols, using GSH as a reducing agent. This process is vital for maintaining cellular redox balance and the balance between reduced (GSH) and oxidized (GSSG) glutathione, as GPx ensures the efficient removal of H_2O_2 , even at low concentrations, by oxidizing GSH to its oxidized form, GSSG.^{65,66} PRDX2, is another enzyme capable of reducing H_2O_2 and organic hydroperoxides to water and alcohols. Peroxiredoxins are a family of thiol-containing enzymes that act as scavengers for H_2O_2 and peroxynitrite in the bloodstream, with PRDX2 being present in high concentrations in RBCs. The catalytic cycle of PRDX2 involves the reduction of oxidized peroxiredoxin by thioredoxin (Trx), which, in turn, is reduced by NADPH via the NADPH-thioredoxin reductase system.^{65,66}

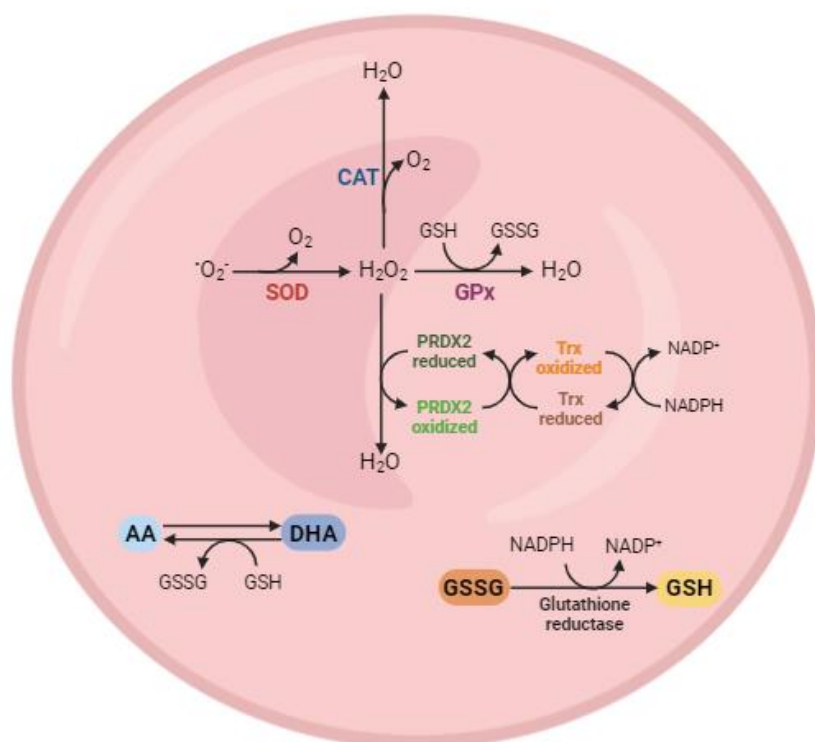


Figure 11 - Schematic representation of the antioxidant defense mechanisms within red blood cells. The antioxidant machinery includes enzymes like superoxide dismutase (SOD), catalase (CAT), glutathione peroxidase (GPx) and peroxiredoxin-2 (PRDX2) in converting harmful ROS like superoxide ($\cdot O_2^-$) and hydrogen peroxide (H_2O_2) into less harmful molecules such as water (H_2O) and molecular oxygen (O_2). Oxidized PRDX2 is reduced by thioredoxin (Trx), which is itself regenerated by thioredoxin reductase (TrxR) using NADPH. Ascorbate donates electrons to neutralize reactive species, becoming DHA in the process. DHA can then be reduced back to

AA, a process facilitated by glutathione (GSH). In this reaction, GSH is oxidized to glutathione disulfide (GSSG). GSSG is subsequently reduced back to GSH by glutathione reductase, using NADPH as a reducing agent.

Alongside these enzymes, MetHb reductase is responsible for reducing oxidized MetHb back into its functional form. In vivo, this reduction mostly occurs through the NADH-cytochrome b5-MetHb reductase system, which requires NADH and cytochrome b5 as cofactors. Other minor pathways, such as the NADPH-dependent MetHb reductase, and direct reduction by intracellular antioxidants like AA and GSH, also contribute to this process.⁶⁶

In both its reduced and oxidized forms, glutathione participates in redox reactions by reversibly oxidizing its active thiol group, allowing it to directly scavenge free radicals or serve as a substrate for GPx and glutathione-S-transferase (GST) during the detoxification of H₂O₂, lipid hydroperoxides, and electrophilic compounds.⁶⁶

In the RBCs the primary source of NADPH needed to reduce GSSG back to GSH is the pentose phosphate pathway (PPP), particularly its oxidative branch.⁶⁷ Some studies indicate that during oxidative stress induced by tert-butylhydroperoxide (tBHP) treatment, the reduction of MetHb to Hb-Fe²⁺ is supported not by increased PPP activity but rather by glycolysis and NADH generation. This results in enhanced glucose metabolism via glycolysis, leading to greater production of pyruvate and NADH, particularly through the activity of glyceraldehyde-3-phosphate dehydrogenase.⁶⁸ In this way, glucose metabolism may have an antioxidant role in RBCs through various pathways.

AA primarily functions to neutralize superoxide, being oxidized to its radical form and then to dehydroascorbic acid (DHA). Additionally, AA scavenges other ROS generated by protein-bound redox metals. In RBCs, DHA is transported through GLUT-type glucose transporters and is reduced back to AA by GSH, further contributing to the cell's antioxidant defense system.^{67,69}

The β93 cysteine (β93Cys) residue in hemoglobin is highly conserved and thought to contribute to the RBC's antioxidant defenses. While its absence does not affect other antioxidant enzymes in RBCs, studies have shown that β93Cys plays a key role in neutralizing reactive species like hydrogen peroxide and chloramines, especially during oxidative stress and inflammation. This suggests that β93Cys enhances hemoglobin's ability to protect RBCs under stressful conditions.⁷⁰

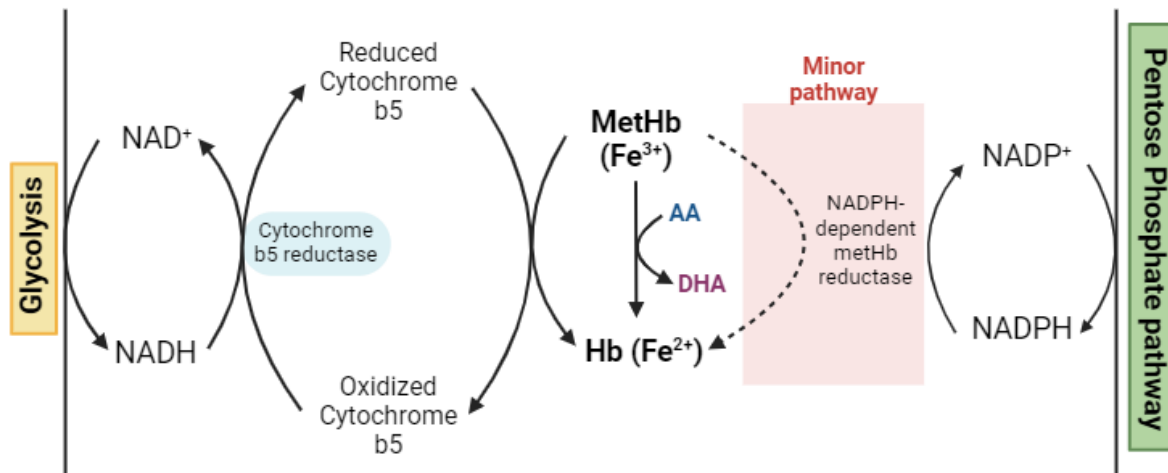


Figure 12 - Schematic illustration of the pathways involved in the reduction of MetHb (Fe^{3+}) to Hb (Fe^{2+}). The major pathway uses NADH, produced in glycolysis, to reduce MetHb via cytochrome b5 reductase and cytochrome b5. The minor pathway involves NADPH, generated in the pentose phosphate pathway (PPP), and NADPH-dependent methemoglobin reductase. Ascorbic acid (AA) and its oxidized form dehydroascorbate (DHA) also contribute to MetHb reduction.

1.4.4. Cell-free hemoglobin

RBCs lack both a nucleus and mitochondria, so damage mostly affects their cell membranes, leading to rupture and Hb release, both inside and outside the vascular system. Under normal physiologic conditions, RBCs live about 100 to 120 days before being removed from circulation by the reticuloendothelial system, particularly in the spleen and bone marrow.^{43,71} Efficient enzymatic defenses within RBCs protect Hb from exposure to the extracellular environment, keeping extracellular Hb levels low (see Section 1.4.3). The concentration of extracellular Hb in circulation remains minimal and is tightly regulated by specific plasma and cellular binding proteins (like haptoglobin) and receptors (such as CD163).^{71,72} However, during pathological conditions such as trauma, blood transfusions, infections, inflammation, or hemolytic diseases such as sickle cell anemia, excess cell-free Hb and heme become toxic, causing oxidative damage in blood vessels and tissues.^{43,71,72}

Within RBCs, Hb exists as a tetramer with iron in its reduced (Fe^{2+}) state, maintained by the cell's antioxidant environment. However, after hemolysis, Hb alternates between tetramers and smaller $\alpha\beta$ heterodimers, with a dimer state predominating at low Hb concentrations in plasma. These dimers can easily penetrate across tissue barriers like the vascular endothelium, renal glomeruli, and the ependymal epithelium, leading to toxic accumulation of Hb and its by-products near vital tissues.⁷² Additionally, when extracellular Hb reacts with NO, similar to its behavior inside RBCs, it oxidizes to MetHb (Fe^{3+}),

releasing heme which is highly cytotoxic and exacerbates tissue damage. Heme also plays a role in immune dysregulation and disrupts cell structures such as the proteasome and cytoskeleton. By binding to toll-like receptor 4 (TLR4), heme triggers inflammatory NF- κ B signaling, as seen in sickle cell anemia murine models.^{72,73} Besides that, cell-free Hb acts as a scavenger for NO produced by endothelial cells, promoting vasoconstriction and hypertension.⁷² It has also been shown that MetHb can be converted into Hb-Fe²⁺, continuing to scavenge NO and causing further vasoconstriction.⁷⁴

During inflammation, cell-free Hb can react with ROS like H₂O₂, forming MetHb and ferrylHb (Hb-Fe⁴⁺), an unstable oxidized Hb form. FerrylHb induces inflammation and increases vascular endothelial cell permeability, altering actin cytoskeleton and upregulating proinflammatory gene expression.⁷⁵ Additionally, Hb-derived free heme and its degradation products can damage endothelial and vascular smooth muscle cells, acting as proinflammatory mediators through inflammatory cell recruitment and by promoting chemokine expression (like IL-8).⁷⁶ Free heme can also oxidize low-density lipoproteins (LDL) and other lipids, converting them into proinflammatory and cytotoxic species, promoting vessel injury through oxidative stress and inflammation.⁷⁶

It has also been shown that HO-1 expression is increased by heme, heavy metals, lipopolysaccharide, and other stimuli. In the brain, HO-1 is induced in conditions like intracerebral (ICH) and subarachnoid hemorrhage (SAH) and other neurodegenerative diseases. While its up-regulation typically has neuroprotective effects, excessive HO-1 activity due to high heme exposure can result in toxicity caused by the iron (product of HO-1 reaction) and serve as a marker of oxidative stress.^{25,77}

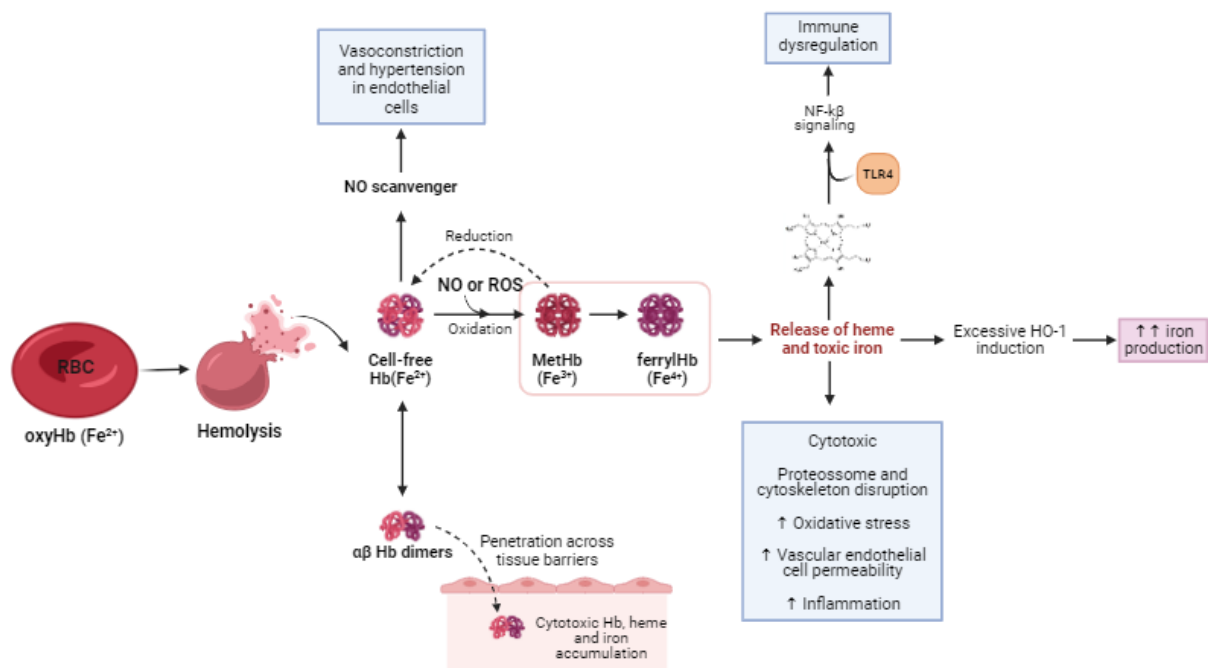


Figure 13 - Schematic representation of the pathways activated by extracellular hemoglobin, released following hemolysis or tissue damage. Oxyhemoglobin (oxyHb (Fe^{2+})) is released into circulation after RBC rupture and rapidly oxidizes into methemoglobin (MetHb (Fe^{3+})) via NO or ROS like H_2O_2 . MetHb can further oxidize to the more toxic ferryl hemoglobin (ferrylHb (Fe^{4+})). The main effects include vasoconstriction and hypertension due to NO scavenging by cell-free reduced Hb, penetration of Hb dimers across tissue barriers, and the release of cytotoxic heme and iron from Hb oxidized forms. This induces oxidative stress, endothelial permeability, and inflammation, activating TLR4 and NF- κ B signaling pathways, which contribute to immune dysregulation. Additionally, excessive induction of HO-1 results in increased iron production, further exacerbating oxidative stress and vascular damage.

In the CNS, Hb is very neurotoxic, causing neuronal cell death and triggering neuroinflammation through the activation of microglia and the release of proinflammatory cytokine release.^{78,79} Elevated levels of MetHb in cerebrospinal fluid after preterm brain hemorrhage has been associated with increased neuroinflammation and higher levels of inflammatory markers.⁸⁰ In several studies with animal models, injecting Hb into the brain has shown BBB leakage, with mechanisms involving NO synthase activity and subsequent NO production, peroxynitrite formation, and MMP-9 activation, further increasing permeability.⁸¹⁻⁸³

In ICH and SAH, Hb released from ruptured RBCs in the CNS induce oxidative stress, inflammation, and BBB disruption by altering tight junction proteins, activating astrocytes, and promoting lipid peroxidation and apoptosis, ultimately increasing BBB permeability.^{12,77,84} These processes illustrate the variety of damaging impacts that cell-free Hb and heme can have on both cellular and organ systems.

1.5. Carboxyhemoglobin (COHb)

CO has a strong affinity for binding to various ferrous heme-containing proteins, especially Hb. CO reversibly binds to Hb with an affinity estimated to be 210-250 times greater than that of O_2 , resulting in the formation of COHb. Because of this high affinity, CO competes with O_2 for the four available binding sites on Hb. Partial occupation of CO at these sites not only reduces the number of sites available for O_2 binding but also inhibits the release of already bound O_2 from the Hb. Consequently, the presence of COHb in the blood decreases the blood's capacity to transport and deliver O_2 effectively.^{30,43}

Under normal physiological conditions, in the absence of significant external CO exposure, most COHb in the blood is generated endogenously through the catabolism of free heme by the enzyme heme-oxygenase (HO), which produces CO as a byproduct. Other hemoproteins, including myoglobin, cytochromes, and peroxidases also contribute to binding about 20-25% of the total quantity of endogenous CO.^{32,85}

The human body is estimated to produce approximately 18.8 μmol of CO *per* hour (0.42 mL per hour), resulting in a total of around 400-500 μmol (12.6 mg) *per* day. This leads to a normal physiological COHb level of about 1–2%, corresponding to 75–150 μM , which is considered to be within the physiological range.³² However, COHb concentrations in blood can rise in response to increased environmental CO exposure or under certain pathological condition that elevate the expression of HO-1 and subsequent CO production.³⁰ Despite its presence, the specific biological role of COHb under normal conditions and its potential protective functions in disease states remain unknown.

1.5.1. COHb does not indicate CO toxicity

The toxicity of CO is likely caused by a combination of factors, including total CO intake, tissue concentrations, the rate at which CO binds to Hb and other hemoproteins, and the specific binding mode of CO with Hb. While CO poisoning is commonly associated with CO binding to Hb (leading to the formation of COHb and reducing oxygen delivery), its cytotoxic effects are more closely related to its binding with hemoproteins like cytochrome c oxidase. This interaction disrupts mitochondrial respiration, resulting in impaired ATP synthesis and oxidative stress, contributing to the toxic effects of CO.^{32,86}

COHb levels are frequently measured in individuals suspected of CO poisoning, with concentrations above 50% typically associated with fatal outcomes. However, the range of COHb concentrations associated with lethal CO poisoning can vary significantly. Severe cases normally present COHb levels exceeding 50%, but some studies have reported fatal outcomes with COHb levels as low as 30% to 40%. This can be due to a number of factors, such as an individual's age, underlying health conditions like coronary artery disease or respiratory insufficiency, and the increased vulnerability of infants and the elderly.^{87–90} On the other hand, the highest reported COHb level in a surviving individual is 73%.⁹⁰ This emphasizes the idea that the clinical presentation or symptoms of CO poisoning do not accurately correlate with the COHb level. Since it has not been demonstrated that the COHb molecule itself has inherent harmful effects, it should only be viewed as a marker of CO exposure instead of a measure of CO toxicity.^{32,90}

In an important *in vivo* experiment by Goldbaum, dogs were exposed to 13% of CO gas by inhalation, leading to COHb levels of 54 to 90%, with all animals dying within 1 hour. Interestingly, a separate group of dogs that received a transfusion of CO-loaded blood, which achieved 80% COHb levels, survived. These results suggest that COHb levels are not reliable predictors of systemic CO toxicity. Additionally, these findings further support the fact that CO toxicity may result from free CO rather than CO bound to Hb.⁹¹

The study above also shows that the impact of CO toxicity varies based on the route of administration due to the way Hb binds with CO. The binding of CO to Hb results in the formation of various forms of COHb complexes ($\text{Hb}_4(\text{O}_2)_4$, $\text{Hb}_4(\text{O}_2)_3(\text{CO})$, $\text{Hb}_4(\text{O}_2)_2(\text{CO})_2$, $\text{Hb}_4(\text{O}_2)(\text{CO})_3$, and $\text{Hb}_4(\text{CO})_4$), with different association constants for each step of the binding. At the same level of COHb%, variations in the composition of these four forms can make a significant difference in terms of toxicity.³²

When COHb levels reach 50% through inhalation, it results in more than just a 50% decrease in the capacity of Hb to carry O_2 . In one way, 50% COHb levels might mean that nearly all Hb molecules carry at least one CO molecule, which would significantly reduce the amount of O_2 carried and also its release to tissues. On the contrary, the experimental determination of 50% COHb may mean that 50% of the total Hb is completely occupied by CO, while the rest remains free, which would mimic anemia rather than acute CO poisoning. In the dog experiments mentioned above, the administration of CO-saturated Hb to reach 60% COHb produced symptoms similar to anemia, indicating a less severe impact on O_2 delivery. However, inhaling CO to achieve the same COHb level would likely result in most Hb molecules binding to CO, impairing O_2 delivery and leading to hypoxia. So, reaching 50% COHb through non-inhalation methods, such as administering CO-saturated Hb, may result in a different distribution of COHb complexes.^{32,91}

This distinction shows why the route of CO administration significantly influences its toxicity. Consequently, the levels of COHb considered dangerous by inhalation may not represent the same risks when CO is administered by other routes.³²

In a 2021 study, Mao et al. used hemoCD1, a synthetic supramolecular compound combining Fe^{2+} porphyrin and a cyclodextrin dimer, to create a precise and sensitive colorimetric assay for quantifying CO in biological samples after CO exposure. Their results revealed that, after inhaling CO gas at a concentration of 400 ppm, blood COHb levels increased linearly over time, while CO levels in tissues like the liver, lungs, cerebrum, cerebellum, heart, and muscles quickly reach a plateau below their saturation limits 10 minutes after exposure. Therefore, continued CO inhalation causes an increase in COHb, whereas CO in tissues reaches a limit. This suggests that COHb formation prevents toxic free CO accumulation in tissues, thereby having a protective function.⁹² Additionally, the study also demonstrated that CO accumulation in organs *ex vivo* was higher than *in vivo*, which indicates that without Hb, more CO can infiltrate tissues. Several other studies have also shown that it is the free CO that diffuses to the tissues and not the fraction bound to Hb that is the primary cause of CO poisoning.⁹²

Lastly, as previously mentioned, CO is produced naturally within the body and is primarily scavenged by Hb, resulting in basal COHb levels of around 1-2%, which are considered physiological. With Hb concentrations around 7.5 mM, 2% COHb corresponds to approximately 150 μM , which is similar or even higher than the peak concentrations of many normally used medications. This suggests that at such concentrations, COHb is not toxic for the organism.³²

1.5.2. COHb as a cytoprotective molecule

Since everything in biological systems is produced for a reason, it is hypothesized that COHb may play an active, biological cytoprotective role rather than being merely a byproduct of CO metabolism.⁹³

1.5.2.1. COHb formation as a protective mechanism against cell-free Hb oxidation and toxicity

As mentioned in Section 1.4.3., Hb is the primary protein within RBCs. During hemolysis, in physiologic or pathologic conditions, RBCs release their intracellular contents, including Hb. Without RBC's protective antioxidant mechanisms, cell-free Hb (Fe^{2+}) can be easily oxidized into toxic forms like MetHb and ferrylHb by oxidants like H_2O_2 and NO. These oxidized forms generate ROS, leading to oxidative stress, protein damage, lipid peroxidation, inflammation and BBB disruption.^{32,43,76}

CO has a strong affinity for reduced Hb, forming COHb, which is resistant to oxidation. Some studies suggest that CO binding prevents the dissociation of cell-free Hb by keeping the ferric heme-iron in a stable ferrous carboxy state, therefore controlling the release of cytotoxic heme and iron. Cell-free COHb exhibits greater stability and reduced toxicity compared to cell-free MetHb, as demonstrated in models of hemolytic malaria, where exposure to CO gas reduced the circulating MetHb and free heme, limiting oxidative stress.^{94,95}

Further research shows that specific Hb mutations, like the Kirklareli mutation (H58L), which promotes Hb auto-oxidation and enhances heme dissociation, may lead to mild anemia. Smokers with this mutation are protected from anemia due to the high affinity of the mutated Hb for CO, which prevents Hb oxidation by binding to CO from cigarette smoke.⁹⁶

Additionally, studies performed on the hemoCD molecule revealed that it binds CO with a very high affinity. In mice treated with this molecule, hemoCD first captures endogenous CO and then CO from circulating COHb, leading to a temporary decrease in blood COHb levels. This depletion then leads to the upregulation of HO-1, increasing endogenous CO production to compensate for the loss of CO in the blood and to restore COHb levels. This shows the need of a compensatory mechanism to maintain a constant level of blood COHb.⁹⁷

All these evidence suggests that COHb might be a part of CO's mechanism of action. The findings support the idea that COHb formation helps limit the oxidation of cell-free reduced Hb, heme release from MetHb, and consequently reduces the deleterious effects associated with these processes.

1.5.2.2. COHb as an antioxidant factor

An in vitro experiment demonstrated that CO treatment of RBCs significantly increased intracellular levels of reduced GSH, from approximately 2 mM to 3 mM. This increase in GSH was not due to enhanced glycolysis but was partially attributed to the activation of the pentose phosphate pathway (PPP). The PPP generates NADPH, which is an essential substrate for the enzyme glutathione reductase, which reduces GSSG to GSH and promotes Hb de-glutathionylation.⁹⁸ The primary source of increased GSH was attributed to Hb de-glutathionylation, releasing GSH from cysteine residues, especially Cys93 and Cys112, due to conformational changes induced by CO binding to Hb, forming COHb. Since Hb is the major protein of RBCs, the COHb-induced Hb conformation alteration results in a significant GSH release. As GSH is a key antioxidant in RBCs, this CO-driven GSH increase, supported by PPP-mediated Hb de-glutathionylation, enhances RBC antioxidant defenses.⁹⁸

Transfusion of RBCs are a primary treatment for hemorrhagic shock. However, hemorrhage and resuscitation by RBC can lead to complications like hepatic ischemia-reperfusion injury, which can potentially result in liver failure. Recent research in this area has shown that this type of injury reduces cytochrome P450 levels and its metabolic activity, increasing free heme, which aggravates hepatic damage and oxidative stress. CO-bound RBCs (CO-RBCs) have been shown to protect the liver by preserving cytochrome P450 activity, reducing the levels of free heme and NO, decreasing lipid peroxidation, and reducing oxidative stress markers, thereby reversing some of the harmful effects of normal RBC transfusions.⁹⁹

Sakai et al. studied the effects of transfusing RBCs or Hb-containing vesicles (liposome encapsulated Hb) exposed to CO gas in a rat model of hemorrhagic shock. Their hypothesis was that CO-bound Hb could improve the results of resuscitation by attenuating the reperfusion injury typically caused by the transfusion of oxygenated blood or Hb-based carriers.¹⁰⁰ The results showed that transfusion with CO-RBCs or COHb vesicles led to improved systemic parameters (parameters related to plasma enzyme levels) and reduced inflammatory oxidative damage in liver and lung tissues compared to oxygenated Hb transfusion. Additionally, it was also observed that the levels of circulating COHb declined from 26-39% following injection to less than 3% within 6 hours.¹⁰⁰

Cabrales et al. also found that when CO-RBCs were injected into hemorrhaging hamsters, they were as effective as regular oxygenated RBCs (O₂-RBCs) in the recovery of the hemorrhagic shock by stabilizing blood pressure and microcirculation. CO-RBCs even showed an increased cytoprotective effect in the subcutaneous microcirculation, reducing tissue damage caused by ischemia-reperfusion injury. Indeed, CO-RBCs transfusion resulted in significantly less apoptotic cells compared to oxygenated RBCs after resuscitation, demonstrating the protective properties of COHb production in RBCs against ischemia-reperfusion injury in a hemorrhagic shock model.¹⁰¹ Furthermore, it has also

been demonstrated that resuscitation with CO-RBCs after hemorrhage not only suppressed ROS production at an early phase but also resulted in lower plasma levels of the pro-inflammatory cytokines IL-6 and TNF- α at a late phase (6 to 24 hours).¹⁰²

Overall, the administration of CO- bound RBCs offers protective antioxidant and anti-inflammatory effects, reducing the oxidative damage normally observed with the use of oxygenated RBC transfusions in hemorrhagic conditions.

1.5.2.3. Other possible protective functions of COHb

In animal studies, CO gas inhalation at 100 to 250 ppm is commonly used because of its protective effects in various tissues and diseases. Depending on the duration of exposure and the specific experimental model, concentrations between 250 and 500 ppm can lead to COHb levels varying from 4.5% to 30%. The observed protective effects may be due to free CO reaching tissues, the presence of COHb in circulation, or a combination of both.^{93,103}

Smokers normally maintain higher levels of COHb compared to non-smokers, with concentrations ranging between 2% to 14%.^{32,104} Although smoking is very harmful and injurious, epidemiological studies have observed a lower incidence of diseases like Parkinson's among smokers. This paradox suggests that, despite the toxicity of cigarettes, smoking might have protective effects against conditions like acute coronary syndrome, stroke, and preeclampsia.²⁸ Even though these benefits are often attributed to free CO, it is a possibility that elevated COHb levels may also contribute. However, we cannot exclude the possibility that other substances in tobacco smoke may also contribute to this effect.⁹³

Some studies have provided evidence suggesting the protective role of COHb formation in elephant seals. These seals have high Hb levels, which account for more than 70% of their total body O₂ storage, allowing them to repeatedly dive for 20-25 minutes, with arterial Hb saturations dropping to as low as 10%. This frequent exposure to hypoxia and reoxygenation increases their risk of tissue damage due to oxidative stress.^{32,105} Adult northern elephant seals exhibit an average COHb level of 8.7%, which is higher than values reported for heavy smokers and comparable to the highest endogenous COHb levels observed in critically ill humans (9.7% COHb). The highest measured COHb value in these seals (10.4%) is close to the 12% COHb levels observed in early clinical trials using inhaled CO as a therapeutic agent. Northern elephant seals may have evolved to depend on their high levels of endogenous CO and COHb to protect their cells and organs during recurrent ischemia-reperfusion, given the established protective effects of low-dose CO.^{32,105}

1.5.3. Advantages of COHb as a potential therapeutic agent

Over the last two decades, there has been growing interest in the signaling functions and therapeutic properties of CO. However, in the research of the cytoprotective mechanisms underlying CO, COHb has only been seen as a measure of CO's toxicity, and avoiding its extensive formation is a crucial consideration during the development of CO-based therapies.

Yet we should start investing in the study of COHb as a possible therapy in the field of CO. Firstly, COHb has advantages over other therapeutic agents as it is an endogenously formed molecule, so the body is already used to its presence. In addition, it always exists at a basal concentration of approximately 150 μM , which is equal to or higher than the maximum concentrations of several commonly used medications. In addition, COHb also has advantages over other types of CO-based therapies currently used, namely the use of CO gas by inhalation and the use of CORMs. With regard to gaseous CO, it is widely known that it is a toxic and lethal gas when inhaled in high concentrations. Although it has been shown in several studies that at low concentrations this gas has several beneficial properties, it is difficult to eliminate the extremely deep-rooted perception of its toxicity, something that would not be a problem with the use of COHb. Regarding the use of CORMs, there are always additional risks related to the xenobiotic molecules that incorporate the CORM structure. After CO is released, the remaining scaffolds, carriers, metabolites and heavy metals can be biologically active and potentially cytotoxic.¹⁰⁶ This would also not be a problem with the use of COHb.

Various Hb-based blood substitutes have also been developed, designed not only to transport and deliver oxygen to tissues but also to serve as fluid replacements. Among these, PEGylated bovine COHb emerged, being capable of delivering both O₂ and CO. This new PEGylated COHb was specifically developed to treat compromised tissue hypoxia while also targeting inflammation and reperfusion injury, making it a potential therapeutic agent for treating conditions such as hemorrhagic and ischemic strokes.¹⁰⁷

2. Aims

Stroke is the leading cause of death in Portugal and a major cause of permanent neurological disability worldwide.¹⁷ Hemorrhagic stroke, though less common, is far more dangerous due to their higher mortality rate.^{20,21} During this vascular dysfunction, whether caused by hemorrhage or ischemia, hemolysis can occur, releasing cell-free hemoglobin (Hb) into the circulation. This cell-free Hb is easily oxidized, forming methemoglobin (Fe³⁺) or ferryl hemoglobin (Fe⁴⁺), both of which contribute to oxidative stress, lipid peroxidation, inflammation, BBB disruption, and neuronal death.^{23–25}

Carbon monoxide (CO) has been recognized for its cytoprotective, anti-inflammatory, antioxidant, and anti-apoptotic effects.^{43,108,109} As a gas, CO diffuses rapidly through tissues and binds to Hb, forming carboxyhemoglobin (COHb). Although COHb is traditionally viewed as an indicator of CO toxicity, recent evidence suggests that it might play an active biological function.³²

We hypothesized that COHb formation is not merely accidental, but instead acts as a biological cytoprotective molecule. Supporting this hypothesis are several points from both literature and our own data: (i) there is no direct correlation between COHb levels and CO toxicity;⁹¹ (ii) COHb demonstrates cytoprotective and antioxidant properties within erythrocytes;⁹⁸ and (iii) COHb prevents oxidative stress following hemorrhagic shock in vivo.¹⁰⁰ Our hypothesis proposes that the formation of COHb prevents the toxic effects of cell-free Hb, particularly its pro-oxidant properties that can induce cell death and inflammation, occurring after physiological or pathological hemolysis.

Therefore, the aim of this project is to investigate the potential biological role of COHb. To achieve this, several cerebral cellular mechanisms were studied:

- Neuronal function and cell death, using the human neuroblastoma cell line SH-SY5Y;
- Neuroinflammatory response of microglia, using the mouse BV-2 microglial cell line;
- BBB integrity, using human brain microvascular endothelial cells, the hCMEC/D3 cell line.

With these cellular models, we aimed to answer whether COHb exhibits anti-inflammatory and neuroprotective effects against MetHb toxicity and other harmful stimuli, and whether it can help maintain BBB integrity.

Scientific community has been studying the cytoprotective mechanisms of CO, however the potential role of COHb has been frequently ignored. Additionally, COHb has been wrongly associated with toxicity or considered an inert by-product of CO detoxification. This study intends to expand the understanding of the physiological role of COHb.

3. Materials and methods

3.1. Cell lines and maintenance

3.1.1. SH-SY5Y

SH-SY5Y cell line is a neuroblastoma clonal human cell line, originally derived from a metastatic bone tumor through a three-time subcloning of the parental SK-N-SH line.¹¹⁰ These cells can be differentiated into neuron-like cells by manipulating the culture media with low concentrations of fetal bovine serum (FBS) and adding retinoic acid (RA).¹¹⁰

3.1.1.1. Maintenance

SH-SY5Y cells were cultured in DMEM-F12 (Dulbecco's Modified Eagle Medium: Nutrient Mixture F-12, Biowest, L0093) basal medium, supplemented with 10% (v/v) inactivated FBS (Gibco, 10500-064) and 2% (v/v) Pen/Strep (Sigma Aldrich, P4333), and maintained in 75 cm² T-flasks at 37 °C and 5% CO₂. When the cells reached 100% confluence, they were passaged at a 1:3 or 1:4 dilution. This guarantees that the cells have enough nutrients and space to continue proliferating. As these cells are adherent, the culture medium was first removed, and the cells were washed with PBS. Next, they were incubated with 0.05% trypsin-EDTA (Gibco, 25300-054) for 2 minutes at 37°C and 5% CO₂. To neutralize the trypsin, the medium containing FBS was added, and the cells were then resuspended in a new 75 cm² T-flask.

When the cells began to exhibit increased aggregation, the T-flask was pre-coated with Matrigel (Sigma Aldrich) 2 hours before the cell passage, following the previously described protocol.

3.1.1.2. Neuronal differentiation and plating

SH-SY5Y cells were plated in 24-well plates at the seedings of 5x10⁴ and 2.5x10⁴ cells/well. On the day following the seeding, the differentiation protocol was initiated by changing the cell medium to a differentiation medium with DMEM-F12 supplemented with a reduced FBS percentage of 1% (v/v), 2% (v/v) Pen/Strep and 10 μM all-trans RA (Thermofisher, 44540). The differentiation process occurred over 6-7 days, changing the media on the fourth day.

As mentioned before, when there was an increase in cell aggregate formation, the plates were pre-coated with Matrigel 2 hours before cell seeding.

3.1.1.3. Thawing

The cells need to be rapidly thawed at 37 °C and then resuspended in 5 mL of prewarmed phosphate buffered saline (PBS). Next, they were centrifuged at 500g for 5 minutes, the supernatant was discarded, and the cells were resuspended in 5 mL of prewarmed maintenance medium. Lastly, the cells were seeded in a 25 cm² T-flask and incubated at 37 °C and 5% CO₂.

3.1.1.4. Freezing

To freeze cells, the proliferation medium was first removed from the 75 cm² T-flask, and the cells were washed with PBS. Next, 1 mL of trypsin was added, and the flask was incubated for 2 minutes at 37 °C. After incubation, 4 mL of the maintenance medium was added, and the cells were centrifuged at 500g for 5 minutes. The supernatant was discarded, and the cell pellet was resuspended in a freezing solution (90% (v/v) FBS and 10% (v/v) DMSO (Merck, D5879)). The cell suspension was then transferred, 1 mL of the cell suspension to each cryovial, to freeze slowly.

3.1.2. BV-2 cell line

The murine BV-2 cell line was produced by introducing a retrovirus (J2) containing the -raf/v-myc oncogene into primary microglial cell cultures.¹¹¹

3.1.2.1. Maintenance

The cells were maintained in 75 cm² T-flasks at 37 °C and 5% CO₂ in RPMI-1640 (Sigma Aldrich, R0883) basal medium, supplemented with 10% (v/v) FBS, 2% glutamine (Sigma Aldrich, G7513) and 1% (v/v) Pen/Strep. When the cells reached 100% confluency, they were passaged at a 1:4 dilution. As semi-adherent cells, they were gently detached from the T-flask using a sterile cell scraper. Once detached, the cells were transferred to a new T-flask, with passage done twice a week.

3.1.2.2. Plating

For experimental assays, BV-2 cells were seeded in 24-well or 96-well plates at the seedings of 2.9×10^4 and 4.8×10^3 cells/well, respectively.

3.1.2.3. Thawing

The thawing process for the BV-2 cells is the same as the one described for the SH-SY5Y cell line.

3.1.2.4. Freezing

To freeze the cells, we first gently scraped them and centrifuged the cell suspension at 500g for 5 minutes. After centrifugation, the supernatant was discarded, and the cells are resuspended in a freezing solution (90% (v/v) FBS and 10% (v/v) DMSO). Lastly, 1 mL of the cell suspension was aliquoted into each cryovial for slow freezing.

3.1.3. hCMEC/D3 cell line

hCMEC/D3 brain microvascular endothelial human cell line was derived from human temporal lobe microvessels obtained during surgical tissue excision. The cells were immortalized sequentially through lentiviral vector transduction with the catalytic subunit of human telomerase (hTERT) and SV40 large T antigen.¹¹²

In optimal culture conditions on collagen-coated surfaces, hCMEC/D3 cells become elongated and form a monolayer. As semi-adherent cells, they require a coated plastic surface in T-flasks to guarantee adequate attachment, growth, and culture maintenance. These cells exhibit characteristics typical of brain endothelial cells, including the development of a strong permeability barrier function.¹¹²

3.1.3.1. Maintenance

All plastic surfaces for hCMEC/D3 culturing must be coated with collagen by adding collagen Rat tail type I (Sigma Aldrich, C7661, 2 mg/mL in a 0.1% solution of acetic acid diluted (1:20) in 0.01M HCl) for 2 hours, then the collagen was removed and the T-flask was washed twice with PBS 1x before seeding the cells.

hCMEC/D3 cells were grown in 75 cm² T-flasks (previously coated) using the proliferation medium described in Table 1 bellow, and then incubated at 37 °C and 5% CO₂. The medium was replaced twice a week, and once the cells reached 100% confluence, they were passaged into a new coated T-flask at a 1:4 dilution. To passage the cells, the medium was first removed and the cells were washed with PBS. They were then trypsinized for 2 minutes at 37°C and 5% CO₂. The trypsinization was stopped by adding the FBS containing medium, after which the cells were resuspended in fresh 75 cm² T-flasks.

3.1.3.2. Cell differentiation and plating

The cells were plated in 6-well and 24-well plates, coated with collagen, at the correspondent seedings of 2.4 cm²/well and 0.475 cm²/well (25% confluence). The endothelial cells were then differentiated for 9-12 days using a differentiation medium described in Table 1. All growth factors (VEGF, IGF, EGF) except basic fibroblast growth factor (bFGF) have to be removed from the differentiation culture medium to promote the expression of junctional proteins.¹¹²

Table 1 - hCMEC/D3 media composition.

Proliferation medium	Differentiation medium
2,5% (v/v) FBS (EGM-2 MV bullet kit)	2,5% (v/v) FBS (Lonza, EGM-2 MV bullet kit)
1% (v/v) Pen/Strep (Sigma Aldrich, P4333)	1% (v/v) Pen/Strep (Sigma Aldrich, P4333)
Hydrocortisone (Lonza, EGM-2 MV bullet kit)	1,4 mM Hydrocortisone (Sigma Aldrich, H0888)
10 mM HEPES (Sigma, CAS: 7365-45-9)	10 mM HEPES (Sigma, CAS: 7365-45-9)
VEGF (Lonza, EGM-2 MV bullet kit)	bFGF 1ng/mL (Gibco, 13256029)
IGF (Lonza, EGM-2 MV bullet kit)	EBM-2 Basal Medium (Lonza, CC-3156)
EGF (Lonza, EGM-2 MV bullet kit)	
bFGF 1ng/mL (Gibco, 13256029)	
EBM-2 Basal Medium (Lonza, CC-3156)	

3.1.3.3. Thawing and freezing

The thawing and freezing processes (and also the freezing solution composition) are the same as described for the SH-SY5Y cell line.

3.2. Preparation of Hemoglobin, Methemoglobin and Carboxyhemoglobin solution

Methemoglobin, reduced hemoglobin and carboxyhemoglobin were prepared using the commercially available human hemoglobin (Sigma-Aldrich, Human Hemoglobin, lyophilized powder, H7379). According to Sigma-Aldrich's indications, the molecular mass of commercial Hb in solution is 16250 g/mol, corresponding to its monomeric form. The preparation of the Hb solutions used for all the assays was the same.

3.2.1. Methemoglobin with Fe³⁺ (MetHb)

Lyophilized Hb powder was dissolved in PBS at a final concentration of 1 mg/mL (~62 μ M). According to Sigma-Aldrich's indications, the Hb (Fe²⁺) in solution is oxidized into Hb (Fe³⁺) when exposed to oxygen.

3.2.2. Reduced hemoglobin with Fe²⁺ (Hb)

A solution of methemoglobin was prepared as described above. Then sodium dithionite (0.2M) (Sigma Aldrich, CAS: 7775-14-6) at a concentration of 20 μ L/mL of Hb solution was added. Since sodium dithionite is a reducing agent, it reacts with the ferric iron (Fe³⁺) on the oxidized hemoglobin and converts it back to its reduced ferrous iron (Fe²⁺) state.

3.2.3. Carboxyhemoglobin (COHb)

After preparing the reduced hemoglobin solution, the COHb was prepared in two different ways: CORM or CO gas. For the first method, 60 μ L of CORMALF826 (2.5 mM) (generously provided by Dr. Carlos C. Romão) was added per mL of reduced Hb solution and then heated at 37 °C for 20 minutes. In the second method, reduced Hb solution was bubbled with CO gas at 100% (kindly supplied by Dr. Carlos C. Romão) for 5 min.

Figure 14 illustrates a schematic representation of the process used to prepare the Hb solutions.

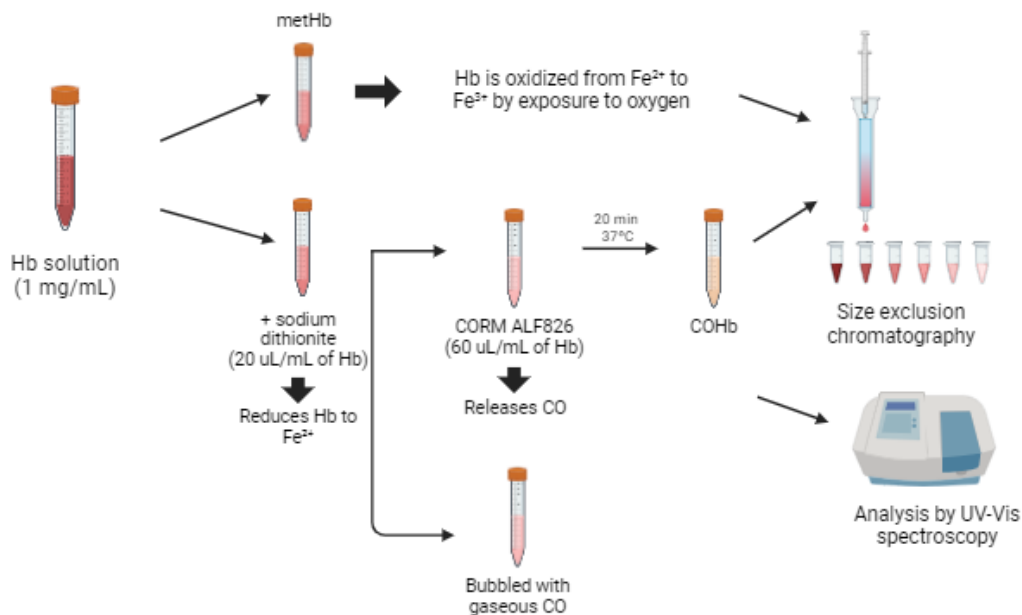


Figure 14 – Schematic representation of the preparation process for methemoglobin, reduced hemoglobin, and carboxyhemoglobin solutions.

According to the manufacturer's instructions, Hb is soluble in water at a concentration of 20 mg/mL. However, a concentration of 1 mg/mL (or approximately 62 μM) was selected for this study, following previous solubility studies carried out in the laboratory that showed higher concentrations led to Hb precipitation. Furthermore, multiple studies have also used 1 mg/mL of Hb in biological experiments.^{113,114}

All the Hb solutions were made using PBS as a buffer so that they could be used in cell culture, more specifically to maintain osmotic pressure in the cells and prevent their lysis.

After preparing all of the Hb solutions, size exclusion chromatography was used to eliminate any residual heme degradation products and free heme groups, products from the sodium dithionite reaction, and/or the molecular structure of ALF826 after release of CO. A Sephadex column (HiTrap Desalting 5mL, Sephadex G-25) was used for the chromatography. Following this step, all solutions were filtrated through a 0.22 μm pore filter (Filter-Lab, JPES022025K) to ensure their sterility.

Following Hb solutions' preparation, Hb redox state was confirmed by UV-Visible (UV-Vis) spectroscopy (Lambda 35, PerkinElmer).

Hemoglobin in its reduced form (Fe^{2+} , bound to oxygen) can be identified by a peak around 415 nm (Soret band) and two additional peaks at approximately 541 and 577 nm. Methemoglobin (Fe^{3+}) has a

peak around 405 nm (Soret band) with two smaller, less distinct peaks around 500 and 631 nm. Carboxyhemoglobin (Fe²⁺-CO) exhibits a peak around 419 nm (Soret band) and two peaks around 540 and 569 nm. These peaks are similar to those of Hb (Fe²⁺), with the difference that COHb peaks are slightly shifted to the left.¹¹⁵

3.3. Griess assay – nitrite quantification

The Griess assay is a colorimetric method used for nitrite (NO₂⁻) quantification in biological samples. This technique uses the Griess diazotization reaction to spectrophotometrically detect nitrite. Quantification of nitrite is an indirect manner for assessing cellular nitric oxide production since nitrite is produced by the spontaneous oxidation of nitric oxide (NO) under physiological conditions.¹¹⁶

The assay is based on the chemical reaction between nitrite in the sample and sulfanilamide under acidic conditions, resulting in the formation of diazonium salt. This salt then reacts with N-(1-naphthyl) ethylenediamine to produce a purple dye. The intensity of the color produced is directly proportional to the nitrite concentration in the sample and can be quantified spectrophotometrically by measuring the absorbance at 548 nm.

3.3.1. Standard calibration curve

A standard calibration curve was done as a control to confirm the proper functioning of the assay reagents (Annex 2). A 30 mM sodium nitrite (NaNO₂, S2252, Sigma-Aldrich) solution in PBS was prepared and used to create serial dilutions. The concentrations for the standard curve were 200 μM, 100 μM, 50 μM, 25 μM, 12.5 μM, 6.25 μM and 0 μM (only PBS). Each concentration was added to a microplate (in triplicates) and mixed with the Griess reagent (GRIESS-ILOSVAY'S nitrite reagent, Sigma, G4410). After incubating for 10 minutes at 37 °C, absorbance was measured at 540 nm using a Tecan Infinite F200 Pro microplate reader.

3.3.2. Griess assay sample preparation

The Griess assay was tested on BV-2 cells seeded in 24-well plates at a density of 2.9x10⁴ cells/well, with 500 μL of BV-2 medium *per* well. After a 24-hour incubation, 250 μL of medium was removed from each well. The cells were then treated with 250 μL PBS (untreated control), or 250 μL of the previously prepared solutions of MetHb, COHb and reduced Hb (four technical replicates *per*

condition). Due to Hb's low solubility, large volumes are required to reach the reported functional concentration of Hb (around 30 μM), which implies that half of the culture medium was removed and replaced with the Hb solutions. The negative (untreated) control groups were treated similarly using only PBS. After an additional 24 hour-incubation, the supernatant was collected and centrifuged for 5 min at 1000g. The supernatant (50 μL) was then mixed with the 50 μL of Griess reagent. Following a 10-minute incubation at 37 °C, absorbance was measured at 540 nm using a Tecan Infinite F200 Pro microplate reader. After the measurement, the Griess reagent was discarded from each well. Figure 15 shows a schematic representation of the Griess assay technique described above.



Figure 15 - Schematic representation of Griess assay protocol.

3.4. ELISA assay – TNF- α quantification

ELISA (Enzyme-Linked Immunosorbent Assay) is a method used to detect and measure specific proteins, antibodies, or hormones in a sample. This technique is based on binding of the target molecule to an enzyme-linked antibody. When a substrate is added, the enzyme catalyzes a reaction that results in a color change that can be measured and associated with the enzyme activity. For this study we used a sandwich ELISA to assess the quantity of the pro-inflammatory cytokine TNF- α (tumor necrosis factor α) in the BV-2 murine microglial cell line.

3.4.1. ELISA assay sample preparation

For ELISA, BV-2 microglia cells were plated in 24-well plates with a seeding of 2.9×10^4 cells/well were used. After a 24-hour incubation, the cells went through the same treatment described in Section 3.3.2. (Griess assay sample preparation). After another 24 hours, cell medium was discarded and 100 μL of RIPA buffer 1x were added to lyse the cells. The samples were then collected in tubes until the assay was performed.

The Human TNF- α Standard ABTS ELISA Development kit (Peprotech) was used following the protocol provided by the manufacturer. Lastly, absorbance was measured at 415 nm with wavelength

correction set at 560 nm, since the reaction product does not absorb at this wavelength, using a Tecan Infinite F200 Pro microplate reader. The absorbance data was then converted to TNF- α concentration values using the standard curves

3.5. DCF assay – ROS quantification

The DCF (2',7'-dichlorofluorescein) is a fluorometric assay commonly used for the detection and quantification of intracellular reactive oxygen species (ROS) in cells. This assay is based on the fact that ROS oxidize the non-fluorescent DCFH-DA (2',7'-dichlorodihydrofluorescein diacetate) into the fluorescent DCF form. Cell membranes allow the DCFH-DA form to freely diffuse through them. Intracellular esterases then hydrolyze the DCFH-DA form to produce DCFH (2',7'-dichlorodihydrofluorescein) which is then oxidized by ROS (more specifically H₂O₂) to form DCF. The fluorescence intensity of DCF is directly proportional to the amount of ROS present within the cells.

3.5.1. DCF assay sample preparation

The DCF test was done on both BV-2 cells and differentiated SH-SY5Y cells, which were seeded in 96-well plates at the seedings of 4.8×10^3 and 8.5×10^3 cells/well, respectively. After a 24-hour incubation, half of the medium (75 μ L) was removed from each well. The cells were then treated with 75 μ L of PBS (untreated control), of MetHb and COHb solutions at 62 μ M.

After a 24-hour incubation, the supernatant was discarded and 100 μ L of a DCFH-DA (Invitrogen) 5 μ M solution was added to each well. After a 15-minute incubation at 37 °C, fluorescence was measured at an excitation wavelength of 485 nm and an emission wavelength of 535 nm, using a Tecan Infinite F200 Pro microplate reader. Following the DCF assay, the reagent was removed from each well, and protein extraction and quantification were performed (described in the next section). In Figure 16 is presented a schematic representation of the previously described protocol.

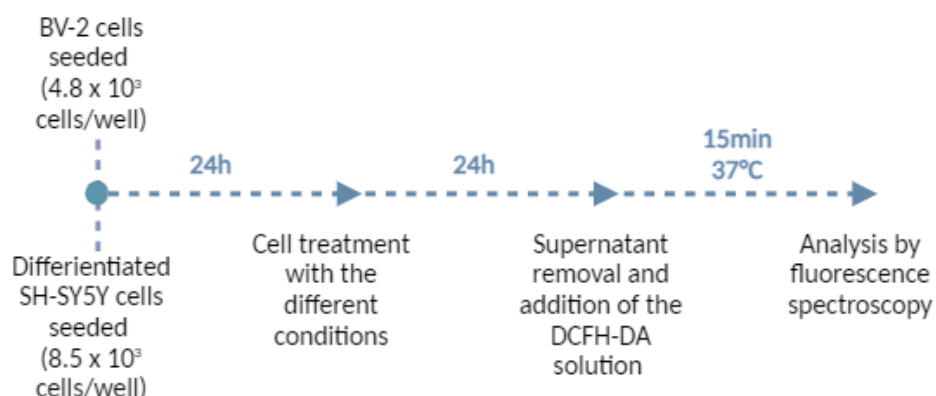


Figure 16 - Schematic representation of DCF assay protocol.

3.6. Protein extraction and quantification

For protein extraction, BV-2 and SH-SY5Y cells were lysed with RIPA buffer (50 mM Tris-HCl, 150 mM NaCl, 0.1% SDS, 1% Sodium Deoxycholate, 1% Triton X100, 1% protease inhibitors). The cell extracts were then transferred into 96-well microplates (25 μ L *per* well). A standard BSA curve with known concentration values (1000 to 15.625 μ g/mL) was also prepared to calculate the protein concentration of the samples. Next, 100 μ L of working reagent from the Pierce BCA Protein Assay kit (Thermo Fisher Scientific, 23227) were added to each well. The plates were incubated for 30 minutes at 37°C, and absorbance values were measured at 560 nm using a Tecan Infinite F200 Pro microplate reader.

3.7. Flow cytometry – cell viability assessment

Flow cytometry is a technique utilized to analyze the physical and chemical characteristics of cells or particles in solution. It uses lasers as light sources to produce scattered and fluorescent light signals, which are detected by specific sensors. As each particle or cell passes through the laser, it is individually measured for properties such as size, granularity and fluorescent intensity. This experiment was performed to assess cell viability by using a propidium iodide (PI) fluorescent dye. PI intercalates into double-stranded DNA but is excluded by intact cell membranes. Therefore, this dye selectively penetrates through the plasmatic membrane and stains dead or dying cells whose membranes have been compromised, emitting red fluorescence when bound to DNA. By measuring PI fluorescence, flow cytometry can distinguish between viable and non-viable cells.

Cellular fluorescence emission was detected by the flow cytometer (Attune® Acoustic Focusing Cytometer, Thermo Scientific) using a blue laser (BL2-A) for excitation. Several parameters are used to differentiate viable and dying (or dead) cells from cellular debris. To specifically examine the target cells, the flow cytometer's settings, or gates, were adjusted. Figure 17 illustrates the flow cytometry gating strategy.

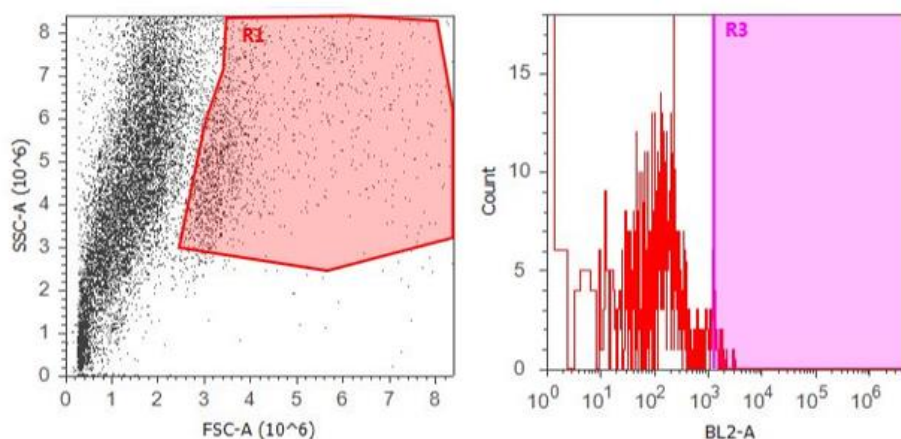


Figure 17 - Flow cytometry gating strategy; **Left panel:** SSC vs FSC density plot. A gate was applied to avoid debris and dead cells and to choose a certain population, with each dot representing a single particle. **Right panel:** PI fluorescence is assessed using a single-parameter histogram; positive datasets are those with light scatter intensities greater than 10^3 .

The gates shown in Figure 4 detect cell population based on size (FSC), and morphology/granularity (SSC). The defined gate (R1) in the left panel distinguishes viable cells from cellular debris, while on the right panel the gate in purple (R3) differentiates dead (or dying) cells from healthy cells by detecting high red fluorescence emitted by PI penetration in compromised cells. In the right panel, only cells present in gate R1 were analyzed.

3.7.1. Flow cytometry sample preparation

Both differentiated and non-differentiated SH-SY5Y cells were used in this viability assay. Cells were seeded at 2.5×10^4 cells/well in 24-well plates. Non-differentiated cells were treated the day after plating whereas for differentiated cells, the medium was replaced with differentiation medium one day after seeding and maintained for 6-7 days before treatment. One group of both cell types was treated with PBS, and MetHb and COHb solutions reaching a final concentration of about $31 \mu\text{M}$. Another group was co-treated with these same solutions plus carbonyl cyanide m-chlorophenyl hydrazone (CCCP,

Sigma Aldrich, C2759) a widely used mitochondrial uncoupler. CCCP (at a concentration of 50 μ M) was used to promote cell death and to assess any protective role of COHb, MetHb or Hb. The cells were then treated with the Hb solutions as described in Section 3.3.2. For each condition, 3 technical replicates (cultured wells) were tested. Cells were treated for 24 hours. Cell viability was measured using the culture supernatant and the trypsinized cells collected into a tube with the addition of fresh medium containing propidium iodide (1:1000)(Invitrogen, P3566). In Figure 18 a schematic representation of the protocol used for the cell viability assay is demonstrated.

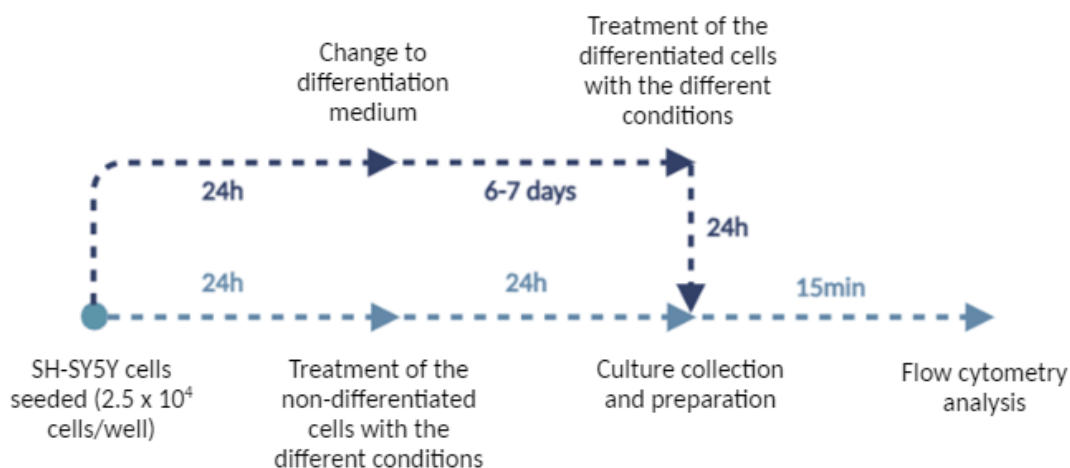


Figure 18 - Schematic representation of cell viability assay protocol.

3.8. Lucifer yellow assay – cell permeability assessment

The paracellular permeability of the hCMEC/D3 cell line under different conditions was evaluated using Lucifer yellow (LY) dye. Cells were initially seeded into inserts (placed into 24-well plates) with a surface area of 0.3 cm^2 at approximately 30% confluence (3 replicates per condition). Within the inserts, the cells occupy the apical side and once fully differentiated, they form a layer of endothelial cells that mimics the blood-brain barrier. To assess the permeability of this barrier, the LY dye was added to the volume inside the inserts, and after determined time intervals, samples were collected from the lower compartment under the insert (basolateral side). The amount of dye that passed through the cellular barrier was measured to determine the permeability coefficient.

3.8.1. Standard calibration curve

A standard calibration curve was done to quantify the concentration of LY. This was achieved by preparing a series of solutions using Hank's Balanced Salt Solution (HBSS, Gibco, 24020-091), which is the medium used in the permeability assay, containing progressively increasing concentrations of the LY dye (Sigma Aldrich, L0259).

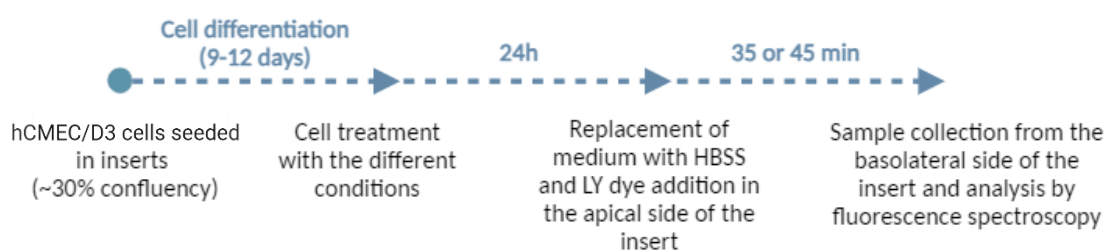
The LY stock solution was prepared at 500 μM in water (molecular weight: 457.25 g/mol). The specific concentrations used for the standard curve were: 10000 nM, 5000 nM, 2500 nM, 1250 nM, 625 nM, 312 nM, 156 nM, and a blank control of 0 nM (only HBSS).

For the calibration curve, 25 μL of each LY solution was added to 100 μL of milli-Q water in triplicate wells on a black-bottom microplate. The fluorescence of each sample was then measured at an excitation wavelength of 485 nm and an emission wavelength of 535 nm using a Tecan Infinite F200 Pro microplate reader.

3.8.2. Sample preparation and calculations

In this assay, 200 μL of medium was added to the inside of each insert in direct contact with the cells, while 500 μL of medium was added to the wells below the inserts. During the differentiation process, only the medium inside the inserts was changed by new medium. After the differentiation period, 100 μL was removed from the insert, and 100 μL of PBS (as a control), MetHb or COHb was added, followed by a 24-hour incubation.

Following the 24-hour incubation, the medium from both the insert and the wells was removed and replaced with Hank's Balanced Salt Solution (HBSS). In the wells 500 μL of HBSS was added, while the inserts were filled with 200 μL in one assay and 500 μL in another. Then, 20 μL of LY dye was added to the apical side of the insert, creating a final concentration of 20 μM . At 35 or 45 minutes after the addition of LY dye, 25 μL samples were collected from the basolateral compartment. These samples were then diluted with 100 μL of milli-Q water and placed in a black-bottom microplate. The fluorescence intensity was measured in the same way as for the standard curve. In Figure 19 a schematic representation of the LY assay protocol is presented.



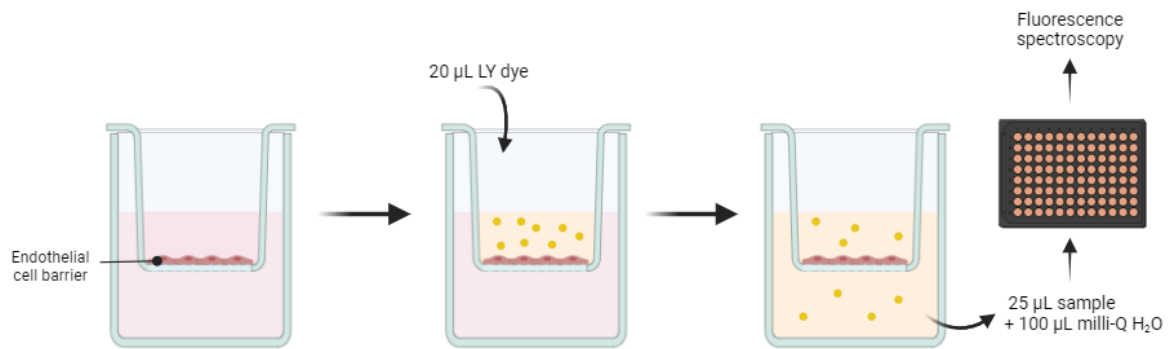


Figure 19 – Schematic representation of the Lucifer yellow assay protocol.

The concentration of LY dye that crossed the cell barrier was determined using the standard calibration curve. The permeability coefficient, which reflects the impact of each cell treatment on the permeabilization of the BBB, was then calculated using the formula presented in Figure 20.¹¹⁷

P_{app} = Apparent permeability coefficient

$$P_{app} \text{ (cm/min)} = \frac{V_B}{A \times \text{time}} \times \frac{\text{Concentration of LY below the insert}}{\text{Initial concentration of LY inside the insert}}$$

Figure 20 - Apparent permeability coefficient (P_{app}) formula. V_B = volume in the basolateral compartment (in cm^3); A = surface area of cell culture (insert) (in cm^2); time (in minutes); both concentrations are in nanoMolar.

3.9. Immunofluorescence microscopy – assessment of tight junction integrity

Immunofluorescence is a technique that uses light microscopy to detect and locate many biomolecules in cells or tissues. It is based on the binding of specific antigens using antibodies that have been tagged with fluorophores. When the fluorophores are excited, they emit light that is detected by a fluorescence microscope, indicating the position and quantity of the target biomolecules.

3.9.1. Sample preparation

For this study, hCMEC/D3 cells were used to assess BBB integrity by analyzing the zonula-occludens-1 (ZO-1) tight junction protein. The cells were plated in 24-well plates with 25% confluence. After the differentiation protocol described in Section 3.1.3.2, and reaching 100% confluence, the cells were treated with the Hb solutions as described in Section 3.3.2 (four technical replicates *per* condition).

After one day of Hb, COHb or MetHb treatments, cells were fixed with 4% paraformaldehyde (PFA) in PBS for 15 minutes. Fixed cells were then washed with PBS and permeabilized with 0.3% Triton X100 in PBS for another 15 minutes. The cells were then blocked with a BlockPerm solution (0.3% Triton X100, 5% FBS in PBS) for 1 hour at RT. After that, the cells were incubated with the primary antibodies, mouse anti-actin (diluted 1:100) (Santa Cruz Biotechnology, sc-8432) and rabbit anti-ZO-1 (diluted 1:50) (Cell Signaling Technology, 8193) in a 0.1% Triton X100, 1% FBS solution, for 4 hours. Following incubation, the cells were washed again and labeled with fluorescent secondary antibodies for 1 and a half hours under low light, goat anti-mouse conjugated to Alexa Fluor 488 (diluted 1:2000) (Invitrogen, A11001) and goat anti-rabbit conjugated to Alexa Fluor 488 (diluted 1:2000) (Invitrogen, A11008). The cells were also incubated with Hoechst diluted 1: 1000 for 10 minutes. Finally, the coverslips were washed with PBS and mounted onto glass slides using mounting medium (ProLong gold antifade reagent, Invitrogen, P10144). Fluorescence imaging was performed with a Zeiss Axio Imager D2 fluorescence microscope.

3.10. Statistical analysis

The data presented throughout this work is the mean \pm standard deviation of replicates (biological or technical depending on the analysis). Comparisons between distinct groups of conditions and treatments were done using the two-tailed and unpaired Student's t-test with Excel. Results with p-values of less than 0.05 were considered statistically significant.

4. Results

4.1. Preparation of the Hemoglobin solution

After preparing the Hb solutions, UV-Vis spectra were obtained to confirm the redox state of iron and whether CO is bound to Hb (Figure 21). This analysis was conducted to validate the effects of sodium dithionite, which serves as a reducing agent for Hb, and to assess the CO release from both the CO-releasing molecule CORM ALF826 and CO gas in the formation of COHb.

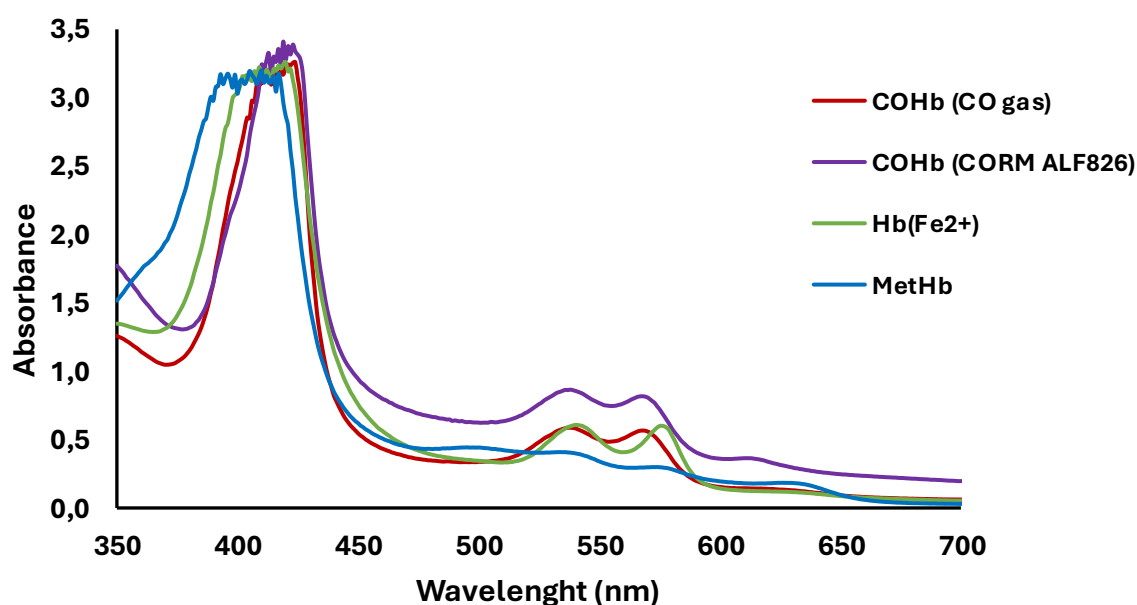


Figure 21 - Hemoglobin absorption spectra from 350 to 700 nm. Methemoglobin (MetHb) was prepared by dissolving lyophilized human hemoglobin powder in PBS at a final concentration of 1 mg/mL (~62 μ M). Reduced hemoglobin (Hb (Fe^{2+})) was prepared by adding sodium dithionite at a concentration of 20 μ L/mL of Hb to a MetHb solution prepared as described previously. Carboxyhemoglobin was prepared either by adding CORM ALF826 at a concentration of 60 μ L/mL of Hb (Fe^{2+}) solution and then heating it at 37 $^{\circ}$ C for 20 minutes – COHb (CORM ALF826) – or by bubbling the Hb (Fe^{2+}) solution with CO gas at 100% for 5 minutes – COHb (CO gas). Hb redox state was confirmed by UV-Visible spectroscopy.

As can be seen in Figure 21, there are differences between the spectra of MetHb (Fe^{3+}) and Hb (Fe^{2+}) between the smaller peaks in the visible spectrum area (around 500 to 600 nm). Because the spectrum is saturated in the region of the Soret peak (around 400 nm), it is not possible to observe defined peaks. To solve this problem, it would be necessary to reduce the concentration of hemoglobin in solution (e.g. by diluting the prepared solution) or to reduce the sensitivity of the spectrophotometer.

In the spectrum corresponding to the reduced form of iron in Hb, there is a slight shift of the Soret peak to the right compared to the peak observed for oxidized iron in MetHb (peak at ~406 nm of MetHb shifts

to ~416 nm in Hb (Fe²⁺). Furthermore, in the visible region of the spectrum, it can also be clearly observed that Hb (Fe²⁺) has two more distinct peaks at around 544 and 578 nm than MetHb (Fe³⁺). The obtained spectrum is in accordance with the characteristic spectrum of reduced Hb found in the literature.¹¹⁵

These results confirm that the addition of sodium dithionite to the MetHb solution (commercial solution) was effective in reducing Fe³⁺ into Fe²⁺, which is important for CO to bind to Hb. The COHb solution was obtained in two different ways: by adding CORMALF826 or by bubbling with 100% CO gas into the Hb (Fe²⁺) solution.

Moreover, in Figure 21, it can also be observed that both COHb (CORMALF826) and COHb (CO gas) spectra show a shift to the right of the peak in the Soret region when compared to the Hb (Fe²⁺), namely from a peak at ~416 nm of Hb (Fe²⁺) to a peak at ~420 nm for COHb. In addition, it is also possible to observe a slight shift to the left of the peaks in the visible region (at 540 and 570 nm) compared to those of the reduced iron Hb spectrum. The COHb (CORMALF826) spectrum generally shows higher absorbance values than those acquired for the other Hb solutions, probably due to a higher concentration of COHb in the solution. However, despite this, both spectra show the characteristic COHb peaks found in the literature.¹¹⁵

4.2. Neuroinflammatory response of microglia – assessment of neuroinflammatory biomarkers after MetHb and COHb treatment

4.2.1. Nitrite quantification

Many physiological processes such as vasodilation, immune modulation, neurotransmission and inflammation are molecularly mediated by nitric oxide (NO). For this reason, NO levels can be used as a measure of cellular inflammatory response.¹¹⁶ A Griess assay was done to quantify nitrite levels, serving as an indirect indicator of cellular NO production by cells. In fact, nitrite is formed through the spontaneous oxidation of endogenous NO under physiological conditions. For this assay, we used BV-2 cells. This cell line has the morphological, phenotypic, and functional characteristics of partially activated microglial cells. Since they are in a semi-activated state, BV-2 can be used to evaluate the effectiveness of treatments aimed at reducing microglial activation or shifting them towards an anti-inflammatory phenotype.¹¹¹ They also demonstrate phagocytic behavior and the ability to release NO, cytokines and lysozymes in response to stimulation.¹¹¹

BV-2 microglial cells were treated with PBS, MetHb, COHb or Hb (Fe²⁺) for 24 hours, and the potential inflammatory response was evaluated.

Because Hb has very low solubility, it was necessary to add high volumes of the Hb solutions prepared in PBS, actually 50% of cell culture volume is Hb-PBS solution. Therefore, the addition of PBS was used as a negative/untreated control. Additionally, when cells were exposed to 50% PBS and 50% medium, the NO levels produced were comparable to those observed with 100% medium, indicating that PBS did not trigger an inflammatory response in the cells (Annex 1). Still, a standard calibration curve of nitrites was done (Annex 2), but it was not possible to apply it since the amount of generated nitrite in our conditions was lower.

In all samples treated with Hb solutions (MetHb, COHb or Hb) there was a great increase in absorbance that should indicate higher levels of nitrite. Because Hb has some color, we questioned whether the observed absorbance values really reflected an increase in nitrite production or if it could be due to the reddish color of the Hb solutions. Given that the Griess assay measures absorbance at 548 nm, a wavelength within the visible spectrum where characteristic Hb peaks occur, we decided to do a control test. This test replicated the Griess protocol exactly as done with the cell culture, but instead used a mixture of 50% medium and 50% of each Hb solution, without cell culture (Figure 22).

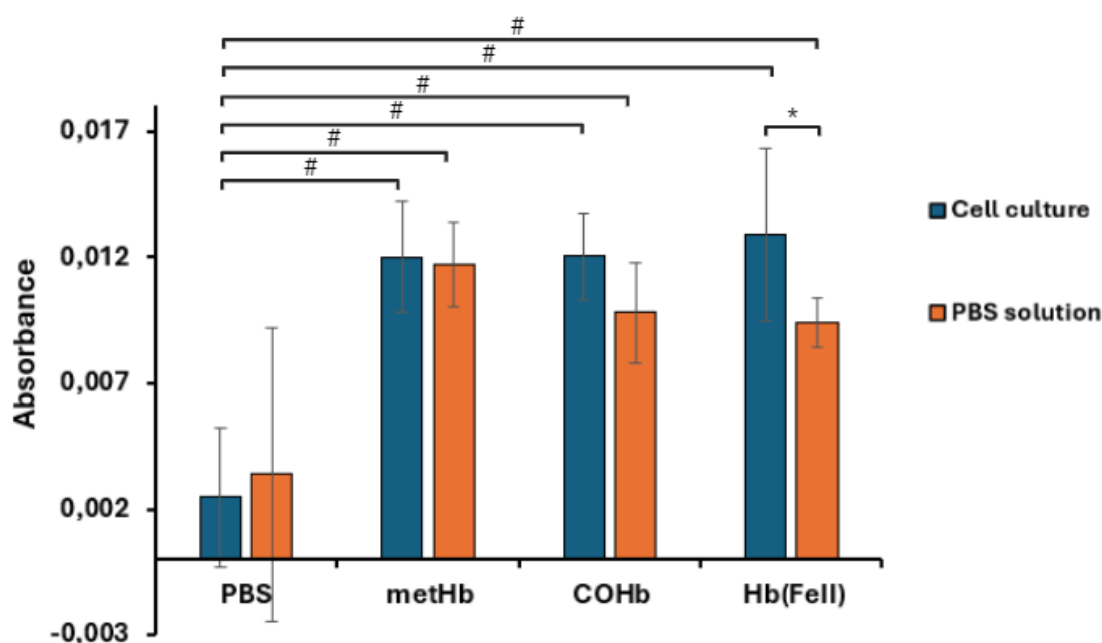


Figure 22 - Comparison between nitrite levels (presented as absorbance values) obtained for cell medium collected from BV-2 cells pre- treated with PBS, MetHb, COHb and Hb (Fe^{2+}) solutions at a concentration of around $30 \mu\text{M}$ for 24 hours (blue) and control samples of 50% medium and 50% of each Hb solution, without cells (orange) by Griess assay. Cells were exposed to 50% of Hb solutions in PBS, with PBS alone serving as the untreated control. Griess assay was done as described in materials and methods. Absorbance was measured at 540 nm. Results are shown as mean \pm SD from 3 independent experiments ($n=3$), each including 3 technical replicates. The asterisk (*) indicates statistically significant differences between treated cells and their respective hemoglobin solution controls. The cardinal (#) indicates significant differences between the untreated control (PBS) from the cell culture and each of the hemoglobin-treated conditions ($p < 0.05$, two-tailed unpaired Student's t-test).

As shown in Figure 22, there is no statistically meaningful difference between the results obtained for the cell culture treated with the different Hb solutions or culture medium in the presence of the Hb solutions, indicating that the higher absorbance is due to Hb molecule and not nitrite production. Therefore, we cannot draw any conclusions about the effects of MetHb and COHb on the inflammatory response assessed by NO production in microglia cells.

4.2.2. ROS quantification

ROS quantification is important because it serves as a biomarker for neuroinflammation, particularly in activated microglia, which release ROS in response to various stimuli, and contribute to inflammatory processes.²²

Thus, we assessed ROS levels in BV-2 cells using a DCFH-DA dye, as ROS are indicative of cellular inflammation and/or stress when present at high concentrations. The non-fluorescent DCFH-DA molecule reacts with products derived from hydrogen peroxide, being converted into the fluorescent DCF form, being a measure of cellular hydrogen peroxide production.

For BV-2 cells (Figure 23), both MetHb and COHb treatments resulted in an increased mean fluorescence intensity, reflecting an increase in ROS production compared to the PBS control. Besides that, MetHb treatment led to an increase of around 55% in the production of cellular ROS compared to COHb (defining PBS as 100%). In conclusion, COHb leads to lower oxidative stress in BV-2 cell line, which may indicate lower neuroinflammatory response.

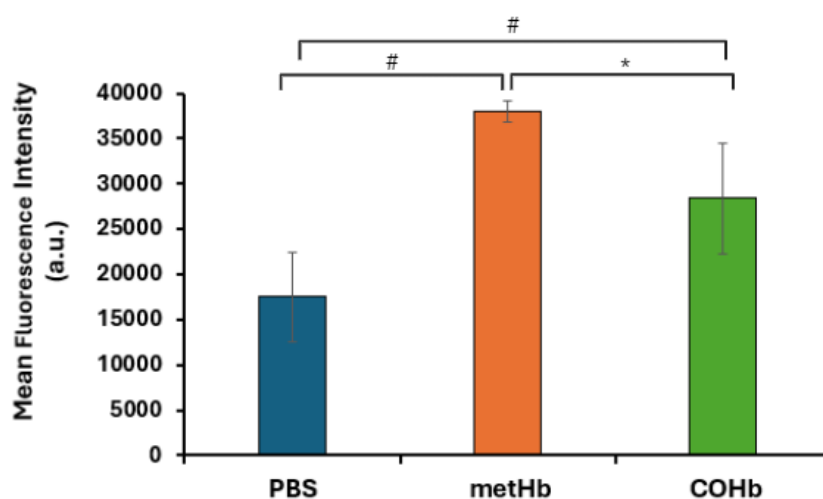


Figure 23 - ROS quantification in BV-2 cells pre-treated with PBS, MetHb and COHb solutions at a concentration of around 30 μM for 24 hours. Cells were exposed to 50% of Hb solutions in PBS, with PBS alone serving as the untreated control. Hydrogen peroxide (H_2O_2) levels were evaluated using a DCFH-DA dye and values presented as Mean Fluorescence Intensity (a.u.). Fluorescence was measured at an excitation wavelength of 485 nm and an emission wavelength of 535 nm. Results are shown as mean \pm SD from 5 independent experiments ($n=5$), each including 3 technical replicates. The asterisk (*) indicates statistically significant differences between MetHb- and COHb-treated cells. The cardinal (#) indicates significant differences between the untreated control (PBS) and each of the hemoglobin-treated conditions ($p < 0.05$, two-tailed unpaired Student's t-test).

4.2.3. TNF- α quantification

To further analyze the neuroinflammatory response of microglia cells exposed to MetHb and COHb, an ELISA assay was performed to quantify TNF- α levels in BV-2 cells. TNF- α is a pro-inflammatory cytokine expressed and released by activated microglia in response to brain injury, infection, or inflammation, being a more specific inflammatory biomarker than ROS.²²

The TNF- α concentration in the PBS-treated group was used as a baseline, set at 100%, for comparison with MetHb and COHb treatments. The standard curves used in these assays are presented in Annex 3.

As shown in Figure 24, results from three independent assays (different panels in Figure 24) using identical treatment conditions reveal considerable variability and inconsistency. In panel A, MetHb significantly decreases TNF- α levels compared to both the PBS control and COHb-treated cells. In panel B, there are no significant differences in TNF- α levels between cells treated with the Hb solutions and the PBS control, nor between the MetHb and COHb treatments. In panel C, both MetHb and COHb treatments result in a reduction in TNF- α levels compared to the PBS control, but there is no significant difference between the two treatments. Along with this inconsistency on the data, the standard curves (Annex 3) used for each assay show values with significantly varying orders of magnitude. This suggests potential errors in the TNF- α quantification across samples.

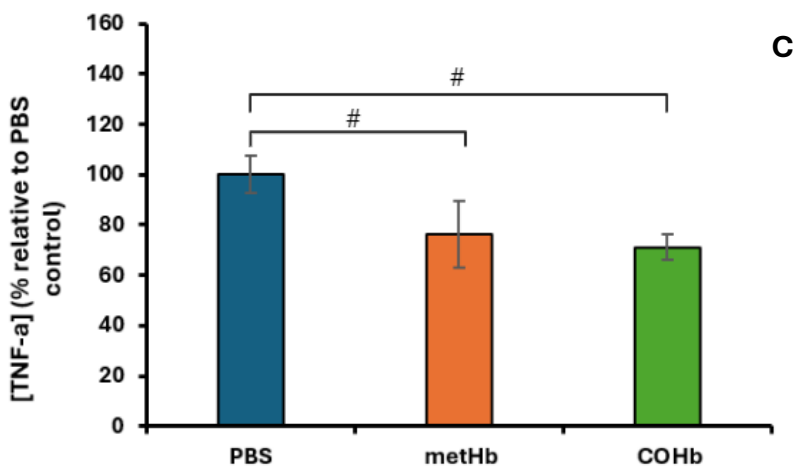
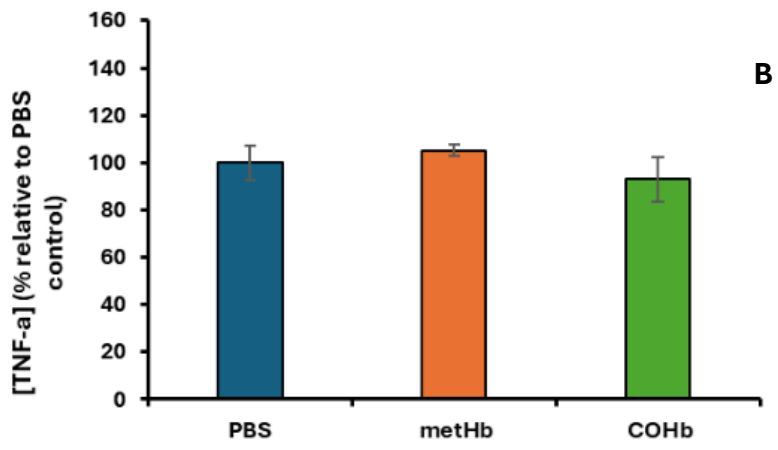
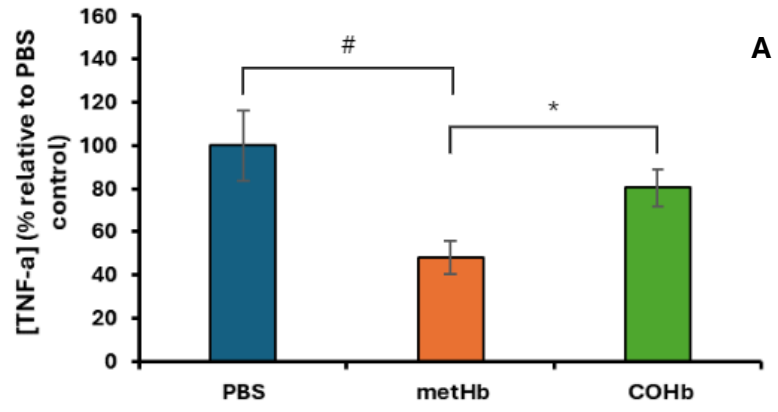


Figure 24 - TNF- α concentration percentage relative to PBS control in cell medium collected from BV-2 cells pre-treated with PBS, MetHb and COHb solutions at a concentration of around 30 μ M for 24 hours. Cells were exposed to 50% of Hb solutions in PBS, with PBS alone serving as the untreated control. TNF- α levels, quantified in pg of TNF- α per mL of cell medium, were determined using an ELISA assay. Absorbance readings were taken at 415 nm, with a wavelength correction at 560 nm, and converted into TNF- α concentrations based on standard curves. Results are shown as mean \pm SD, each panel (A, B and C) corresponding to one biological replicate that includes 3 technical replicates. The asterisk (*) indicates statistically significant differences between MetHb - and COHb-treated cells. The cardinal (#) indicates significant differences between the untreated control (PBS) and each of the hemoglobin-treated conditions ($p < 0.05$, two-tailed unpaired Student's t-test). The presented statistics represent technical reproducibility rather than biological significance.

Overall, due to the high variability, the results remain inconclusive regarding the effects of MetHb and COHb on TNF- α production in microglial cells. Still, it can also indicate that there is no change in TNF- α generation in response to MetHb or COHb.

For future experiments, neuroinflammation stimuli, such as LPS pre-treatment before the addition of Hb solutions could be a possible approach. LPS acts as a strong inflammatory stimulus that activates microglia and triggers a proinflammatory response.^{56,111} By treating the BV-2 cells with LPS prior to adding MetHb and COHb, it would be possible to assess if the Hb solutions either amplify the inflammatory response (synergistic effect) or if COHb has a protective effect by reducing the LPS-induced TNF- α production.

4.3. Neuronal viability and oxidative stress – assessment of cell death and stress biomarkers after MetHb and COHb treatment

4.3.1. Neuronal viability in differentiated and non-differentiated SH-SY5Y cells

For this viability assay, both differentiated and non-differentiated SH-SY5Y cells were used. Although non-differentiated SH-SY5Y cells are considered a homogenous cell line, it contains both neuroblast-like cells (N-type) and epithelial-like cells (S-type).¹¹⁰ Upon neuronal differentiation, induced by retinoic acid and a low concentration of FBS, the cells exhibit a different morphology compared to the undifferentiated ones, including reduced proliferation, enhanced neurite development and extension, and increased expression of neuronal markers.¹¹⁰

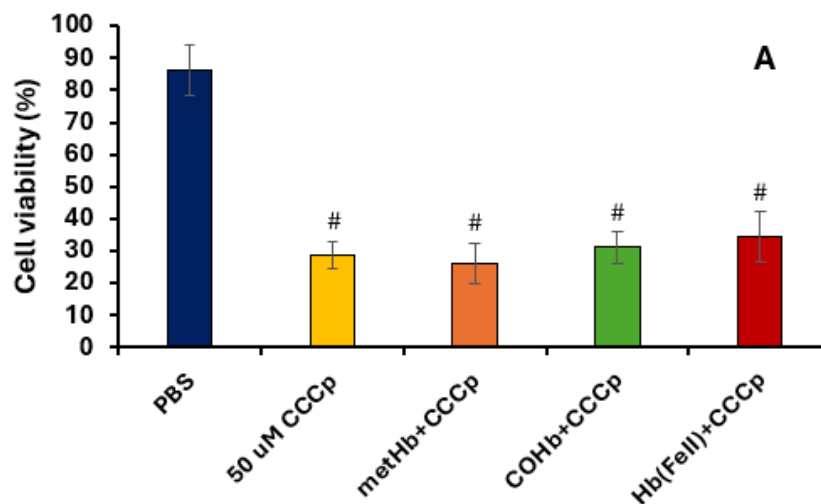
Differentiated cells more accurately mimic physiological neurons, while non-differentiated cells maintain a more tumor-like, undifferentiated state. By assessing the cytotoxic effects of MetHb and

potential protective effects of COHb on both of these cellular states, we expected to see differences related to cell's sensitivity. Differentiated SH-SY5Y cells are more responsive to oxidative stress and susceptible to cell death, while non-differentiated cells, being less specialized, are expected to be more resistant to toxic stimuli, allowing for a comparison of how these cell types react to the same treatments.

Non-differentiated and differentiated SH-SY5Y cells were pre-treated with PBS (used as a positive control for cell viability), MetHb, COHb, and Hb solutions, then CCCp, which was added to induce cell death for the evaluation of any protective or toxic effect derived from COHb, MetHb, or Hb. CCCp is an uncoupler molecule generating mitochondrial stress and cell death when applied at high concentrations. After 24 hours of CCCp treatment, cell viability was assessed through the cellular internalization of propidium iodide assessed by flow cytometry.

For both non-differentiated and differentiated cells not co-treated with CCCp (Annex 4), it is observed that MetHb, COHb, and Hb (Fe^{2+}) did not significantly affect cell viability, with values remaining close to those of the control (PBS) group. In conclusion MetHb, COHb nor Hb are toxic for undifferentiated and differentiated SH-SY5Y cells.

Figure 25 shows the results, with panel A corresponding to the non-differentiated cells and panel B showing the differentiated neuron-like cells. Only CCCp treatment leads to a significant reduction in cell viability, both in non-differentiated cells and differentiated cells. Furthermore, there is no significant difference in viability between cells treated with MetHb and those treated with COHb in both differentiated and non-differentiated conditions.



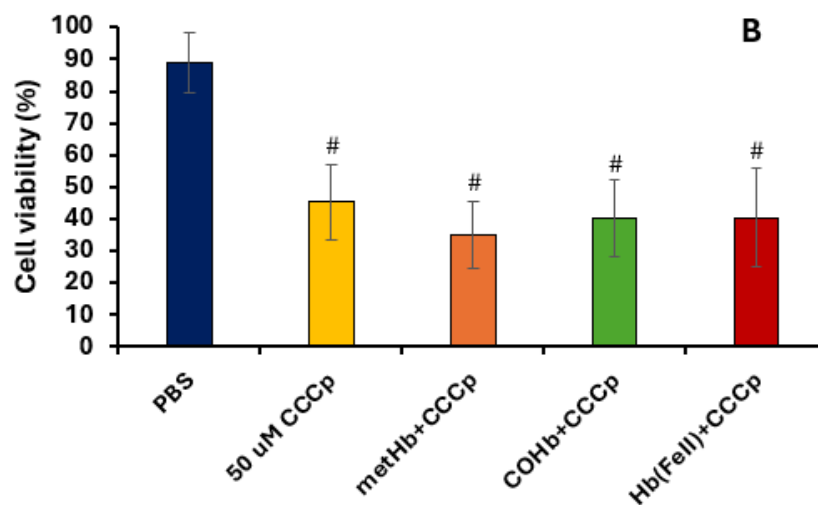


Figure 25 - Cell viability (%) assessment of non-differentiated (A) and differentiated (B) SH-SY5Y cells pre-treated with PBS, MetHb, COHb and Hb (Fe²⁺) solutions at a concentration of around 30 μM and co-treated with a mitochondrial uncoupler (CCCp) at a concentration of 50 μM for 24 hours. Cells were exposed to 50% of Hb solutions in PBS, with PBS alone serving as the untreated control. Cell viability was assessed by propidium iodide staining quantification by flow cytometry. Results are shown as mean ± SD from 3 independent experiments (n=3) for non-differentiated cells and 5 independent experiments (n=5) for differentiated cells, each including 3 technical replicates. The cardinal (#) indicates statistically significant differences between the untreated control (PBS) and both the treated control (PBS + 50 μM CCCp) and each of the hemoglobin-treated conditions (p < 0.05, two-tailed unpaired Student's t-test).

The results suggest that neither MetHb exhibits a toxic effect nor COHb provides a protective effect. MetHb causes a slight decrease in cell viability, while COHb appears to slightly increase it, in both differentiated and undifferentiated cells. However, these differences are not statistically significant.

For future experiments, it may be beneficial to use lower concentrations of CCCp, reducing the overall cell death and allowing a better understanding of COHb's potential protective effect.

4.3.2. ROS quantification

MetHb is a potent pro-oxidant molecule that exacerbates oxidative stress by generating ROS like superoxide anions (O₂⁻) and hydrogen peroxide (H₂O₂).⁴³ The oxidized form of Hb easily loses its heme, further promoting heme-mediated ROS generation, mainly due to the redox function of heme iron (Fe³⁺). This oxidative stress significantly contributes to neuroinflammation and neuronal injury.⁴³ Therefore, ROS quantification serves as an important biomarker of oxidative stress in cells.

We assessed ROS levels in differentiated neuron-like SH-SY5Y cells using a DCFH-DA dye, as ROS are indicative of cellular stress when present at high concentrations. We used the same procedure as for the BV-2 cells, mentioned in Section 4.2.2.

In differentiated SH-SY5Y cells (Figure 26), cells exhibited a significant increase in ROS production following treatment with either MetHb or COHb. However, there is no statistically significant difference between the ROS levels in cells treated with MetHb and those treated with COHb, as the mean fluorescence intensity values are very similar.

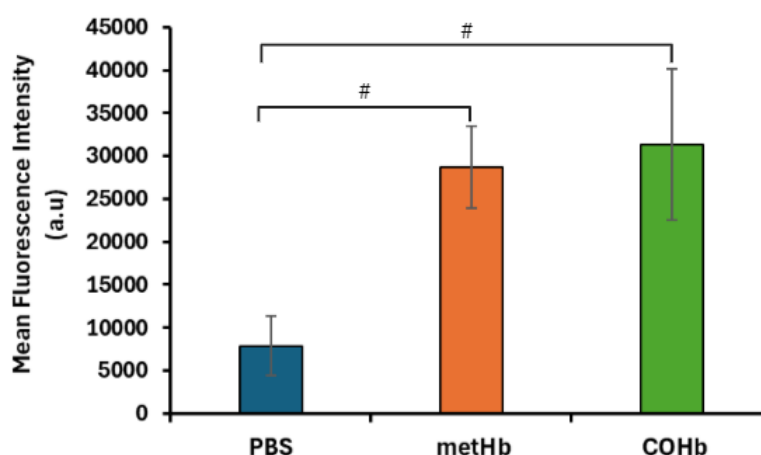


Figure 26 - ROS quantification in differentiated SH-SY5Y cells pre-treated with PBS, MetHb and COHb solutions at a concentration of around 30 μ M for 24 hours. Cells were exposed to 50% of Hb solutions in PBS, with PBS alone serving as the untreated control. Hydrogen peroxide (H_2O_2) levels were evaluated using a DCFH-DA dye and values presented as Mean Fluorescence Intensity (a.u.). Fluorescence was measured at an excitation wavelength of 485 nm and an emission wavelength of 535 nm. Results are shown as mean \pm SD from 4 independent experiments (n=4), each including 3 technical replicates. The cardinal (#) indicates statistically significant differences between the untreated control (PBS) and each of the hemoglobin-treated conditions ($p < 0.05$, two-tailed unpaired Student's t-test).

4.4. Blood-brain barrier (BBB) integrity – assessment of BBB permeability and tight junction integrity

4.4.1. BBB permeability assay

Under optimal culture conditions, hCMEC/D3 cells differentiate into elongated cells that form a monolayer, displaying characteristics of brain endothelial cells. This includes the expression of mature

adherens junction and tight junction proteins, such as VE-cadherin, claudin-3, claudin-5, and occludin, as well as scaffolding proteins like β -catenin and ZO-1 and ZO-2. These features contribute to a strong permeability barrier function.¹¹²

Given their ability to mimic the BBB, we used hCMEC/D3 cells to assess the effects of MetHb and COHb on BBB permeability. Lucifer yellow, a fluorescent tracer molecule, was used to evaluate the disruption of BBB integrity as it passes through only when permeability increases.

The results are presented as permeability coefficient values, calculated using the formula described in the Materials and Methods (Section 3.8.2.).

Because the generated data was not consistent, it is presented separately the results derived from two different time points, each one from two distinct biological replicates in Figure 27.

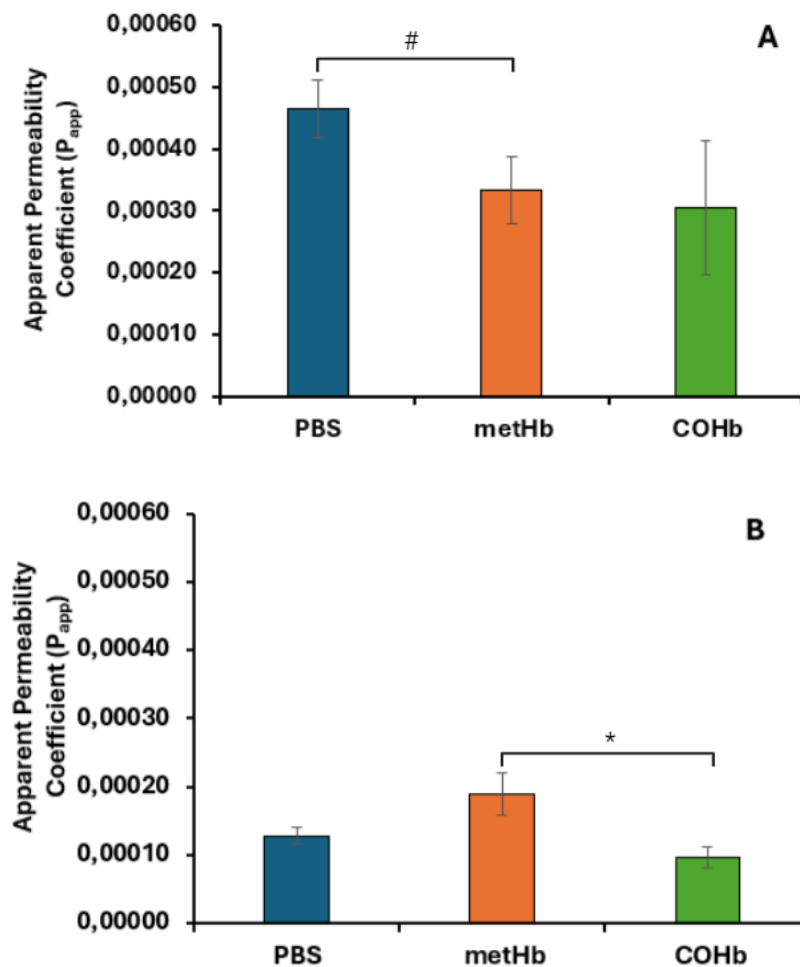


Figure 27 - Apparent permeability coefficient values of brain microvascular endothelial hCMEC/D3 cells pre-treated with PBS, MetHb and COHb solutions at a concentration of around 30 μ M for 24 hours. Cells were exposed to 50% of Hb solutions in PBS, with PBS alone serving as the untreated control. Cells were seeded into transwell inserts (placed into 24-well plates) with a surface area of 0,3 cm² and differentiated for 12 days into a cell monolayer. Samples collected from the basolateral compartment at 35 (**A**) and 45 minutes (**B**) after the addition of the Lucifer yellow dye to the apical compartment. Fluorescence was measured at an excitation wavelength of 485 nm and an emission wavelength of 535 nm. Results are shown as mean \pm SD, each panel corresponding to one biological replicate that includes 3 technical replicates. The asterisk (*) indicates statistically significant differences between MetHb- and COHb-treated cells. The cardinal (#) indicates significant differences between the untreated control (PBS) and each of the hemoglobin-treated conditions ($p < 0.05$, two-tailed unpaired Student's t-test). The presented statistics represent technical reproducibility rather than biological significance.

The permeability coefficient values show no clear tendency in any sample recovery time point (35 and 45 minutes) after the addition of the LY dye (Figure 7). After 35 min of LY treatment, MetHb decreases permeability compared to the PBS control. Following 45 min of LY treatment, permeability of MetHb treated cells is higher than barrier permeability of COHb-treated cells, but with no significant difference between the treatment conditions (MetHb and COHb) and the control (PBS).

The significant difference in MetHb effect on permeability coefficient values between 35 and 45 min of Lucifer yellow treatment does not allow any consistent conclusion about Hb effect on BBB function. This incongruity can be caused by issues related to cell confluence. If the hCMEC/D3 cells did not reach full confluence, it could indicate incomplete differentiation, and no barrier formation, which leads to insufficient or incorrect expression of tight junction proteins. This would impair the cells' ability to form a cohesive cell barrier that accurately mimics the BBB, affecting the permeability results.

4.4.2. Endothelial tight junction (ZO-1) integrity – immunofluorescence microscopy

To better understand whether COHb has any protective effects against the toxic impact of MetHb on the BBB, we did an immunofluorescence assay using hCMEC/D3 cells. These cells were treated with the Hb solutions for 24 hours, and the integrity of the BBB was assessed by examining the ZO-1 tight junction protein (Figure 28).

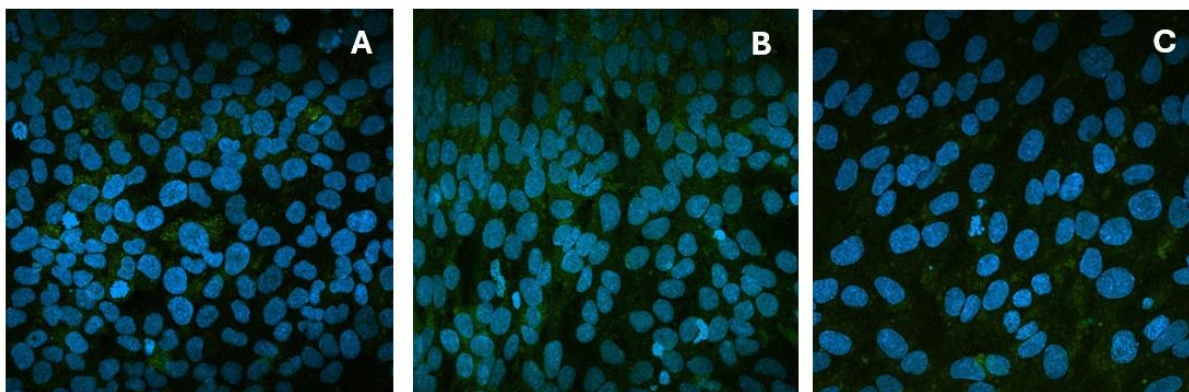


Figure 28 - Confocal microscopy images of immunofluorescence staining of the tight junction protein zonula occludens-1 (ZO-1) in hCMEC/D3 cells pre-treated with PBS (A), MetHb (B) and COHb (C) solutions at a concentration of around 30 μ M for 24 hours. Cells were exposed to 50% of Hb solutions in PBS, with PBS alone serving as the untreated control. Cells were seeded into 24-well plates and differentiated for 9 to 12 days. Then they were incubated with rabbit anti-ZO-1 primary antibody (diluted 1:50) for 4 hours and then with Alexa Fluor 488 (green) as a secondary antibody (diluted 1:2000). Cell nuclei were stained using Hoechst (blue) (diluted 1:1000) for 10 minutes. (original magnification 400x)

ZO-1 is a scaffolding protein that plays a key role in the formation and maintenance of tight junctions, which are essential for preserving the integrity and selective permeability of the BBB.^{2,9} Tight junctions are found at the contact points between adjacent endothelial cells, so ZO-1 staining is typically observed as a continuous or punctuate line along the edges of the cells, marking the presence of intact tight junctions where cells are connected. If the staining pattern is disrupted, it can indicate a loss of tight junction integrity or barrier dysfunction, which is often expected with treatments like MetHb.

In this case, we expected to observe a well-defined labeling along the cell borders where cells make contact. However, this expected pattern was not observed, preventing us from taking any conclusions from the results.

The non-specific and incorrect staining could be attributed to various factors, such as errors in the protocol (like incorrect antibody concentration or incubation time), the quality of the antibodies, or issues with the cells themselves. Moreover, the insufficient cell confluence and lack of barrier formation may be the main reason for weak tight junction protein expression, and incomplete or improper differentiation of the cells could also affect the results. If this is the case, it can explain the high variability of permeability coefficient values shown in Section 4.4.1 (BBB permeability assay).

In future experiments, it is essential to ensure that the cells reach full confluence before starting the experiment. If necessary, the differentiation period should be extended, and confluence must be verified before initiating the treatment with PBS, MetHb or COHb solutions. Another possible approach would be to optimize antibody concentrations and incubation times, as the non-specific staining may be due to incorrect concentrations. Besides that, increasing the primary antibody incubation time and reducing the

secondary antibody exposure could also reduce background staining. Additionally, confirming ZO-1 expression levels in hCMEC/D3 cells through a Western blot before the staining protocol would ensure the presence of the tight junction protein, would exclude issues related to low protein expression. Lastly, verifying that the fixation protocol preserves ZO-1 is essential, as prolonged storage after paraformaldehyde fixation may compromise protein integrity.

5. Discussion and conclusions

Hemorrhagic stroke is particularly dangerous due to its elevated mortality rate.^{20,21} During this condition, hemolysis results in the release of cell-free Hb, which rapidly oxidizes into MetHb (Fe³⁺). This oxidized form of Hb contributes to oxidative stress, lipid peroxidation, inflammation, BBB disruption, and neuronal death.²³⁻²⁵ In this context, microglia, neurons, and cerebral endothelial cells are all essential and play key roles in disease progression, whether they are favorable or deleterious.

Addressing the harmful effects of pro-oxidant MetHb represents a potential therapeutic strategy for hemorrhagic stroke. CO, a gas endogenously produced by the stress-response enzyme heme-oxygenase (HO), has been shown to have cytoprotective, anti-inflammatory, antioxidant, and anti-apoptotic effects.^{43,108} CO binds to reduced Hb with high affinity forming COHb, which is traditionally considered a marker of CO toxicity.³² However, emerging evidence suggests that COHb may have a protective biological role with potential therapeutic applications, as it stabilizes Hb in a less toxic and stable ferrous state by preventing its oxidation into cytotoxic MetHb.^{94,95}

Thus, this work aimed to understand whether COHb has a protective effect against the oxidative damage and inflammation induced by cell-free oxidized Hb. Specifically, if COHb formation could limit neuroinflammation, protect neurons, and preserve BBB integrity. For this purpose, three cell models were used: BV-2 microglia cell line (to study neuroinflammation), SH-SY5Y neuroblastoma cell line (to assess neuronal protection), and hCMEC/D3 brain microvascular endothelial cell line (to evaluate BBB permeability).

The results from this novel project, although still very preliminary, align with the hypothesis that COHb might be a cytoprotective molecule. In summary, it was demonstrated that COHb reduces inflammation measured by ROS production in microglial cells when compared to its oxidized form MetHb. These data suggest that COHb might stabilize cell-free Hb, preventing the release of toxic heme and iron by keeping the iron in a more stable state. The findings regarding neuronal viability and blood-brain barrier (BBB) integrity were inconclusive, so further investigation is necessary to fully understand the biological role of COHb in brain cells.

In microglia, both MetHb and COHb treatments increased ROS production, with MetHb inducing a stronger oxidative response than COHb. Although both forms of Hb triggered inflammation, COHb induced a less severe increase in ROS, suggesting its comparatively lower toxicity. While ROS results (Figure 23) supported the hypothesis, nitrite and TNF- α quantifications were inconclusive because Griess technique cannot be used to measure nitrite and TNF- α quantification was not robust. For future experiments, pre-treating the cells with LPS could serve as a strong inflammatory stimulus, fully activating the microglia and triggering an inflammatory response before treatment with MetHb and COHb. This approach would allow a better assessment of whether Hb solutions amplify or reduce the

existing LPS-induced TNF- α production. In hemorrhagic stroke, early inflammation is triggered by blood components like thrombin, fibrin, and hemoglobin, which act as damage-associated molecular patterns (DAMPs) and activate microglia to amplify the inflammatory response.^{22,23} The addition of the Hb solutions at a concentration of $\sim 30 \mu\text{M}$ may not have been sufficient to induce a significant activation state of cells and subsequent cytokine production, explaining the variability in the results. Additionally, analyzing other inflammatory markers such as surface receptors (CD14, CD45, CD68, CD11B, CX3CR1, MHC-II), chemokines (CCL2, CCL5, CCL20 and CXCL10), pro-inflammatory cytokines (IL-1 β , IL-6), iNOS, Iba-1 and matrix metalloproteinases (MMP2/9) could also provide a better understanding of the neuroinflammatory response.¹¹⁸⁻¹²⁰ Future work could involve Western blot techniques to quantify protein levels (iNOS, surface receptors, Iba-1), immunostaining for Iba-1 to assess microglial morphology, and ELISA for IL-1 β and IL-6. Flow cytometry could be employed to measure the percentage of cells expressing these markers and their mean fluorescence intensity. Quantitative RT-PCR could also be used to analyze mRNA levels for these genes. For NO quantification, a fluorometric probe like 2,3-diaminonaphthalene (DAN) or diaminofluoresceins (DAF) would surpass the interference caused by the reddish color of the Hb solutions.¹²¹ This approach would ensure more accurate assessment of NO levels, eliminating potential errors caused by Hb's natural color.

Neuronal viability assays in both differentiated and undifferentiated SH-SY5Y cells revealed no toxic effect from MetHb nor any protective effect from COHb. The disruption of mitochondrial membrane potential by CCCp leads to cell death through ATP depletion and increased oxidative stress. The results suggest that the extensive mitochondrial damage caused by CCCp might outweigh any protective effects of COHb, as COHb may not have a strong enough mechanism to counteract the toxic effects of CCCp. Lowering the CCCp concentration may reduce overall cell death, allowing for a better understanding of COHb's potential protective effects in future experiments. In the absence of CCCp co-treatment, neither MetHb nor COHb significantly affected cell viability, suggesting that none of the Hb forms were toxic to the neuronal cells. However, based on previous experiments and the observed ROS increase in cells treated with MetHb and COHb (Figure 26), higher cell death, particularly with MetHb, was expected in differentiated SH-SY5Y cells. One possible explanation is that the concentration of Hb used in the experiments may not have been sufficient to induce significant oxidative stress or cytotoxicity, as MetHb toxicity is dose-dependent.¹²² To further assess cell death/viability, alternative methods such as measuring cleaved caspase-3 levels (an apoptosis marker) via Western blot should be considered in future studies.¹²²

It was expected that differentiated SH-SY5Y cells, which more closely resemble physiological neurons, would be more sensitive to cytotoxic treatments, while non-differentiated cells, being less specialized and more tumor-like, would show greater resistance. However, the results revealed little difference in cell viability between the two types of cells. Since CCCp directly disrupts the mitochondrial membrane potential, its cytotoxic effect may be equally potent in both cell types, leading to similar cell death levels.

BBB permeability studies and ZO-1 tight junction analysis did not offer any clear conclusion. In this experimental approach there were some technical problems related to the cell culture confluency and barrier formation. Thus, there is still room for improvements in the future. Moreover, other techniques such as trans-endothelial electrical resistance (TEER) - electric analysis of the barrier - or the study of additional tight junction proteins could provide clearer insights into COHb's potential protective effects on the BBB.¹²³

Research into PEGylated COHb, a COHb-based oxygen carrier developed as blood substitute for transfusions, has shown promising results in vivo models of hemorrhagic shock¹²⁴ and patients with subarachnoid hemorrhage.¹²⁵ These studies demonstrated an improvement in cerebral blood flow and neuroprotection, which can be attributed to increased mean arterial pressure and enhanced tissue oxygenation, suggesting a potential COHb biological function and therapeutic potential.

Additionally, COHb has also been found to enhance the antioxidant capacity of RBCs, increasing intracellular GSH levels and strengthening the antioxidant defense system.⁹⁸ Moreover, COHb levels naturally rise in response to stress like inflammation and oxidative stress, suggesting its potential involvement in adaptive cellular responses.⁹³

Continuing the study of COHb's biological role, especially in pathological conditions, will be essential to comprehend its biological significance and potential therapeutic use. Although more research is needed to confirm the results of the present work and to further understand the molecular mechanisms underlying the effects of COHb in brain cells, these findings provide important information about the protective role COHb may have in human physiology, particularly in the context of hemorrhagic stroke.

6. References

1. Carter, Rita, et al. "The human brain book (1st American ed)." London [England], New York, NY (2009).
2. Brady, S. T. & Tai, L. Cell Biology of the Nervous System. in *Basic Neurochemistry: Principles of Molecular, Cellular, and Medical Neurobiology: Eighth Edition* 3–25 (Elsevier, 2011). doi:10.1016/B978-0-12-374947-5.00001-8.
3. Brodal, Per. *The Central Nervous System: Structure and Function*. (oxford university Press, 2010).
4. Südhof, T. C. The cell biology of synapse formation. *Journal of Cell Biology* vol. 220 Preprint at <https://doi.org/10.1083/jcb.202103052> (2021).
5. Martin, E. A., Lasseigne, A. M. & Miller, A. C. Understanding the Molecular and Cell Biological Mechanisms of Electrical Synapse Formation. *Frontiers in Neuroanatomy* vol. 14 Preprint at <https://doi.org/10.3389/fnana.2020.00012> (2020).
6. Jäkel, S. & Dimou, L. Glial cells and their function in the adult brain: A journey through the history of their ablation. *Frontiers in Cellular Neuroscience* vol. 11 Preprint at <https://doi.org/10.3389/fncel.2017.00024> (2017).
7. Jessen, K. R. Glial cells. *International Journal of Biochemistry and Cell Biology* vol. 36 1861–1867 Preprint at <https://doi.org/10.1016/j.biocel.2004.02.023> (2004).
8. Gomes, F. C. A., Spohr, T. C. L. S., Martinez, R. & Neto, V. M. *Cross-Talk between Neurons and Glia: Highlights on Soluble Factors*. *Braz J Med Biol Res* vol. 34 (2001).
9. Ludewig, P., Winneberger, J. & Magnus, T. The cerebral endothelial cell as a key regulator of inflammatory processes in sterile inflammation. *Journal of Neuroimmunology* vol. 326 38–44 Preprint at <https://doi.org/10.1016/j.jneuroim.2018.10.012> (2019).
10. Risau, W. & Wolburg, H. *Development of the Blood-Brain Barrier*. (1990).
11. Sweeney, M. D., Zhao, Z., Montagne, A., Nelson, A. R. & Zlokovic, B. V. From Physiology to Disease and Back. *Physiol Rev* **99**, 21–78 (2019).
12. Keep, R. F. *et al.* Vascular disruption and blood-brain barrier dysfunction in intracerebral hemorrhage. *Fluids Barriers CNS* **11**, (2014).
13. Feigin, V. L. *et al.* World Stroke Organization (WSO): Global Stroke Fact Sheet 2022. *International Journal of Stroke* vol. 17 18–29 Preprint at <https://doi.org/10.1177/17474930211065917> (2022).
14. European Observatory on Health Systems, and Policies. State of Health in the EU Portugal: Country Health Profile 2021 (2021).
15. Kuriakose, D. & Xiao, Z. Pathophysiology and treatment of stroke: Present status and future perspectives. *International Journal of Molecular Sciences* vol. 21 1–24 Preprint at <https://doi.org/10.3390/ijms21207609> (2020).

16. Kojic, B., Burina, A., Hodzic, R., Pasic, Z. & Sinanovic, O. RISK FACTORS IMPACT ON THE LONG-TERM SURVIVAL AFTER ISCHEMIC STROKE. *Acta Medica Saliniana* **41**, (2013).
17. Deb, P., Sharma, S. & Hassan, K. M. Pathophysiologic mechanisms of acute ischemic stroke: An overview with emphasis on therapeutic significance beyond thrombolysis. *Pathophysiology* vol. 17 197–218 Preprint at <https://doi.org/10.1016/j.pathophys.2009.12.001> (2010).
18. Stein, M. *et al.* Intracerebral hemorrhage in the very old: Future demographic trends of an aging population. *Stroke* **43**, 1126–1128 (2012).
19. Testai, F. D. & Aiyagari, V. Acute Hemorrhagic Stroke Pathophysiology and Medical Interventions: Blood Pressure Control, Management of Anticoagulant-Associated Brain Hemorrhage and General Management Principles. *Neurologic Clinics* vol. 26 963–985 Preprint at <https://doi.org/10.1016/j.ncl.2008.06.001> (2008).
20. Shi, Z. Pathophysiology of Hemorrhagic Stroke. in 77–96 (2017). doi:10.1007/978-981-10-5804-2_5.
21. Aronowski, J. & Zhao, X. Molecular pathophysiology of cerebral hemorrhage: Secondary brain injury. *Stroke* vol. 42 1781–1786 Preprint at <https://doi.org/10.1161/STROKEAHA.110.596718> (2011).
22. Mracsko, E. & Veltkamp, R. Neuroinflammation after intracerebral hemorrhage. *Front Cell Neurosci* **8**, (2014).
23. Alsbrook, D. L. *et al.* Neuroinflammation in Acute Ischemic and Hemorrhagic Stroke. *Current Neurology and Neuroscience Reports* vol. 23 407–431 Preprint at <https://doi.org/10.1007/s11910-023-01282-2> (2023).
24. Taylor, R. A. & Sansing, L. H. Microglial responses after ischemic stroke and intracerebral hemorrhage. *Clinical and Developmental Immunology* vol. 2013 Preprint at <https://doi.org/10.1155/2013/746068> (2013).
25. Imai, T. *et al.* Intracellular Fe²⁺ accumulation in endothelial cells and pericytes induces blood-brain barrier dysfunction in secondary brain injury after brain hemorrhage. *Sci Rep* **9**, (2019).
26. Lapchak, P. A. & Araujo, D. M. Advances in hemorrhagic stroke therapy: Conventional and novel approaches. *Expert Opinion on Emerging Drugs* vol. 12 389–406 Preprint at <https://doi.org/10.1517/14728214.12.3.389> (2007).
27. A David Mendelow. *Stroke: Pathophysiology, Diagnosis, and Management*. vol. Section I, Chapter 8 (2015).
28. Hopper, C. P., Zambrana, P. N., Goebel, U. & Wollborn, J. A brief history of carbon monoxide and its therapeutic origins. *Nitric Oxide - Biology and Chemistry* vols 111–112 45–63 Preprint at <https://doi.org/10.1016/j.niox.2021.04.001> (2021).
29. Tenhunen, R., Marver, H. S. & Schmid, R. Microsomal Heme Oxygenase. *Journal of Biological Chemistry* **244**, 6388–6394 (1969).
30. Ryter, S. W., Alam, J. & Choi, A. M. K. Heme Oxygenase-1/Carbon Monoxide: From Basic Science to Therapeutic Applications. (2006) doi:10.1152/physrev.00011.2005.-The.

31. Idriss, N. K., Blann, A. D. & Lip, G. Y. H. Hemoxygenase-1 in Cardiovascular Disease. *Journal of the American College of Cardiology* vol. 52 971–978 Preprint at <https://doi.org/10.1016/j.jacc.2008.06.019> (2008).
32. Bansal, S., Liu, D., Mao, Q., Bauer, N. & Wang, B. Carbon Monoxide as a Potential Therapeutic Agent: A Molecular Analysis of Its Safety Profiles. *Journal of Medicinal Chemistry* vol. 67 9789–9815 Preprint at <https://doi.org/10.1021/acs.jmedchem.4c00823> (2024).
33. Sammut, I. A. *et al.* Carbon monoxide is a major contributor to the regulation of vascular tone in aortas expressing high levels of haeme oxygenase-1. *Br J Pharmacol* **125**, 1437–1444 (1998).
34. Motterlini, R. *et al.* Heme Oxygenase-1-Derived Carbon Monoxide Contributes to the Suppression of Acute Hypertensive Responses In Vivo. <http://circres.ahajournals.org/> (1998).
35. Duckers, Henricus J., *et al.* "Heme oxygenase-1 protects against vascular constriction and proliferation." *Nature medicine* 7.6 (2001): 693-698.
36. Józkwicz, Alicja, *et al.* "Heme oxygenase and angiogenic activity of endothelial cells: stimulation by carbon monoxide and inhibition by tin protoporphyrin-IX." *Antioxidants and Redox Signaling* 5.2 (2003): 155-162.
37. Wagener, F. A. D. T. G. *et al.* Different faces of the heme-heme oxygenase system in inflammation. *Pharmacological Reviews* vol. 55 551–571 Preprint at <https://doi.org/10.1124/pr.55.3.5> (2003).
38. Carbon monoxide has anti-inflammatory effects involving the mitogen-activated protein kinase pathway.
39. Brouard, S. *et al.* Carbon Monoxide Generated by Heme Oxygenase 1 Suppresses Endothelial Cell Apoptosis. *J. Exp. Med* vol. 192 <http://www.jem.org/cgi/content/full/192/7/1015> (2000).
40. Silva, G., Cunha, A., Grégoire, I. P., Seldon, M. P. & Soares, M. P. The Antiapoptotic Effect of Heme Oxygenase-1 in Endothelial Cells Involves the Degradation of p38 α MAPK Isoform. *The Journal of Immunology* **177**, 1894–1903 (2006).
41. Physiology, C. *et al.* Cellular Physiology Cellular Physiology Cellular Physiology Cellular Physiology Carbon Monoxide Protects Against Ischemia-Reperfusion Injury in Vitro via Antioxidant Properties. *Original Paper Cell Physiol Biochem* vol. 29 www.karger.com www.karger.com/cpb (2012).
42. Morita, T. Heme oxygenase and atherosclerosis. *Arteriosclerosis, Thrombosis, and Vascular Biology* vol. 25 1786–1795 Preprint at <https://doi.org/10.1161/01.ATV.0000178169.95781.49> (2005).
43. Quaye, I. K. Extracellular hemoglobin: The case of a friend turned foe. *Front Physiol* **6**, (2015).
44. Rochette, L., Cottin, Y., Zeller, M. & Vergely, C. Carbon monoxide: Mechanisms of action and potential clinical implications. *Pharmacology and Therapeutics* vol. 137 133–152 Preprint at <https://doi.org/10.1016/j.pharmthera.2012.09.007> (2013).
45. Leffler, C. W., Parfenova, H. & Jaggar, J. H. Carbon monoxide as an endogenous vascular modulator. *Am J Physiol Heart Circ Physiol* **301**, (2011).

46. Ramos, Kenneth S., Hua Lin, and James J. McGrath. "Modulation of cyclic guanosine monophosphate levels in cultured aortic smooth muscle cells by carbon monoxide." *Biochemical pharmacology* 38.8 (1989): 1368-1370.
47. Morita, T., Perrellat, M. A., Leeti, M.-E., Kourembanas, S. & Avery, M. E. *Smooth Muscle Cell-Derived Carbon Monoxide Is a Regulator of Vascular CGMP (Hypoxia/Vessel Tone/Gene Regulation) Communicated By*. vol. 92 (1995).
48. Wang, R., Lingyun Wu, and Zunzhe Wang. "The direct effect of carbon monoxide on K Ca channels in vascular smooth muscle cells." *Pflügers Archiv* 434 (1997): 285-291.
49. Lim, I. *et al.* Carbon monoxide activates human intestinal smooth muscle L-type Ca²⁺ channels through a nitric oxide-dependent mechanism Carbon monoxide activates human intestinal smooth muscle L-type Ca²⁺ channels through a nitric oxide-dependent mechanism Human Jejunal Circular Smooth Muscle Cell Preparation. *Am J Physiol Gastrointest Liver Physiol* **288**, 7–14 (2005).
50. Amersi, F. *et al.* Ex vivo exposure to carbon monoxide prevents hepatic ischemia/reperfusion injury through p38 MAP kinase pathway. *Hepatology* **35**, 815–823 (2002).
51. Almeida, A. S., Soares, N. L., Vieira, M., Gramsbergen, J. B. & Vieira, H. L. A. Carbon monoxide releasing molecule-A1 (CORM-A1) improves neurogenesis: Increase of neuronal differentiation yield by preventing cell death. *PLoS One* **11**, AR (2016).
52. Vieira, H. L. A., Queiroga, C. S. F. & Alves, P. M. Pre-conditioning induced by carbon monoxide provides neuronal protection against apoptosis. *J Neurochem* **107**, 375–384 (2008).
53. Almeida, A. S., Queiroga, C. S. F., Sousa, M. F. Q., Alves, P. M. & Vieira, H. L. A. Carbon monoxide modulates apoptosis by reinforcing oxidative metabolism in astrocytes: Role of Bcl-2. *Journal of Biological Chemistry* **287**, 10761–10770 (2012).
54. Oliveira, S. R., Figueiredo-Pereira, C., Duarte, C. B. & Vieira, H. L. A. P2X7 Receptors Mediate CO-Induced Alterations in Gene Expression in Cultured Cortical Astrocytes—Transcriptomic Study. *Mol Neurobiol* **56**, 3159–3174 (2019).
55. Bani-Hani, M. G., Greenstein, D., Mann, B. E., Green, C. J. & Motterlini, R. Modulation of thrombin-induced neuroinflammation in BV-2 microglia by carbon monoxide-releasing molecule 3. *Journal of Pharmacology and Experimental Therapeutics* **318**, 1315–1322 (2006).
56. Soares, N. L. *et al.* Carbon Monoxide Modulation of Microglia-Neuron Communication: Anti-Neuroinflammatory and Neurotrophic Role. *Mol Neurobiol* **59**, 872–889 (2022).
57. Figueiredo-Pereira, C., Dias-Pedroso, D., Soares, N. L. & Vieira, H. L. A. CO-mediated cytoprotection is dependent on cell metabolism modulation. *Redox Biology* vol. 32 Preprint at <https://doi.org/10.1016/j.redox.2020.101470> (2020).
58. Motterlini, R. & Otterbein, L. E. The therapeutic potential of carbon monoxide. *Nature Reviews Drug Discovery* vol. 9 728–743 Preprint at <https://doi.org/10.1038/nrd3228> (2010).
59. Roux-Dalvai, F. *et al.* Extensive analysis of the cytoplasmic proteome of human erythrocytes using the peptide ligand library technology and advanced mass spectrometry. *Molecular and Cellular Proteomics* **7**, 2254–2269 (2008).

60. Billet, H. H. Hemoglobin and hematocrit. *In: Walker HK, Hall WD, Hurst JW, editors. Clinical Methods: The History, Physical, and Laboratory Examinations. 3rd edition. Boston: Butterworths; 1990. Chapter 151. Available from: <https://www.ncbi.nlm.nih.gov/books/NBK259/>.*
61. Jensen, B. & Fago, A. A Novel Possible Role for Met Hemoglobin as Carrier of Hydrogen Sulfide in the Blood. *Antioxidants and Redox Signaling* vol. 32 258–265 Preprint at <https://doi.org/10.1089/ars.2019.7877> (2020).
62. Cummins, E. P., Selfridge, A. C., Sporn, P. H., Sznajder, J. I. & Taylor, C. T. Carbon dioxide-sensing in organisms and its implications for human disease. *Cellular and Molecular Life Sciences* vol. 71 831–845 Preprint at <https://doi.org/10.1007/s00018-013-1470-6> (2014).
63. Mairbäurl, H. & Weber, R. E. Oxygen transport by hemoglobin. *Compr Physiol* **2**, 1463–1489 (2012).
64. Umbreit, J. Methemoglobin - It's not just blue: A concise review. *American Journal of Hematology* vol. 82 134–144 Preprint at <https://doi.org/10.1002/ajh.20738> (2007).
65. Rifkind, J. M. & Nagababu, E. Hemoglobin redox reactions and red blood cell aging. *Antioxidants and Redox Signaling* vol. 18 2274–2283 Preprint at <https://doi.org/10.1089/ars.2012.4867> (2013).
66. Çimen, M. Y. B. Free radical metabolism in human erythrocytes. *Clinica Chimica Acta* vol. 390 1–11 Preprint at <https://doi.org/10.1016/j.cca.2007.12.025> (2008).
67. May, J. M., Qu, Z.-C. & Morrow, J. D. *Mechanisms of Ascorbic Acid Recycling in Human Erythrocytes*. www.bba-direct.com.
68. Ogasawara, Y., Funakoshi, M. & Ishii, K. Glucose metabolism is accelerated by exposure to t-butylhydroperoxide during NADH consumption in human erythrocytes. *Blood Cells Mol Dis* **41**, 237–243 (2008).
69. Buehler, P. W. & Alayash, A. I. *Redox Biology of Blood Revisited: The Role of Red Blood Cells in Maintaining Circulatory Reductive Capacity. Mini Review ANTIOXIDANTS & REDOX SIGNALING* vol. 7 (2005).
70. Vitturi, D. A. *et al.* Antioxidant functions for the hemoglobin β 93 cysteine residue in erythrocytes and in the vascular compartment in vivo. *Free Radic Biol Med* **55**, 119–129 (2013).
71. Buehler, P. W. & Agnillo, F. D. ' *Toxicological Consequences of Extracellular Hemoglobin: Biochemical and Physiological Perspectives*. www.liebertonline.com=ars.
72. Drvenica, I. T., Stančić, A. Z., Maslovarić, I. S., Trivanović, D. I. & Ilić, V. L. Extracellular Hemoglobin: Modulation of Cellular Functions and Pathophysiological Effects. *Biomolecules* vol. 12 Preprint at <https://doi.org/10.3390/biom12111708> (2022).
73. Vallelian, F., Buehler, P. W. & Schaer, D. J. *Hemolysis, Free Hemoglobin Toxicity, and Scavenger Protein Therapeutics*. http://ashpublications.org/blood/article-pdf/140/17/1837/2052037/blood_bld-2022-015596-c-main.pdf.
74. Wang, D. *et al.* In vivo reduction of cell-free methemoglobin to oxyhemoglobin results in vasoconstriction in canines. *Transfusion (Paris)* **53**, 3149–3163 (2013).

75. Silva, G. *et al.* Oxidized hemoglobin is an endogenous proinflammatory agonist that targets vascular endothelial cells. *Journal of Biological Chemistry* **284**, 29582–29595 (2009).
76. Schaer, D. J. & Buehler, P. W. Cell-free hemoglobin and its scavenger proteins: New disease models leading the way to targeted therapies. *Cold Spring Harb Perspect Med* **3**, (2013).
77. Butt, O. I., Buehler, P. W. & D’Agnillo, F. Blood-brain barrier disruption and oxidative stress in guinea pig after systemic exposure to modified cell-free hemoglobin. *American Journal of Pathology* **178**, 1316–1328 (2011).
78. Kaiser, S. *et al.* Neuroprotection after hemorrhagic stroke depends on cerebral heme oxygenase-1. *Antioxidants* **8**, (2019).
79. Zhou, Y., Wang, Y., Wang, J., Anne Stetler, R. & Yang, Q. W. Inflammation in intracerebral hemorrhage: From mechanisms to clinical translation. *Progress in Neurobiology* vol. 115 25–44 Preprint at <https://doi.org/10.1016/j.pneurobio.2013.11.003> (2014).
80. Gram, M. *et al.* Hemoglobin Induces Inflammation after Preterm Intraventricular Hemorrhage by Methemoglobin Formation. <http://www.jneuroinflammation.com/content/10/1/100> (2013).
81. Ding, R. *et al.* Peroxynitrite decomposition catalyst prevents matrix metalloproteinase-9 activation and neurovascular injury after hemoglobin injection into the caudate nucleus of rats. *Neuroscience* **297**, 182–193 (2015).
82. Katsu, M. *et al.* Hemoglobin-induced oxidative stress contributes to matrix metalloproteinase activation and blood-brain barrier dysfunction in vivo. *Journal of Cerebral Blood Flow and Metabolism* **30**, 1939–1950 (2010).
83. Yang, S. *et al.* Hemoglobin-induced nitric oxide synthase overexpression and nitric oxide production contribute to blood-brain barrier disruption in the rat. *Journal of Molecular Neuroscience* **51**, 352–363 (2013).
84. Keep, R. F. *et al.* Brain endothelial cell junctions after cerebral hemorrhage: Changes, mechanisms and therapeutic targets. *Journal of Cerebral Blood Flow and Metabolism* vol. 38 1255–1275 Preprint at <https://doi.org/10.1177/0271678X18774666> (2018).
85. Owens, E. O. Endogenous carbon monoxide production in disease. *Clinical Biochemistry* vol. 43 1183–1188 Preprint at <https://doi.org/10.1016/j.clinbiochem.2010.07.011> (2010).
86. Stucki, D. & Stahl, W. Carbon monoxide – beyond toxicity? *Toxicology Letters* vol. 333 251–260 Preprint at <https://doi.org/10.1016/j.toxlet.2020.08.010> (2020).
87. Widdop, B. *Analysis of Carbon Monoxide*. *Ann Clin Biochem* vol. 39 (2002).
88. Boumba, V. A. & Vougiouklakis, T. Evaluation of the methods used for carboxyhemoglobin analysis in postmortem blood. *Int J Toxicol* **24**, 275–281 (2005).
89. Olson, K. N., Hillyer, M. A., Kloss, J. S., Geiselhart, R. J. & Apple, F. S. Accident or arson: Is CO-oximetry reliable for carboxyhemoglobin measurement postmortem? *Clin Chem* **56**, 515–519 (2010).
90. Hampson, N. B. *Carboxyhemoglobin: A Primer for Clinicians*. vol. 45 (2018).
91. Goldbaum, L. R.; Ramirez, R.G.; Absalon, K.B. What is the Mechanism of Carbon Monoxide Toxicity? *Aviat. Space Environ. Med.* **46**, 1289-1291 (1976).

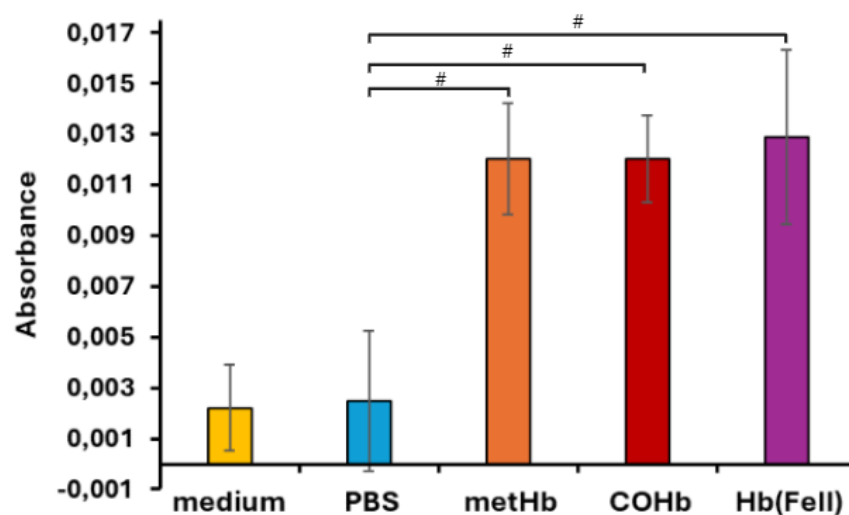
92. Mao, Q. *et al.* Sensitive quantification of carbon monoxide in vivo reveals a protective role of circulating hemoglobin in CO intoxication. *Commun Biol* **4**, (2021).
93. Carrola, A., Romão, C. C. & Vieira, H. L. A. Carboxyhemoglobin (COHb): Unavoidable Bystander or Protective Player? *Antioxidants* vol. 12 Preprint at <https://doi.org/10.3390/antiox12061198> (2023).
94. Sher, E. A., Shaklai, M. & Shaklai, N. Carbon monoxide promotes respiratory hemoproteins iron reduction using peroxides as electron donors. *PLoS One* **7**, (2012).
95. Pamplona, A. *et al.* Heme oxygenase-1 and carbon monoxide suppress the pathogenesis of experimental cerebral malaria. *Nat Med* **13**, 703–710 (2007).
96. Bissé, E. *et al.* Hemoglobin Kirklareli (α H58L), a new variant associated with iron deficiency and increased CO binding. *Journal of Biological Chemistry* **292**, 2542–2555 (2017).
97. Kitagishi, H. *et al.* Feedback Response to Selective Depletion of Endogenous Carbon Monoxide in the Blood. *J Am Chem Soc* **138**, 5417–5425 (2016).
98. Metere, A. *et al.* Carbon monoxide signaling in human red blood cells: Evidence for pentose phosphate pathway activation and protein Deglutathionylation. *Antioxid Redox Signal* **20**, 403–416 (2014).
99. Ogaki, S. *et al.* Carbon monoxide-bound red blood cell resuscitation ameliorates hepatic injury induced by massive hemorrhage and red blood cell resuscitation via hepatic cytochrome P450 protection in hemorrhagic shock rats. *J Pharm Sci* **103**, 2199–2206 (2014).
100. Sakai, H., Horinouchi, H., Tsuchida, E. & Kobayashi, K. Hemoglobin vesicles and red blood cells as carriers of carbon monoxide prior to oxygen for resuscitation after hemorrhagic shock in a rat model. *Shock* **31**, 507–514 (2009).
101. Cabrales, P., Tsai, A. G. & Intaglietta, M. Hemorrhagic shock resuscitation with carbon monoxide saturated blood. *Resuscitation* **72**, 306–318 (2007).
102. Ogaki, S. *et al.* Kupffer cell inactivation by carbon monoxide bound to red blood cells preserves hepatic cytochrome P450 via anti-oxidant and anti-inflammatory effects exerted through the HMGB1/TLR-4 pathway during resuscitation from hemorrhagic shock. *Biochem Pharmacol* **97**, 310–319 (2015).
103. Ryter, S. W. & Choi, A. M. K. Targeting heme oxygenase-1 and carbon monoxide for therapeutic modulation of inflammation. *Translational Research* vol. 167 7–34 Preprint at <https://doi.org/10.1016/j.trsl.2015.06.011> (2016).
104. Ji, X. *et al.* Toward Carbon Monoxide-Based Therapeutics: Critical Drug Delivery and Developability Issues. *Journal of Pharmaceutical Sciences* vol. 105 406–416 Preprint at <https://doi.org/10.1016/j.xphs.2015.10.018> (2016).
105. Tift, M. S., Ponganis, P. J. & Crocker, D. E. Elevated carboxyhemoglobin in a marine mammal, the northern elephant seal. *Journal of Experimental Biology* **217**, 1752–1757 (2014).
106. Romão, C. C., Blättler, W. A., Seixas, J. D. & Bernardes, G. J. L. Developing drug molecules for therapy with carbon monoxide. *Chem Soc Rev* **41**, 3571–3583 (2012).
107. Abuchowski, A. SANGUINATE (PEGylated Carboxyhemoglobin Bovine): Mechanism of Action and Clinical Update. *Artif Organs* **41**, 346–350 (2017).

108. Motterlini, R. & Foresti, R. Biological signaling by carbon monoxide and carbon monoxide-releasing molecules. *Am J Physiol Cell Physiol* **312**, 302–313 (2017).
109. Queiroga, C. S. F., Vercelli, A. & Vieira, H. L. A. Carbon monoxide and the CNS: Challenges and achievements. *British Journal of Pharmacology* vol. 172 1533–1545 Preprint at <https://doi.org/10.1111/bph.12729> (2015).
110. Simões, R. F. *et al.* Refinement of a differentiation protocol using neuroblastoma SH-SY5Y cells for use in neurotoxicology research. *Food and Chemical Toxicology* **149**, (2021).
111. Blasi, E., Barluzzi, R., Bocchini, V., Mazzolla, R. & Bistoni, F. *Immortalization of Murine Microglial Cells by a V-Raf/v-Myc Carrying Retrovirus*. *Journal of Neuroimmunology* vol. 27 (1990).
112. Weksler, B., Romero, I. A. & Couraud, P. O. The hCMEC/D3 cell line as a model of the human blood brain barrier. *Fluids and Barriers of the CNS* vol. 10 Preprint at <https://doi.org/10.1186/2045-8118-10-16> (2013).
113. Nakai, K. *et al.* Inhibition of endothelium-dependent relaxation by hemoglobin in rabbit aortic strips: comparison between acellular hemoglobin derivatives and cellular hemoglobins. *J Cardiovasc Pharmacol* **28**, 115–123 (1996).
114. Kuck, J. L. *et al.* Ascorbic acid attenuates endothelial permeability triggered by cell-free hemoglobin. *Biochem Biophys Res Commun* **495**, 433–437 (2018).
115. Surgenor, D. M. N. *The Red Blood Cell: Volume II*. vols 2, Chapter 17 (Elsevier Science, 2013).
116. Sharma, J. N., Al-Omran, A. & Parvathy, S. S. Role of nitric oxide in inflammatory diseases. *Inflammopharmacology* vol. 15 252–259 Preprint at <https://doi.org/10.1007/s10787-007-0013-x> (2007).
117. Eigenmann, D. E. *et al.* *Comparative Study of Four Immortalized Human Brain Capillary Endothelial Cell Lines, HCMEC/D3, HBMEC, TY10, and BB19, and Optimization of Culture Conditions, for an in Vitro Blood-Brain Barrier Model for Drug Permeability Studies* *FLUIDS AND BARRIERS OF THE CNS Comparative Study of Four Immortalized Human Brain Capillary Endothelial Cell Lines, HCMEC/D3, HBMEC, TY10, and BB19, and Optimization of Culture Conditions, for an in Vitro Blood-Brain Barrier Model for Drug Permeability Studies*. *Fluids and Barriers of the CNS* vol. 10 <http://www.fluidsbarrierscns.com/content/10/1/33> (2013).
118. Rock, R. B. *et al.* Role of microglia in central nervous system infections. *Clinical Microbiology Reviews* vol. 17 942–964 Preprint at <https://doi.org/10.1128/CMR.17.4.942-964.2004> (2004).
119. Maguire, E. *et al.* Assaying Microglia Functions In Vitro. *Cells* vol. 11 Preprint at <https://doi.org/10.3390/cells11213414> (2022).
120. Bi, R., Fang, Z., You, M., He, Q. & Hu, B. Microglia Phenotype and Intracerebral Hemorrhage: A Balance of Yin and Yang. *Frontiers in Cellular Neuroscience* vol. 15 Preprint at <https://doi.org/10.3389/fncel.2021.765205> (2021).
121. Goshi, E., Zhou, G. & He, Q. Nitric oxide detection methods in vitro and in vivo. *Medical Gas Research* vol. 9 192–207 Preprint at <https://doi.org/10.4103/2045-9912.273957> (2019).

122. Wang, X., Mori, T., Sumii, T. & Lo, E. H. Hemoglobin-induced cytotoxicity in rat cerebral cortical neurons: Caspase activation and oxidative stress. *Stroke* **33**, 1882–1888 (2002).
123. Helms, H. C. *et al.* In vitro models of the blood-brain barrier: An overview of commonly used brain endothelial cell culture models and guidelines for their use. *Journal of Cerebral Blood Flow and Metabolism* vol. 36 862–890 Preprint at <https://doi.org/10.1177/0271678X16630991> (2015).
124. Nugent, W. H. *et al.* Effects of sanguinate on systemic and microcirculatory variables in a model of prolonged hemorrhagic shock. *Shock* **52**, 108–115 (2019).
125. Dhar, R., Misra, H. & Diringier, M. N. SANGUINATE™ (PEGylated Carboxyhemoglobin Bovine) Improves Cerebral Blood Flow to Vulnerable Brain Regions at Risk of Delayed Cerebral Ischemia After Subarachnoid Hemorrhage. *Neurocrit Care* **27**, 341–349 (2017).

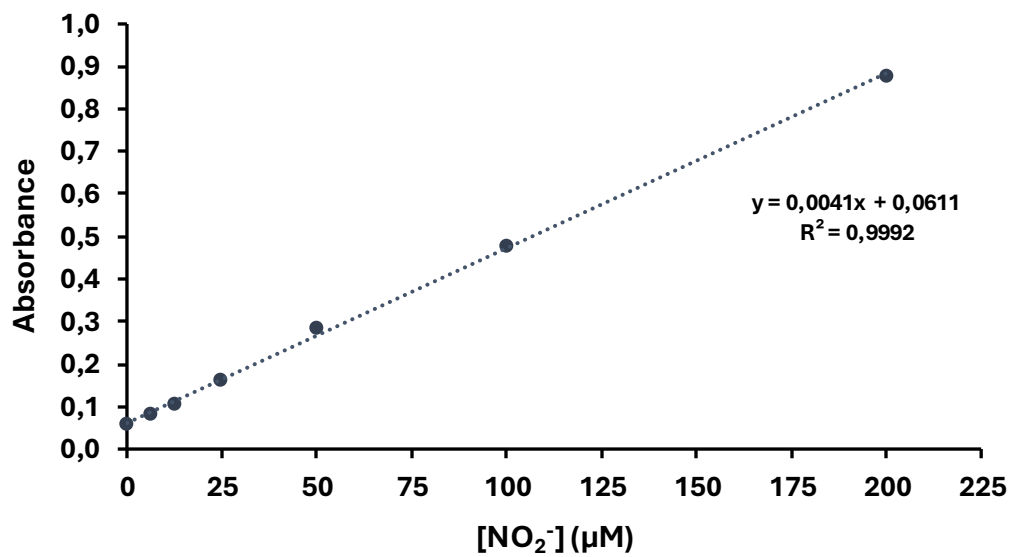
7. Annexes

Annex 1: Griess assay (NO quantification) - BV-2 microglial cells treatment with PBS, MetHb, COHb and Hb (Fe²⁺) for 24 hours



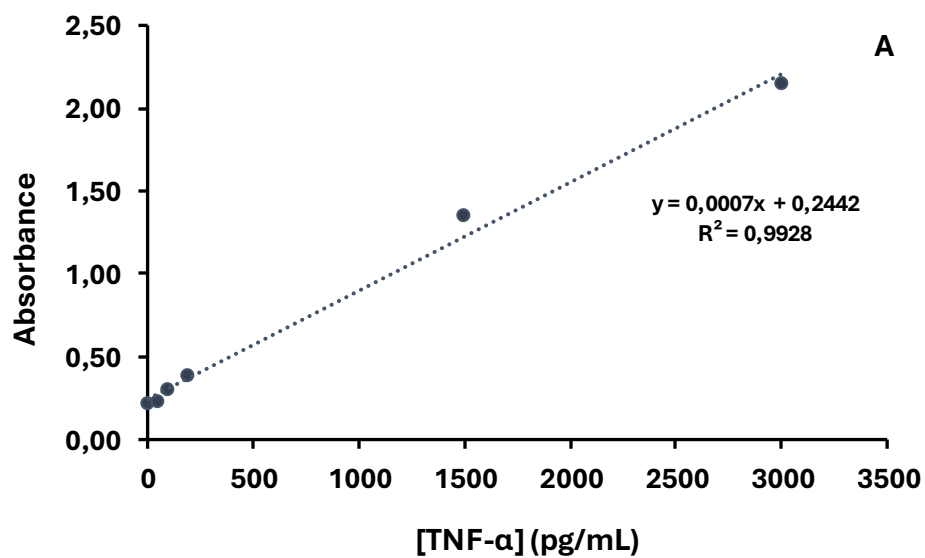
Annex Figure 1 – Quantification of nitrite (NO₂⁻) levels (presented in the graph as absorbance values) in cell medium collected from BV-2 cells pre-treated with PBS, MetHb, COHb and Hb (Fe²⁺) solutions at a concentration of around 30 μM for 24 hours by Griess assay. Cells were exposed to 50% of Hb solutions in PBS, with PBS alone serving as the untreated control. Griess assay was done as described in materials and methods. Absorbance was measured at 540 nm. Results are shown as mean ± SD from 3 independent experiments (n=3), each including 3 technical replicates. The cardinal (#) indicates significant differences between the untreated control (PBS) and each of the hemoglobin-treated conditions (p < 0.05, two-tailed unpaired Student's t-test).

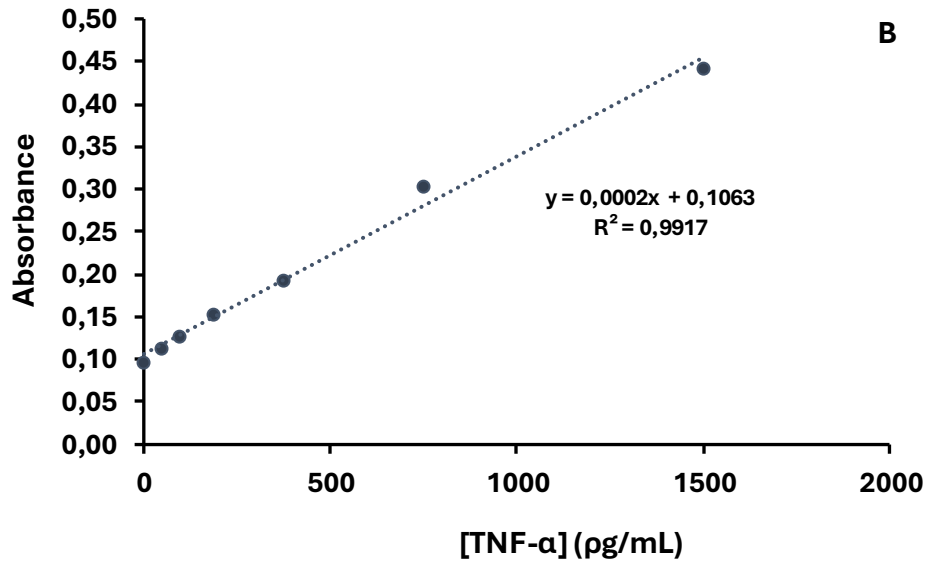
Annex 2: Griess assay standard curve



Annex Figure 2 - Griess assay standard curve. Absorbance of seven different standard solutions of sodium nitrite (NaNO_2) in PBS (0, 6.25, 12.5, 25, 50, 100 and 200 μM) was measured at 540 nm wavelength. $[\text{NO}_2^-]$ – Nitrite concentration presented in micromolar. Each point on the graph represents the mean value for each concentration, calculated from three replicates.

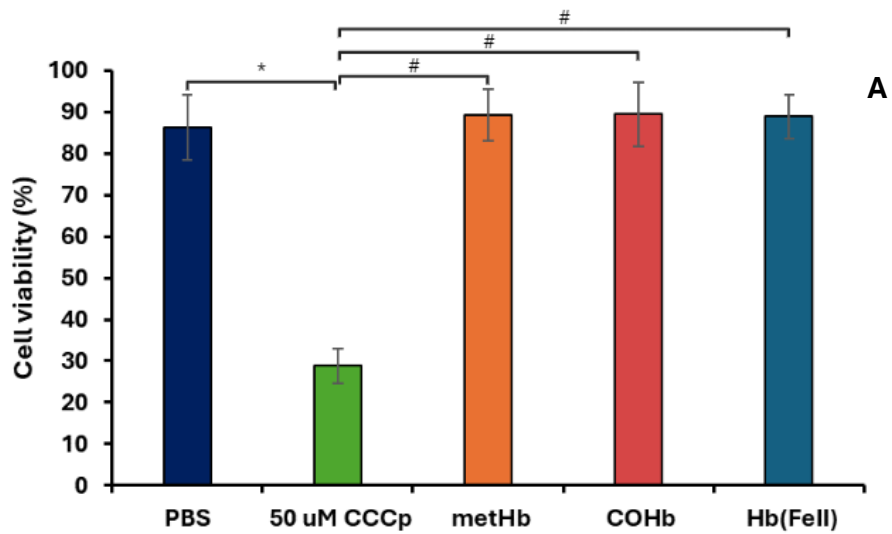
Annex 3: ELISA assay standard curves

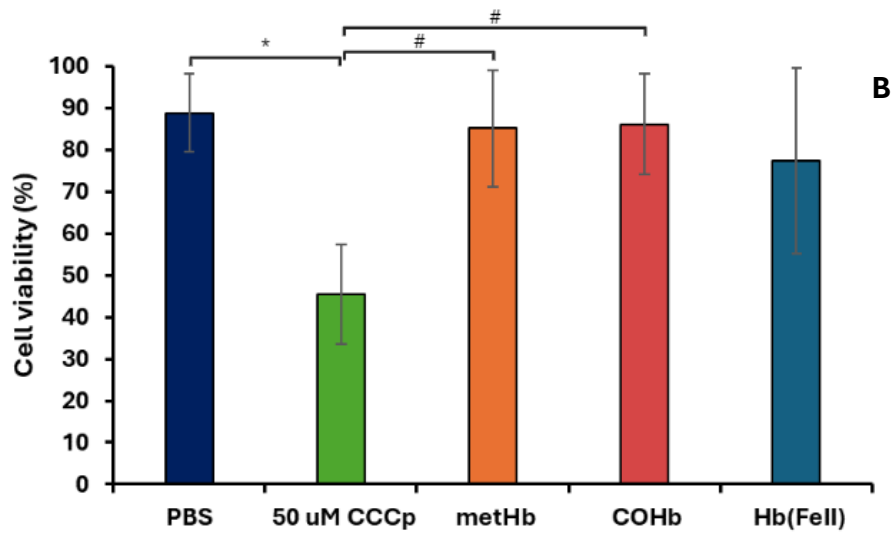




Annex Figure 3 - ELISA assay standard curves. (A) Absorbance of six different standard solutions of the pro-inflammatory cytokine tumor necrosis factor-alpha (TNF- α) (0, 46.87, 93.75, 187.5, 1500 and 3000 pg/mL). (B) Absorbance of seven different standard solutions of TNF- α (0, 46.87, 93.75, 187.5, 375, 750 and 1500 pg/mL). Absorbances were measured at 415 nm with wavelength correction set at 560 nm. Each point on the graph represents the mean value for each concentration, calculated from three replicates.

Annex 4: Neuronal viability – non-differentiated and differentiated SH-SY5Y cells treatment with PBS, CCCp, MetHb, COHb and Hb (Fe²⁺) for 24 hours





Annex Figure 4 - Cell viability (%) assessment of non-differentiated (A) and differentiated (B) SH-SY5Y cells pre-treated with PBS, MetHb, COHb and Hb (Fe²⁺) solutions at a concentration of around 30 μ M for 24 hours. Cells were exposed to 50% of Hb solutions in PBS, with PBS alone serving as the untreated control. Cells treated with a mitochondrial uncoupler (CCCp) at a concentration of 50 μ M were used as a control of induced cell death. Cell viability was assessed by propidium iodide staining quantification by flow cytometry. Results are shown as mean \pm SD from 3 independent experiments (n=3) for non-differentiated cells and 5 independent experiments (n=5) for differentiated cells, each including 3 technical replicates. The asterisk (*) indicates statistically significant differences between the untreated (PBS) and the treated control (50 μ M CCCp). The cardinal (#) indicates statistically significant differences between the treated control (50 μ M CCCp) and each of the hemoglobin-treated conditions ($p < 0.05$, two-tailed unpaired Student's t-test).



2024 Tatiana Fernandes

THE POTENTIAL NEUROPROTECTIVE ROLE OF CARBOXYHEMOGLOBIN (COHB) AGAINST HEMORRHAGIC STROKE